Lawrence Berkeley National Laboratory
Recent Work

Title

BIOPHYSICAL BASES OF HUMAN PLASMA LIPOPROTEIN POLYDISPERSITY: ROLE OF SURFACE MODIFICATION

Permalink

https://escholarship.org/uc/item/1r02z098

Author

Shahrokh, Z.

Publication Date

1984-11-01

Lawrence Berkeley Laboratory

UNIVERSITY OF CALIFORNIA

BIOPHYSICAL BASES OF HUMAN PLASMA LIPOPROTEIN
POLYDISPERSITY: ROLE OF SURFACE MODIFICATION

Z. Shahrokh
(Ph.D. Thesis)

November 1984

Donner Laboratory

**Biology &
Medicine
Division**

DISCLAIMER

BIOPHYSICAL BASES OF HUMAN PLASMA LIPOPROTEIN POLYDISPERSITY: ROLE OF SURFACE MODIFICATION

Zahra Shahrokh

Ph.D. Thesis

Lawrence Berkeley Laboratory
University of California
Berkeley, California 94720

November 1984

Biophysical Bases of Human Plasma Lipoprotein
Polydispersity: Role of Surface Modification

Zahra Shahrokh

Biophysical Bases of Human Plasma Lipoprotein
Polydispersity: Role of Surface Modification

Zahra Shahrokh

Abstract

Metabolic depletion of the core of the triglyceride-rich lipoproteins via lipolysis results in the production of polydisperse species of particles within the density range of low density lipoproteins (LDL). Modification of surface properties of plasma LDL may further contribute to LDL polydispersity. In this dissertation, we study the interactions with LDL of models of lipolysis-related surface products (i.e., phosphatidylcholine vesicles (PCV) and discoidal complexes (DC) of apoprotein AI and phosphatidylcholine) and examine the influence on such interactions of high density lipoproteins (HDL) and other relevant plasma components (lecithin:cholesterol acyltransferase (LCAT), lipid transfer proteins (LTPs), albumin, lysolecithin (LPC)).

Incubation (37°C, 6h) of LDL with PCV alone results in formation of aggregates of LDL and PCV without any change in the apparent particle diameter (APD) of unaggregated LDL.

Addition of the ultracentrifugal plasma d>1.20 g/ml fraction (bottom fraction, BF) produces an increase in LDL APD value. Further addition of components capable of PC uptake (e.g., HDL) modulates the extent of such APD increase. Incubation (6h) of LDL with DC also produces an increase in LDL APD value, primarily due to PL uptake by LDL. LDL APD change due to PL uptake is associated with decreased susceptibility to trypsin digestion of apoprotein B on the LDL surface. Interaction of LDL with DC or PCV also results in formation of association complexes (290-412A; class II products) comprised of LDL-sized species. Disruption of apoprotein B by trypsin prior to interaction with PL prevents formation of class II products as well as of aggregates of LDL with PCV. Trypsin-treated LDL are 5-10A smaller; however, they undergo an increase in APD value upon interaction with PCV and BF.

In incubation mixtures with DC, BF enhances LDL APD increase, primarily due to enhanced PL uptake by LDL. In incubations with either PCV or DC, albumin alone can simulate the effect of BF, whereas plasma PL transfer protein can not. In the presence of a PL acceptor (HDL), albumin returns the APD of PL-enriched LDL to its original value.

Interaction of another surface-reactive agent, LPC, with LDL, also results in LDL APD increase and formation of class II products.

Based on the studies obtained in this dissertation LDL surface modification may contribute to LDL polydispersity. Since HDL is a major acceptor of PL, formation of surface-modified LDL (e.g., PL-enriched, large LDL) in vivo would depend on LDL/HDL weight ratio in plasma.

Alex V Michts 11/14/84

Dedication

With my warmest gratitude, I present this thesis to a perceptive scientist, a giving teacher, and a wonderful person: my advisor, Dr. Alex Nichols. The work in this thesis began at the time of a revolution and survived some difficult socio-cultural encounters. Dr. Nichols and his associates, Elaine Gong and Pat Blanche, were as supportive and encouraging as my own family could be.

I acknowledge Dr. Virgie Shore and Nancy Shen for production of antibodies and gel electrophoresis of apoproteins; Dr. Ron Krauss for his scientific discussions on LDL; Dr. Trudy Forte and Bob Nordhausen for their assistance in the use of the electron microscope; Laura Glines and Joseph Orr for performing the analytical ultracentrifuge; and Gerry Adamson who reconciliated between me and the computers when all else failed.

Former colleagues, Drs. James Hunter and John Babiak, together with Richard Thrift and Christine Giotas, have been my good friends who made those weary hours in the lab fulfilling with scientific, and often not-so-scientific, talks.

To all those dearest girl-friends who still remained caring and understanding when I often spent more time with the thesis than with them.

To Saïd, a special person, who in marriage during final moments with the thesis, has given me new insights.

Mother,

Father,

together we have shared

harsh and happy times;

this thesis is for the two of you.

Grant Acknowledgment

Abbreviations

AUC: analytical ultracentrifugation

APD: apparent particle diameter

BF: plasma d>1.20 g/ml fraction (bottom fraction)

CE: cholesteryl ester

CF: cystic fibrosis patients

CFPI+: cystic fibrosis patients with pancreatic insufficiency

CFPI-: cystic fibrosis patients without pancreatic insufficiency

DC: discoidal complexes (comprised of apoprotein AI and phosphatidylcholine)

DTNB: dithiobis-(2-nitrobenzoic acid)

EM: electron microscopy

GGE: gradient gel electrophoresis

GnHCl: guanidine hydrochloride

GSH: reduced glutathione

HDL: high density lipoproteins

HMW: high molecular weight

HTG: hypertriglyceridemic patients

IDL: intermediate density lipoproteins

Kd: kilodaltons

LCAT: lecithin:cholesterol acyltransferase

LDL: low density lipoproteins

LPC: lysophosphatidylcholine (lysolecithin)

LPL: lipoprotein lipase

LTP: lipid transfer protein

mu: migration units

MW: molecular weight

N: normal subjects

NEFA: nonesterified fatty acids

N-LDL: native low density lipoproteins

NTG: normotriglyceridemic subjects

PC: phosphatidylcholine

PCMPS: p-chloromercuriphenyl sulfonic acid

PCV: phosphatidylcholine vesicles

PE: phosphatidylethanolamine

PL: phospholipid

PLTP: phospholipid transfer protein

PMSF: phenylmethylsulfonyl fluoride

PX: paraoxon

rmu: relative migration units

SDS-PAGE: sodium dodecylsulfate polyacrylamide gel electrophoresis

TG: triglyceride

TLC: thin layer chromatography

T-LDL: trypsin-treated low density lipoproteins

UC: unesterified cholesterol

VLDL: very low density lipoproteins

Table of Contents

I. Introduction

A. Lipoprotein Structure

Human plasma lipids of dietary or endogenous origin fall into two categories: polar lipids (phospholipids (PL),* unesterified cholesterol (UC), nonesterified fatty acids (NEFA), lysolecithin (LPC)) and nonpolar lipids (triglycerides (TG), cholesteryl esters (CE)). Due to their insolubility in water, transport of nonpolar lipids either from the intestine (their site of absorption), or from liver (their site of endogenous synthesis), to various tissues requires their incorporation into spheroidal complexes called lipoproteins (1). Physico-chemical techniques have established that the nonpolar lipids are located in the central region or the core of lipoproteins and are stabilized in aqueous solution by a surface shell of polar lipids and apoproteins.

Based on the size and composition of lipoprotein species, and molecular volumes of the separate lipoprotein components, Shen et al (2) have proposed a unifying model of lipoprotein organization (Fig. 1). Consistent with X-ray diffraction (3) and other spectroscopic (for review, see ref 4) data, the model proposes that lipoprotein particles are spherical structures of radius r, with a core of radius (r-

*See Abbreviations section for alphabetical listing of abbreviations used in this dissertation.

Fig 1. Model of human plasma LDL structure.

r (A)

r (A)

core | surface
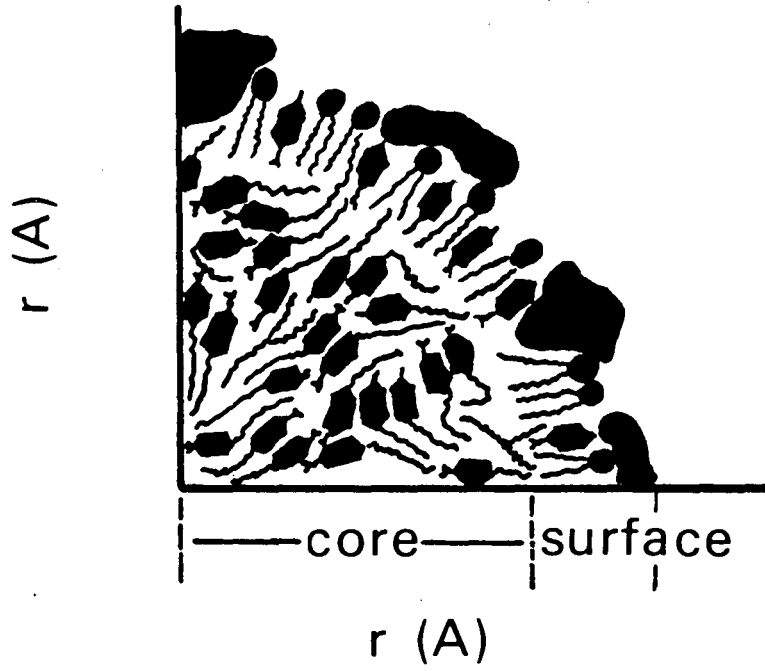
apoprotein

cholesteryl ester

phospholipid

triglyceride

unesterified cholesterol

XBL 848-7864

20A) consisting of TG and CE. The core is surrounded by a monolayer (20A thick) of PL and protein; the protein is in close association with the hydrophilic head groups of the PL. The UC is near to the surface of the lipoprotein particle and is packed adjacent to the hydrophobic tails of the PL; it is also considered to be masked by the protein. Recent studies take a more dynamic view of lipoprotein structure. Surface (UC) and core (TG and CE) lipids are shown to partition between the two compartments (5) and the boundary between the two compartments is less well-defined. Whatever the determinants of lipoprotein organization, our current understanding is that lipoprotein structure is the result of a series of metabolic interactions such as those occurring during: (1) enzymatic lipolysis of the lipoprotein TG, (2) exchange of PL, CE and TG among lipoprotein particles via lipid transfer proteins, and (3) build up of apolar core in lipoproteins during enzymatic esterification of cholesterol in plasma.

B. Lipoprotein Classification

The early work of Gofman et al (6) characterized plasma lipoproteins by their rate of flotation in salt solutions of specified density in the analytical ultracentrifuge. These studies established the existence of separate density classes, based on their relative content of lipid and protein. The major density classes of lipoproteins (Table 1) have hydrophobic cores that are either TG-enriched

Table 1 -Physico-chemical properties of major classes of human plasma lipoproteins.

lipoprotein class	density (g/ml)	particle diameter (A)	molecular weight (dalton)	flotation rate (Svedberg$\times 10^{13}$)	major apoproteins	protein (weight%)	major core lipid
chylomicron	0.95	10^3-10^4	10^9-10^{10}	S_f^o 400	apo B, C	1.5-2.5	triglyceride
VLDL	0.95-1.006	300-750	5×10^6-10^7	S_f^o 20-400	apo B, E, C	5-10	triglyceride
IDL	1.006-1.019	278-300	4.5×10^6	S_f^o 12-20	apo B	15-20	triglyceride
LDL	1.019-1.063	218-300	2-2.5×10^6	S_f^o 0-12	apo B	20-25	cholesteryl ester
HDL	1.063-1.20	50-120	1.9-3.9×10^5	$F_{1.20}^o$ 0-9	apo AI, AII	40-55	cholesteryl ester

*VLDL, very low density lipoproteins; IDL, intermediate density lipoproteins; LDL, low density lipoproteins; HDL, high density lipoproteins.

(chylomicrons, very low density lipoproteins (VLDL), and intermediate density lipoproteins (IDL), which are contained within the d<1.019 g/ml plasma fraction), or CE-enriched (low density lipoproteins (LDL, d 1.019-1.063 g/ml) and high density lipoproteins (HDL, d 1.063-1.20 g/ml)). With increasing density, the particle size, molecular weight, and flotation rate of lipoproteins decrease (Table 1).

Although density is generally used as a basis for the isolation and definition of lipoprotein classes, a recent method of classification based on constituent apoprotein moieties (7), has gained interest. The interest is primarily based on the understanding that functional properties of lipoproteins are determined, in major part, by their apoprotein moieties. Each lipoprotein is characterized by a specific apoprotein profile. This profile reflects metabolic events that are involved in the remodeling of a particular lipoprotein species and determine its fate. Apo AI, for example, is the major activator of the plasma cholesterol esterifying enzyme of plasma, lecithin:cholesterol acyltransferase (LCAT). Members of the apoprotein C family regulate the activity of lipoprotein lipase (LPL), while apo B and apo E interact with specific receptors, signaling for lipoprotein catabolism.

C. Interrelationships Among Lipoprotein Classes: Metabolic Schemes

The various density classes of lipoproteins are inter-related not only structurally but also functionally. Once newly-synthesized TG-rich lipoproteins, containing primarily apoproteins B and AI, enter the blood circulation from intestine or liver, they pick up apoproteins C and E from HDL (for review, see references 1,8). As their TG is rapidly hydrolysed by the capillary-bound LPL, remnant particles are produced, containing primarily apoproteins B and E. Remnants are removed in part by the liver cells, and are partly converted to LDL (with mainly apoprotein B). During lipolysis, transfer of apoproteins C and E to the TG-rich lipoproteins from HDL is important for both activation of lipases by apoprotein CII and removal of remnants by apo E-receptor-mediated pathway. During degradation of the TG-rich lipoproteins, apoproteins C, E, and AI are transferred to HDL. In contrast to the recycling of these apoproteins, apoprotein B (apo B) is retained during degradation of TG-rich lipoproteins to LDL. Thus, the d<1.063 g/ml lipoproteins, also known as apo B-containing lipoproteins, represent products of a metabolic cascade in which lipolysis plays a major role.

The cascade of core removal from the larger, less dense species gives rise to excess surface components (PL, UC, and apoproteins) which are released in part as vesicular (9,10) and discoidal (11,12) structures. Discoidal complexes are

considered to be major precursors to plasma HDL (13,14) and are transformed to spherical species during conversion of their UC to CE by catalysis via LCAT (15). Spherical HDL can further interact with excess surface products of lipolysis and in conjunction with LCAT activity give rise to larger, less dense HDL species (16). Catabolism of HDL leads to the ultimate clearance of the excess surface products from plasma, completing the metabolic events occurring upon core depletion of TG-rich lipoproteins.

D. Functional Properties of Lipoprotein Classes

Plasma lipoproteins are responsible for the distribution of lipids among tissues. Fatty acids produced during lipolysis of the TG-rich lipoproteins are delivered to cells where they can be either utilized directly or stored. The CE-enriched lipoproteins, on the other hand, are involved in cellular cholesterol homeostasis. The final by-product of lipolysis, LDL, is the main deliverer of cholesterol to cells. Apo B-receptor-mediated uptake of LDL from the blood circulation triggers a set of cellular responses, such as decreased number of cell surface receptors recognizing apo B and reduced endogenous synthesis of cholesterol (17). These responses prevent accumulation of cholesterol within the cell. On the other hand, both the interaction of HDL with cells and the transformation of nascent HDL species in conjunction with LCAT activity seem to be essential for removal of cellular cholesterol. The clinical consequences of

abnormalities in lipid transport and delivery by lipoproteins are apparent in such genetic disorders as LCAT-deficiency (associated with abnormal HDL structure and composition (15)), deficiency in apo B-receptor (associated with hypercholesterolemia (18)), or simultaneous deficiency in apo AI and apo C III (associated with negligible levels of HDL of abnormal composition (19)). In LCAT deficiency, the disruption in cholesterol esterification leads to accumulation of cellular cholesterol content and clinical symptoms including anemia and renal failure (20). In the other cases cited above, CE accumulates in arterial cells and premature vascular disease is frequently encountered.

E. Human Plasma LDL: Structure and Metabolism

In view of the important role of LDL in the normal function of the lipid transport system, particularly in cellular cholesterol homeostasis, and in the correlation of blood lipid levels with the development of coronary heart disease, many studies have examined LDL structure and metabolism. Recent studies indicate considerable LDL polydispersity and have raised questions with respect to its metabolic origin and pathologic implications. I shall first review the current understanding of the structural properties of LDL, in particular those pertinent to their polydispersity

1. Core Organization

Differential scanning calorimetry (21) and X-ray diffraction (3) studies on intact human LDL, as well as NMR (22) studies on reconstituted LDL, consistently show a thermal transition between smectic (ordered) to liquid-like (disordered) states of core CE in the temperature range of 20-40°C. The peak of the transition temperature is slightly below body temperature and reflects not only the degree of saturation of the cholesterol ester but also with CE/TG ratio in the LDL. Below the phase transition, the core consists of a radially-oriented arrangement of two concentric layers of CE interspersed with TG (Fig 1). In the large, CE-enriched LDL from Cynomolgus monkeys on atherogenic diets (23), the core consists of three (instead of the usual two) concentric layers of CE below phase transition.

2. Apoproteins of LDL

More than 97% of LDL protein is apo B. Minor amounts of apo C and apo E (24) are also detected in the LDL density range (d 1.019-1.063 g/ml). Unlike other apoproteins, apo B is insoluble in aqueous solutions and has a tendency to aggregate once separated from LDL lipids. This has complicated investigation of the basic properties of apo B, such as its amino acid sequence. Depending on the technique used for delipidation, solubilization, and determination of molecular weight (MW), different values for molecular weight have been assigned to apo B. Thus, apo B has been reported as a single subunit of about 540 kilodaltons (Kd (25)), or two subunits of 250 Kd each (26), or even several

polypeptides, 14 Kd-200 Kd (27). The susceptibility of LDL to oxidation and proteolysis (28) can result in several small MW polypeptides. Inconsistent observations among laboratories in studies on apo B have been attributed to lack of attention to protective measures, such as chelating agents, antioxidants, antibacterial reagents, protease inhibitors, and adequate storage conditions (29). Two out of the fourteen sylfhydryl groups of apo B are free and susceptible to interaction with peroxides of fatty acyl moieties (30). Trace metals (28) are thought to be responsible for initiating oxidative aggregation of apo B.

Apo B is a glycoprotein with 8-10% carbohydrate content (31). Although its amino acid and carbohydrate compositions have been determined, the primary structure has not yet been assigned. Immunochemical characterization of partially-cleaved apo B has suggested the presence of repeated sequences (32). Recently a partial sequence of a proteolytic fragment of apo B (33) has been described and work is directed at isolation of apo B mRNA. The latter may prove fruitful in determination of apo B properties through the use of recombinant DNA technology.

Two immunochemically distinct variants of apo B have been detected (25). The one (apo B-48) from the intestine is found mainly in chylomicron and intestinal VLDL, and the other (apo B-100) from liver is commonly seen in LDL and hepatic VLDL. Often, two minor components (apo B-74 and apo B-26) are also present in LDL preparations which may

represent proteolytic fragments of apo B-100 (34). By means of monoclonal antibodies to apo B, two allelic variants to apo B have been recently identified (35). Polymorphism in apo B may prove to be of clinical significance as implicated by the work of Mao et al (36). Their studies show that patients with coronary heart disease have a significant increase in a form of plasma apo B that is recognizable specifically by one out of the four monoclonal anti-apo B antibodies they have produced.

3. Polydispersity Among LDL: Physical-chemical Evidence

Lipoproteins within the density class of LDL (from different individuals as well as from a single human subject) are particles that exhibit a range of size (37,38), molecular weight (39,40), hydrated density, flotation rate, and chemical composition (24, 41-44). Early work of Lindgren et al (43) and Adams et al (44) reported at least three subclasses of LDL differing in density, S^o_f rate and lipid/protein ratio in plasma of a single subject. Fisher et al (45) postulated that, for the same amount of apoprotein within each of the major LDL subclasses (S^o_f rate 20, 10, 4) the larger molecular weight components may be generated by the addition of specific increments of lipids, particularly TG and PL.

Subfractionation of LDL from a single individual by equilibrium density gradient ultracentrifugation indicated the presence of three (24) to six (38) density classes. By means of polyacrylamide gradient gel electrophoresis in the

latter study, multiple discrete subspecies were found within each density fraction as well as within the unfractionated LDL. A progressive decrease in average particle diameter, peak S^o_f rate, and TG/CE ratio was seen with increasing density. A major reduction in the core CE and surface constituents (PL, UC) was observed with increasing density and decreasing particle size. With increasing density, there was an initial decrease in core TG content, however, there was an abrupt increase in TG in the most dense LDL species (41), suggesting a different metabolic origin for these species. The major density subfractions of human plasma are classified in Table 2.

Despite polydispersity within the LDL obtained from a single individual, characteristic LDL profiles have been found in individuals in similar metabolic states. For example, molecular weight and ultracentrifugal peak flotation rates are generally larger in women than men. Interrelationships between LDL and other lipoprotein subclasses have also been established (43,46). Levels of LDL of S^o_f rate 3-5 are inversely and significantly correlated, in both cross-sectional and longitudinal studies, with levels of HDL, particularly the faster floating HDL_2 component. Thus, females generally have lower levels of the S^o_f rate 3-5 than males and this is associated with substantially higher HDL_2 levels. In addition, lipoprotein distributions with predominantly faster floating LDL (and HDL) species (such as those observed in most females) are characteristic of plasma with

Table 2 -Major subclasses of human plasma LDL

density range (g/ml)	1.025-1.035	1.035-1.040	1.040-1.050	1.050-1.060
size range (A)	278-255	255-246	246-232	232-218
S_f^o range (Svedberg $\times 10^{13}$)	10-7.5	7.5-5.7	5.7-4.0	4.0-1.0
NL ♀*	minor‡	major‡		
NL ♂	minor	minor	major	
FHCS (♀/♂)*	major	minor		
HTG (♀/♂)*			major	minor
severe HTG (♀/♂)*			major	major

*NL, normolipidemia; FHCS, familial hypercholesterolemia; HTG, hypertriglyceridemia (plasma triglyceride level > 250 mg/dl); severe HTG is defined by plasma triglyceride level in the range of 500-1000 mg/dl.

‡'minor' and 'major' signify that the component is either a minor or a major contributor to the pattern.

low VLDL levels. In other studies (47), a positive correlation between plasma VLDL levels and the total core content (hence size) of LDL (and HDL) has been reported. These relationships are consistent with the observations that subjects with high plasma VLDL levels typically exhibit small, more dense LDL (and HDL) species. In extreme cases of familial hypertriglyceridemia (HTG), the major LDL component is comprised of the slow floating S^o_f 0-4 (45), small (230-245A, this dissertation), relatively TG-rich species. Such LDL distributions are frequently associated with low HDL levels (mainly HDL_3 species).

Recently, however, an exception to this general relationship has been noted in some normotriglyceridemic (NTG) subjects. Despite their normal plasma VLDL levels, these subjects have small, dense, and relatively "apo B-enriched" (CE-poor) LDL species (48), that are somewhat similar to those found in hypertriglyceridemic subjects. The presence of such "apo B-enriched" LDL species in subjects with normal or elevated plasma lipid levels has been termed as hyperapobetalipoproteinemia. When hyperapobetalipoproteinemia is found in subjects with normal plasma TG levels, the subjects frequently have a history of coronary heart disease. This has created interest in further characterization of LDL properties in such individuals, since the new notion of a CE-poor (smaller and more dense) LDL being associated with atherogenesis is in contrast to the observation of the presence of CE-enriched (larger and less dense) LDL species in

patients most prone to premature coronary disease, those with familial hypercholesterolemia (18).

Of the properties of LDL, other than lipid composition, that may contribute to LDL polydispersity, structural polymorphism of apo B has recently gained interest. In their study of immunoreactivity of LDL towards various monoclonal antibodies against apo B, Schonfeld et al (49) reported marked variation in epitope expression of LDL from different individuals. With some antibodies, the number of epitopes expressed in LDL from different individuals correlated positively with the precentage of LDL-PL; with other antibodies, epitope expression correlated positively with the percentage of cholesterol and negatively with the percentage of TG, suggesting that both surface and core constituents of LDL may influence the exposure of apo B epitopes to antibodies. Recent data[†] demonstrate a decrease in epitope expression, using selected monoclonal anti-apo B antibodies, with increasing density (decreasing cholesterol/protein weight ratio) of LDL. Reduced apo B epitope expression, particularly in the most dense LDL may either be due to the presence of minor apoproteins (e.g. apo C (24)), or might imply differences in apo B conformational properties across the LDL spectrum. Though earlier findings (50) have shown that molecular domains in LDL susceptible to trypsin cleavage are invariable in LDL from different

---

[†]Krauss R.M. and Marcel, I., personal communication.

donors, the new findings with monoclonal antibodies imply that lipoprotein polydispersity is also related to differences in apo B organization.

4. Metabolic Bases of LDL Polydispersity

Metabolically LDL arise predominantly from lipolysis of TG-rich lipoproteins. Understanding how lipolysis leads to LDL formation may provide insight into the metabolic origins of LDL polydispersity. In addition, LDL polydispersity may result from de novo cellular biosynthesis of LDL and interconversion (i.e., shifts in distribution due to interaction with cells, lipolytic enzymes, proteolytic enzymes, and lipid transfer proteins) among species within the LDL density range.

a. Origins of LDL: Direct Cellular Synthesis

Early turnover studies (51) suggested that VLDL production was sufficient to account for all of the LDL production observed in normolipidemic individuals. Later studies showed a discrepancy between the turnover of VLDL apo B, IDL apo B, and LDL apo B (52-55). This was observed in familial hypercholesterolemia (52,53), individuals on high carbohydrate diets (54), and in familial hypertriglyceridemia (55). These studies showed that 20-72% of plasma LDL may be derived from precursors other than VLDL and IDL.

The properties of newly-synthesized LDL are not known. In the rat, LDL appear in the S_f^o rate range of 0-5, 65% of which enter plasma independent of VLDL secretion (56). Human

Hep G2 cells in culture appear to secrete negligible amounts of VLDL, but do secrete two discrete species of cholesterol-poor, TG-rich and PL-rich species within the LDL density range (140). Properties of LDL in interstitial fluids (57)[*] or liver cells (58), and the contribution of these LDL to plasma LDL polydispersity have yet to be evaluated.

b. Origins of LDL: Lipolysis of TG-rich Lipoproteins ("Core Pathway")

The molecular mechanisms involved in production of LDL from VLDL have been studied <u>in vitro</u> (51, 59-62). During core degradation, excess surface PL, UC and apo C and E are released (11). The product LDL formed <u>in vitro</u> are apo B-rich and appear in the d 1.019-1.063 g/ml. These "LDL" are larger, more heterogeneous and contain surplus CE molecules (60).

The processes leading to conversion of these "LDL" to LDL of normal composition and size are still not known. It has been postulated (59-60) that conversion of such "LDL" to LDL with normal size and composition involves, firstly, CE depletion of the core of the "LDL" particles in exchange for TG, and secondly lipolysis of the core. Core exchange plus lipolysis leads to formation of smaller, more dense species with reduced core contents. In plasma, such core exchange

---

*Also see Forte, T.M., Reichl, D., Hong, J.L., and Ruda, D.N., abstract submitted to American Heart Association.

can be facilitated by lipid transfer proteins (for review
see ref 62) and the donor of TG is mainly VLDL. The amount
of TG available (as VLDL) for core exchange presumably
determines the extent of core TG enrichment of the "LDL".
The particle size and hydrated density of the final LDL pro-
ducts are presumably determined by the extent of lipolysis
of this TG. Support for this comes from the observation
that plasma VLDL levels (hence the TG available for exchange
with the LDL core moiety) directly correlate with the mass
of the LDL core components (which is indicative of LDL par-
ticle size and density).

c. Interconversion Among LDL Subpopulations: "Core
Pathway" and "Surface Pathway"

Core exchange and depletion via lipolysis can also
occur for particles within native plasma LDL density range,
producing a shift in LDL distribution to smaller, more dense
species. Such a "core pathway" may contribute to LDL
polydispersity. In addition to the "core pathway", LDL
interconversion may also occur via reduction in content of
surface components. For example, conversion of LDL to
smaller species could result from a decrease in surface
lipids (e.g. via transesterification of surface PC and UC by
LCAT or lipolysis via phospholipases) or degradation of sur-
face protein (e.g. via proteolysis). A recent report (63)
has described interconversion of LDL to more dense species
when when plasma was incubated without an LCAT inhibitor. In
these LDL, the percentage of core lipids increased, but the

content of surface components decreased. Electron micros-copy did not reveal any significant changes in LDL particle size or shape. The opposing effects of core versus surface alteration on LDL particle size remains to be assessed with more sensitive methods. In this thesis, the first part of the Results section describes an investigation of changes in LDL properties associated with LCAT activity during plasma incubation.

Recent in vivo studies (64) indicate bidirectional shifts of apo B to higher (as well as lower) density LDL species following injection of specific radiolabelled LDL subpopulations. Whereas transformation to smaller, more dense species may occur due to core depletion and passive loss of surface constituents during lipolysis, interconversion to larger species would probably require either core and/or surface enrichment of the smaller species. Surface enrichment would most likely result from interaction with surface components of lipolysis (i.e. vesicular and discoidal complexes of PL, UC, and apoprotein). Surface enrichment in the case of HDL, both in vivo (65) and in vitro (11,66,67), leads to conversion to larger, less dense species via increase in surface PL. The half life of LDL in plasma (68) is long enough that it, too, can interact with surface-derived components in vivo. The possible inter-conversion of LDL upon interaction with surface components and the role of LCAT, lipid transfer proteins, and other plasma proteins in such interactions has not previously been

studied and is a major focus of this thesis.

II. Overview of Thesis

To investigate changes or interconversions in LDL that might be initiated by interaction of LDL with excess surface products during lipolysis of TG-rich lipoproteins, in vitro incubation studies were carried out. As analogues to surface-derived structures, vesicles of PC (PCV) and discoidal complexes of PC and apoproteins (DC) were used. Initial studies investigated the effects of plasma incubation on LDL properties in the absence of PCV. In these baseline studies, the role of plasma factors that may participate in LDL and PC interaction, namely LCAT and LTPs, was evaluated. Incubation studies on plasma plus PCV were carried out and changes in LDL particle size and distribution were detected by gradient gel electrophoresis (GGE). By means of reconstitution experiments, essential determinants of LDL particle size and distributions changes were identified. The role of factors such as HDL and the plasma d>1.20 g/ml fraction was assessed. Several biophysical techniques were utilized to characterize the LDL products formed at various stages of particle size and distribution changes. Subfractionation of incubation mixtures for the purpose of chemical analysis of the LDL products was attempted. Difficulties were encountered in separating PCV from LDL and other interaction products. Hence, emphasis was placed on studies evaluating the interaction of LDL with a different surface product of lipolysis, namely discoidal complexes of PL and apoprotein. Discoidal complexes (DC) were used and

these proved to be particularly suitable for fractionation from LDL products. To evaluate whether effects previously seen with PCV could also be demonstrated with DC, similar experimental approaches were used as with PCV. The particle size increases observed by us during incubation of LDL with PCV and other plasma components (HDL, the plasma d>1.20 g/ml fraction) also occurred with DC. However, not all of the effects observed with PCV were seen with the latter. Fractionation of incubation mixtures containing DC provided insight into the bases for particle size change. PL uptake by LDL was found to be the major contributor and changes in apoprotein structural properties accompanied PL uptake.

III. Methods

A. Lipoprotein Preparation

Blood was drawn from human subjects after an overnight fast into tubes containing K_2EDTA (2.5mM). An alphabetical list of the subjects used in this dissertation is provided in Table 3. Plasma was separated by centrifugation (twice at 1800 rpm, 4^OC, 20 min). Sodium azide (0.2 mg/ml) or ethylmercurithiosalicylic acid (merthiolate, 0.12 mM), and 5 μl/ml penicillin-streptomycin (10000 units/ml-10000 g/ml; Gibco) were immediately added as antibacterial agents. For certain incubation studies, phenylmethylsulfonylfluoride (PMSF, 2mM; Sigma), or reduced glutathione (GSH, 1.6 mM; Sigma), were also added to plasma in order to inhibit possible proteolysis or lipid oxidation, respectively. When necessary, dithiobis-(2-nitrobenzoic acid) (DTNB, 2 mM), 2mM p-chloromercuriphenylsulfonic acid (PCMPS, Sigma), or 1.4 mM diethyl p-nitrophenyl phosphate (paraoxon, PX; Sigma), were added as inhibitors of LCAT.

Lipoproteins were isolated by sequential ultracentrifugation (Beckman 40.3 rotor, 24h, 400000 rpm, 15^OC) after appropriate density adjustment with solid NaBr. Routinely, only two ultracentrifugal steps were used to isolate each lipoprotein class. First, plasma adjusted to d 1.063 was spun and the top 2 ml, containing VLDL, IDL, and LDL was removed. Then this fraction (the d<1.063 g/ml) was layered under 4 ml of a d 1.006 solution and centrifuged. The VLDL

Table 3 -Alphabetical list of subjects

subject	age	sex	plasma TG status
AP	26	M	NTG*
BG	29	M	120 mg/dl
CB	33	F	130 mg/dl
DJ	30	M	NTG
DR	41	F	@1000 mg/dl
EB	48	M	198 mg/dl
GH	49	F	NTG
GK	30	F	NTG
JB	--	F	@1000 mg/dl
JG	52	M	550 mg/dl
KP	--	F	NTG
LS	40	M	@1000 mg/dl
MB	--	F	NTG
RM	--	F	109 mg/dl
TI	52	M	550 mg/dl

*NTG, normotriglyceridemic (plasma triglyceride level < 250 mg/dl); actual values not available.

and IDL (d<1.020 g/ml) appeared in the top 2 ml and the LDL (d 1.020-1.063 g/ml) appeared in the bottom 2 ml. HDL (d 1,.063-1.20 g/ml) were isolated from flotation at d 1.20 g/ml of the ultracentrifugal d>1.063 g/ml plasma fraction. An Lp(a)-enriched fraction (d 1.050-1.19 g/ml) was also isolated from certain plasmas using a two-step sequential ultracentrifugation. Plasma was first spun at d 1.050 g/ml, the top 2 ml was removed, and the bottom 4 ml was then respun at d 1.19 g/ml. The Lp(a)-enriched fraction appearing in the top 1 ml was removed.

Single-step ultracentrifugation (Beckman 50.3 rotor, 24h, 50000 rpm, 15°C) of plasma adjusted to d 1.20 g/ml was used for isolation of fresh d>1.20 g/ml plasma proteins ("bottom fraction" designated BF) at the bottom 2/3 of the tubes. In this case, the d<1.20 g/ml lipoprotein-containing fraction (top 1 ml) was removed and fractionated by gel filtration in order to obtain separate classes of lipoproteins. Gel filtration was performed on 6% beaded agarose gel (2.5x100 cm Bio-Rad column, 30 ml/h, 4°C), using either 0.01 M Tris-0.19 M NaCl, 0.27 mM Na_2EDTA, 0.12 mM merthiolate, pH 7.4 (buffer A) or 0.01 M Tris- 0.15 M NaCl, 0.27 mM Na_2EDTA, 0.12 mM merthiolate, pH 8.0 (buffer B). Following gel filtration, fractions from the elution profile were characterized by gradient gel electrophoresis (GGE). Fractions containing the HDL and the LDL were separately pooled and concentrated (Amicon XM-100) to 4-6 mg/ml protein for subsequent incubation studies. The HDL fraction purified by gel

filtration was free of albumin or other plasma protein contaminants, and was thus used for apo AI isolation.

B. Phospholipid Vesicle Preparation

One hundred mg egg yolk L-α-lecithin (20 mg/ml in ethanol; Supelco) was dried under N_2 (room temperature), and vortexed in 5 ml buffer A (see Methods, section A) PC vesicles (PCV) were prepared by sonication (Ultrasonics; 3 times at 5 min intervals, 40 watts, under N_2 and on ice). Large aggregates and metal chips were removed by ultracentrifugation (Beckman 40.3 rotor, 15000 rpm, 10 min, 15° C), and the vesicles were stored in screw cap glass vials (under N_2, 4°C). As assessed by thin-layer chromatography (TLC), vesicles could be stored for at most one month without appearance of oxidation products.

C. Preparation of Discoidal Complexes Comprised of PC and Apo AI

Discoidal complexes of human apo AI and egg yolk phosphatidylcholine (DC) were prepared, using a detergent dialysis technique (69). To prepare apo AI, the HDL (obtained from gel filtration of the d<1.20 g/ml plasma fraction) were incubated (3h, 37°C) in 4 M guanidine hydrochloride (GnHCl). The GnHCl was removed by dialysis (Spectropor 1 tubing, 6000-8000 MW cutoff; 4°C) against buffer B, adjusted to d 1.20 g/ml with NaBr, and the mixture was ultracentrifuged (Beckman 50.3 rotor, 50000 rpm, 24h, 15°C).

The dissociated apo AI, which appeared in the ultracentrifugal bottom 1.5 ml was removed and dialysed to buffer B. Isolated apo AI gave a single-band on 2-16% sodium dodecyl sulfate-polyacrylamide gel electrophoresis (SDS-PAGE; see Fig 2).

Egg-yolk phosphatidylcholine (15.4 mg in ethanol) was dried under N_2, dispersed in sodium cholate (23.25 mg in buffer B), and incubated (30 min, $37^{O}C$). Apo AI (6.35 mg) was added while vortexing, and the mixture (total volume, 5 ml) was incubated ($4^{O}C$, overnight). For removal of the sodium cholate, samples were first dialysed (Spectropor 1 tubing, 6000-8000 MW cutoff) against buffer B ($4^{O}C$, 2 l, 3 changes in 24h). After dialysis, any residual cholate was removed by passing the samples through a Bio-Gel P-4 column (2.0x50 cm, 20 ml/h, room temperature) using buffer B. The material eluting in the void volume contained discoidal complexes of polydisperse particle size (Fig 3, lane 1). Using gel filtration on 6% beaded agarose gel (2.5x100 cm, 30 ml/h, $4^{O}C$) the major species (class 3, peak diameter 94A, Fig 3, lane 3) in addition to minor components (169A, class 4, and 80A, class 2, Fig 3, lane 3) were isolated from larger complexes in the unfractionated disc preparation (Fig 3, lane 1). This sample had a final PL:protein molar ratio within the range of 88:1 to 100:1 and was used for incubation studies with LDL.

Fig 2. Examination of the purity of a human apo AI prepara-
tion by SDS-polyacrylamide gel electrophoresis. Ten µl of a
preparation of apo AI (3.44 mg/ml) in a Tris-NaCl buffer
(buffer B, see Methods, section A) was added to ten µl of a
denaturing buffer (buffer C, see Methods, section G3), and
heated (60°C, 15 min). 10 µl of this mixture (lane 1) and
of a solution of molecular weight markers (Pharmacia HMW
protein mixture; 1 mg/ml in buffer C, lane 2) were
separately mixed with 5 µl of a sucrose-containing solution
(40% sucrose, 0.01% bromphenol blue in buffer B) and elec-
trophoresed on a 2-16% polyacrylamide gradient gel.
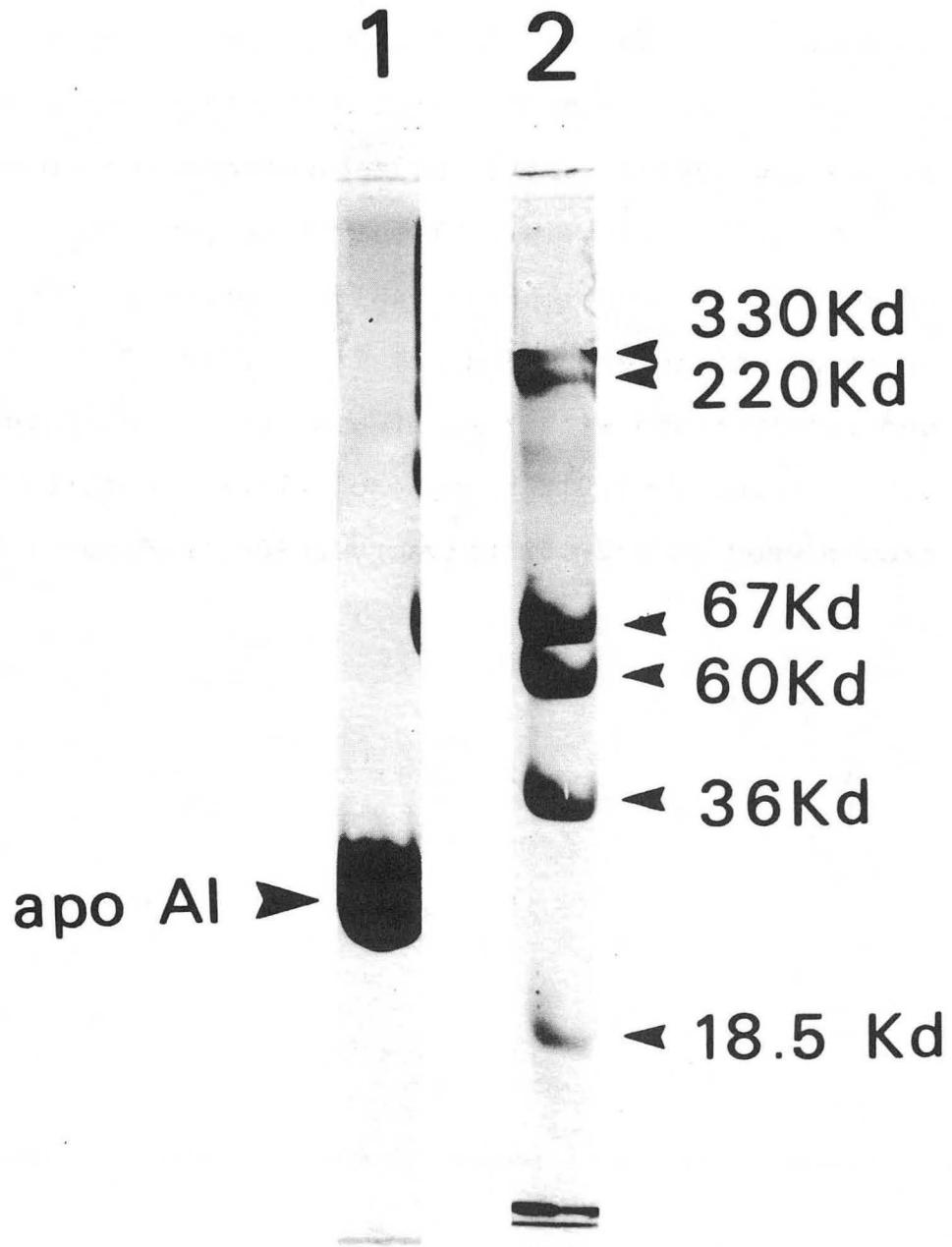
XBB 849-6742

Fig 3. Gradient gel electrophoresis (4-30%) of discoidal complexes of PC and apo AI (88:1 molar ratio). Discoidal complexes were prepared as described in Methods, section C. GGE (using 4-30% gels) was performed on unfractionated discoidal complexes (lane 1), a mixture of class 3 and 2 discoidal complexes (lane 3) isolated by gel filtration, and particle size calibration proteins (lanes 2 and 4).

class 3 ►
class 2 ►

1 2   3 4

Thyroglobulin

apoferritin

catalase

lactate dehydrogenase

bovine serum albumin
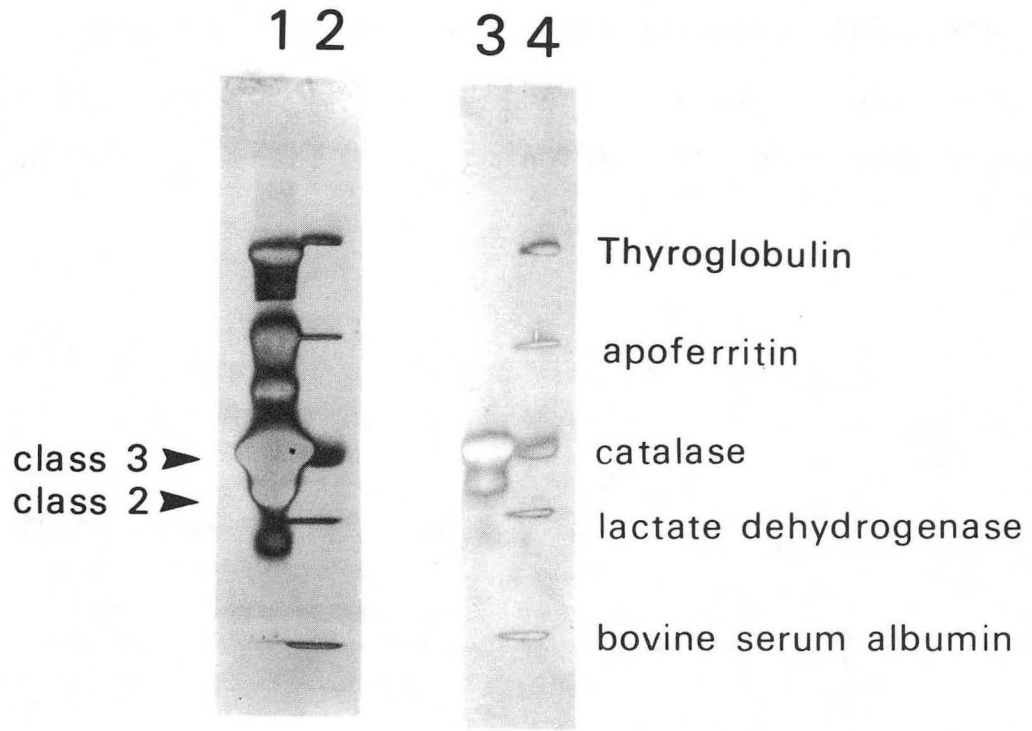
XBB 849-6741

D. Incubation of Experimental Mixtures

Before incubation, all samples were dialysed against either buffer A (1980-83)[*] or buffer B (1983-84). In general, incubation mixtures (0.5 ml to 12 ml) contained either 0.6 mg/ml LDL-protein in incubation with PCV (0.2-0.4 mg/ml PC) or 0.3 mg/ml LDL-protein in incubations with DC (0.4-1.9 mg/ml PC). Where investigated, the following components were incorporated into the interaction mixtures at the levels indicated: HDL (0.7 to 1.5 mg/ml protein), the d>1.20 g/ml plasma fraction (at concentrations equivalent to plasma level), human serum albumin (fraction V, fatty acid free, 35 mg/ml), and partially-purified PL or cholesteryl ester transfer proteins[**] (80 µg/ml). Specific compositions of incubation mixtures used in the various studies of this thesis are described with each experiment in the text.

Incubations (37°C, 15 min to 24h) were performed under N$_2$ either in screw cap glass vials or in snap-cap plastic Eppendorf tubes (0.5 ml samples). Upon completion of incubation, the samples were chilled on ice and immediately subjected to isolation (ultracentrifugation or gel filtration) and characterization by GGE. In incubation mixtures containing either the d>1.20 g/ml plasma fraction or albumin, isolation of lipoprotein products was achieved by raising

---

[*]A change in buffer at 1983 came about because of the recommended use of higher pH for preparation of discoidal complexes.
[**]Gift of Dr. A.Tall.

the density of the mixture either to d 1.063 g/ml or to d 1.20 g/ml, and ultracentrifugation (Beckman 50.3 rotor, 50000 rpm, 24h, 15°C).

To assess the possibility that changes in LDL surface organization, particularly the apo B conformation, may induce changes in LDL electrophoretic mobility, LDL was exposed to a denaturing agent, GnHCl. Incubation (37°C, 6h) in the presence of GnHCl (Sigma, 1M-6M) was carried out following addition of dry GnHCl directly to LDL (100 μg protein) in a total volume of 1 ml. and gentle vortexing. After incubation, the mixture was either analysed directly by GGE or was dialysed (initially at room temperature for 3 washes, and subsequently at 4°C for 3 washes) against buffer B.

E. Ultracentrifugal Procedures

1. Isopycnic density gradient ultracentrifugation (IPDGUC)

Different subclasses of LDL were isolated using an equilibrium density gradient ultracentrifugation technique developed by Shen et al (41). An LDL-containing mixture (typically 2 ml d<1.063 g/ml) was first dialysed to d 1.040 g/ml NaCl-NaBr solution and then layered above a d 1.054 g/ml (2.5 ml) solution in a 1/2"x 1/2" cellulose nitrate centrifuge tube. Then, 2.5 ml of a d 1.0275 g/ml solution was layered above the LDL. After ultracentrifugation (Beckman SW 45 rotor, 40000 rpm, 40h, 15°C), the top 0.5 ml and

six 1 ml fractions were removed and identified by GGE. The value of the background salt density was used to estimate LDL hydrated density.

When a shallow gradient was desired for further sub-fractionation of LDL, 0.5 ml sample (dialysed to 1.067 g/ml) was overlaid with 11.5 ml of a linear gradient (d 1.037 g/ml to 1.049 g/ml) and ultracentrifuged (Beckman SW 41 rotor, 40000 rpm, 40 h, 20^OC). This procedure was designated 2-grad. The tubes were scanned (455 nm) with an RFT scanning densitometer and then 1 ml frac|ions were removed for chemical analysis.

2. Analytical Ultracentrifugation

Lipoprotein concentrations and flotation coefficients were measured using analytical ultracentrifugation of lipoproteins at either d 1.063 g/ml or d 1.20 g/ml in a Spinco Model E ultracentrifuge with schlieren optics, as previously described (70).

F. Gel Filtration

Gel filtration on 6% beaded agarose gel was used for isolation of (1) different lipoprotein classes from plasma (Bio-Rad 2.5x100 cm column, 30 ml/h, 4^OC, buffer A) and (2) LDL from incubation mixtures containing DC (Bio-Rad 1.6x100 cm column, 20 ml/h, 4^OC, buffer B). Gravity-driven elution under constant hydrostatic pressure was used in all cases.

Before pouring the columns, the beads were washed three times in appropriate elution buffer and degassed. The freshly-poured columns were first equilibrated with plasma lipids by passing a concentrated d<1.20 g/ml lipoprotein sample through the column and then eluting with several bed volumes of buffer. Void volume was estimated using Blue Dextran (Sigma).

Samples (10 ml for 2.5x100 cm column, 1-2 ml for 1.6x100 cm column) were applied the top of the column with a long glass pipette, and introduced completely into the gel. The column walls were washed with about 2 ml buffer, prior to the start of fraction collection (4 to 5 ml/fraction).

G. Electrophoretic Techniques

1. Gradient Gel Electrophoresis:

Electrophoresis (Pharmacia Apparatus) of LDL-containing samples (less than 20 μg protein) was carried out in precast 2-16% polyacrylamide gradient gels (PAA 2/16; Pharmacia Fine Chemical) using buffer (pH 8.3) containing 0.09 M Tris-0.08 M boric acid, 27 mM EDTA, and 0.12 mM merthiolate. Gels were pre-electrophoresed (125V, 15 min) prior to loading samples. Approximately 20 μl samples, containing 1 part by volume of a 40% sucrose solution, 0.01% bromphenol blue, and 1.75 mg/ml thyroglobulin (internal standard), were applied. Routinely, experiments were designed so as to apply twelve lipoprotein-containing samples and one reference protein mixture (Pharmacia HMW protein mixture), to each gel.

Samples and reference proteins were pre-electrophoresed (10 min each at 25V, 50V, and 75V) for entry of samples and reference proteins into the gel. Then 4 µl diluted (1:10 vol:vol) carboxylated latex beads (Dow Diagnostics), used for particle size calibration, was applied to the reference protein lane.

Following electrophoresis (125V constant voltage, 24h, $10^{O}C$ in 1980-83, $15^{O}C$ in 1983-84), the gels were fixed (0.5 h) in 10% sulfosalicylic acid, stained for protein (1h) in 0.04% Coomassie G-250 in 3.5% perchloric acid, and destained in 5% acetic acid. For lipid staining, the gels were heated (55°C, 4-10h) in 0.04% Oil Red O in 60% ethanol immediately after electophoresis and destained in 5% acetic acid. The gels were then scanned with a model RFT densitometer (Transidyne) at 603 nm (protein stain) or 530 nm (lipid stain).

Electrophoresis of HDL or DC was carried out in precast 4-30% polyacrylamide gradient gels (PAA 4/30; Pharmacia) in a manner similar to that described for 2-16% gels. The reference protein mixture, used for particle size calibration contained thyroglobulin (hog thyroid, 170A), apoferritin (horse spleen, 122A), catalase (beef liver, not used for particle size measurements), lactate dehydrogenase (beef heart, 81A), and bovine serum albumin (71A). Area under peaks (protein stain) within established size ranges of normal HDL subpopulations were measured to provide estimates of lipoprotein concentration within each size range (71).

2. Agarose Gel Electrophoresis

Lipoprotein patterns obtained by using electrophoresis on agarose gels were determined according to the procedures described by Hatch et al (72).

3. SDS-Polyacrylamide Gel Electrophoresis

Apoprotein composition of samples was determined by electrophoresis (10 ma/tube, 3-4 h, or 120V/slab, 1h; $18^{O}C$) in 0.01 M phosphate buffer, 0.01% SDS, pH 7.1 (buffer C), using either uniform polyacrylamide tube gels (10% and 4%), or 2-16% (Pharmacia) polyacrylamide gradient slab gels. The gels were pre-electrophoresed (1.25 ma/tube for 0.5h, or 120V/slab, 0.5h) prior to sample loading. Samples were either delipidated with chloroform/methanol (73) or were heated ($100^{O}C$, 2-5 min) in the presence of a denaturing buffer (buffer C: 0.01 M phosphate buffer, pH 7.4, 2% SDS, 2% mercaptoethanol). Aliquots containing 10-50 µg protein were mixed with a solution containing 40% sucrose and 0.01% Bromphenol Blue (4 parts sample to 1 part dye solution) prior to loading on the gels.

Electrophoresis was stopped when the tracking dye band reached a distance of about 1 cm from the gel bottom. Frozen samples of trypsin-treated or DC-exposed LDL (typically 100 µg protein) were first lyophilized, then the major part of lipids and salts removed by several washes with acetone/water (90:1 by volume). Denaturing solution (buffer C) was added and the mixture was incubated (room

temperature, overnight). Electrophoresis under denaturing conditions was carried out, as previously described (74), in 3-27% polyacrylamide gradient gels. 40-50 μgm samples were generally applied to the gels in order to assure detection of the trypsinized LDL peptides.

The gels were fixed (40% methanol, 7% acetic acid, 10h), stained (0.25% Coomassie Blue R-250 in 45% methanol and 9% acetic acid; 1h), and destained (5% methanol, 7.5% acetic acid). Cross-linked hemocyanin (Sigma), containing five species of known molecular weight (70,000, 140,000, 210,000, 280,000, 350,000), and the Pharmacia HMW protein mixture (thyroglobulin, 330,000; apoferritin, 220,000 and 18,500; albumin, 67,000; catalase, 60,000; lactate dehydrogenase, 36,000) were applied to large pore gels (4% or 2-16% gels) as molecular weight markers. The Pharmacia LMW protein mixture (phosphorylase b, 94,000; albumin, 67,000; ovalbumin, 43,000; carbonic anhdrase, 30,000; trypsin inhibitor, 20100; a-lactalbumin, 14,400) was also used for estimation of molecular weight in the small pore (10%, 2-16%, 3-27%) gels.

H. Thin Layer Chromatography

Intactness of PC following PCV preparation was assessed by analytical TLC. Silica-coated plates (Redi Coat H; Supelco) were preheated (100°C, 1h). 200 μg PCV and 10 μl standard polar lipid mix (lysophosphatidylcholine (LPC), phosphatidylcholine (PC), phosphatidylethanolamine (PE),

unesterified cholesterol (UC); 6.25 mg/ml each; Supelco) were applied and the plates were developed in chloroform:methanol:water (140:60:10). Lipid location was visualized by charring with concentrated sulfuric acid and heating for a few minutes at $100^{\circ}C$.

Quantitative TLC was also used to evaluate any changes in phospholipid species during incubation of LDL with apo AI-PCDC. Total lipids were extracted from incubation mixtures with chloroform/methanol (2:1 by volume), as previously described (73). 150-300 µg extracted lipids and 500 µg standard lipid mix were separately applied to the plates. Following identification of the lipid spots by iodine vapor (75), LPC spot and the pooled PC, PE, sphingomyelin spots were scraped off the plates, extracted with methanol, and analysed for phosphorous (76).

I. Compositional Analysis

Protein and phosphorous were measured according to the method of Lowry (77) and Bartlett (76), respectively. Total and unesterified cholesterol were quantitated, either enzymatically (Cholesterol Reagent Set, Boehringer-Mannheim), or by gas-liquid chromatography of the N,O bis-(trimethylsilyl)-trifluoroacetamide derivative of cholesterol, according to the method of Hindriks et al (78). Triglyceride was measured enzymatically (Triglyceride Reagent Set, Boehringer-Mannheim).

$\underline{J}$. $\underline{Proteolysis}$ $\underline{of}$ $\underline{LDL}$

To study the role of intact apo B in the interaction of LDL with either PCV or DC, trypsinized LDL (T-LDL) was prepared (123). LDL (5.2 mg protein in buffer A) was incubated ($37^{\circ}C$, 2h) with trypsin (Sigma; 5:1 LDL-protein:enzyme weight ratio). Proteolysis was stopped by addition of soybean trypsin inhibitor (Calbiochem; 2 mg). Released proteolytic fragments were separated from the trypsinized LDL by gel filtraton on 6% beaded agarose gel (2.0x100 cm column, 30 ml/h, $4^{\circ}C$). Fractions containing T-LDL were pooled, concentrated (Amicon XM-100A), and used for incubation studies with PC sources.

The susceptibility of LDL (before and after interaction with PCV or DC) to proteolytic attack was examined by subjecting isolated LDL products (100 µg protein in buffer B) to limited tryptic digestion ($37^{\circ}C$, 1h to 4h, LDL-protein/enzyme weight ratio, 100:1). Immediately following proteolysis, the samples were frozen prior to analysis of peptide fragments by SDS-PAGE.

The effect of trypsin on the particle size distribution of LDL (before and after interaction with PCV or DC) was studied by subjecting the LDL (either 430 µgm protein of PCV-exposed LDL or 100 µgm DC-exposed isolated LDL) to limited tryptic digestion ($37^{\circ}C$; 0.5 h, LDL-protein/enzyme weight ratio of 5:1). Digestion was immediately followed by electrophoresis of the total incubation mixture on 2-16% polyacrylamide gels under non-denaturing conditions.

K. Assay for LCAT Activity

LCAT activity in incubation mixtures was assessed by direct measurement of cholesteryl ester formed or by using radiolabelled proteoliposome substrates (apo AI:PC:UC, 1:320:6.5 mole ratio containing 1.2 μcurie 14C-UC per ml) according to a previously reported method (79). When required, LCAT activity was inhibited by addition of either DTNB, PCMPS, or PX.

IV. RESULTS

A. Application of Gradient Gel Electrophoresis to Analysis of Low Density Lipoproteins

Electrophoresis in gels, which have a higher viscosity and frictional resistance relative to liquid media, separates particles primarily according to particle size not according to charge. In gradient gel electrophoresis, particles migrate through a gel network of progressively decreasing effective pore size and are retarded as they approach their exclusion limit. For globular proteins which are not highly asymmetrical or flexible, the exclusion limit correlates with the particle's hydrodynamic volume and can be used to determine the Stokes radius of the particle.

Prior to study of LDL polydispersity with slab gradient gels (2-16% polyacrylamide), several parameters were evalutated for their potential effects on the determination of particle size.

1. Electrophoresis Time

For estimation of LDL particle size by GGE, it was necessary to establish the time required for particles in the size range of LDL to reach their exclusion limit. Thus, the relationship between migration distance and electrophoresis time of major LDL components and calibration proteins was determined.

LDL (within d<1.063 g/ml plasma fraction) were obtained from plasma of subject KT. The GGE pattern of KT's LDL after 24h electrophoresis (Fig 4A) consisted of one major (230 migration units, mu) and three minor (174, 261, 288, mu) components. Figure 5 shows that the migration distance of the peaks of both the LDL and the calibration proteins increased between 24h and 36h, and subsequently a plateau was reached between 36h and 48h. Longer electrophoresis times (between 48h and 68.5 h) surprisingly resulted, once again, in an increase in migration distance with time and were associated with a decrease in area under the LDL peaks (Fig 4B and Fig 4C). This observation indicated that alterations in gel properties (e.g. increased porosity) and/or lipoprotein properties occurred at electrophoresis times greater than 48h, leading to apparent loss of protein species from the gel into the chamber.[*]

Since particles approached their exclusion limit between 24h and 36h, and the rate of change in migration distance (between 24h and 36h) was similar for LDL (3.250 mu per h; Fig 5) and for standard proteins (thyroglobulin, 3.500 mu per h; apoferritin, 3.417 mu per h), a convenient electrophoresis time of 24h, was chosen for estimation of

*For both the LDL and calibration protein standards, increased protein staining material at the top of the gel occurred together with decrease in area under the GGE peaks (Fig 4B). Because the buffer was recirculated in the chamber, the appearance of staining material at the top of the gel may have been due to re-electrophoresis of protein material lost into the chamber.

Fig 4. The effect of electrophoresis time (24h, Fig 4A; 68.5h, Fig 4B) on the gradient gel electrophoretic (GGE) pattern of LDL (within the plasma d<1.063 g/ml fraction) and on the areas under the LDL peaks (Fig 4C). The migration distance in arbitrary units (mu) is indicated with each peak. An internal standard protein (thyroglobulin; mu: 461 in Fig 4A and 542 in Fig 4B) was added to each sample. GGE was performed on 2-16% gels and the areas (between arrow heads) under LDL peaks were measured.
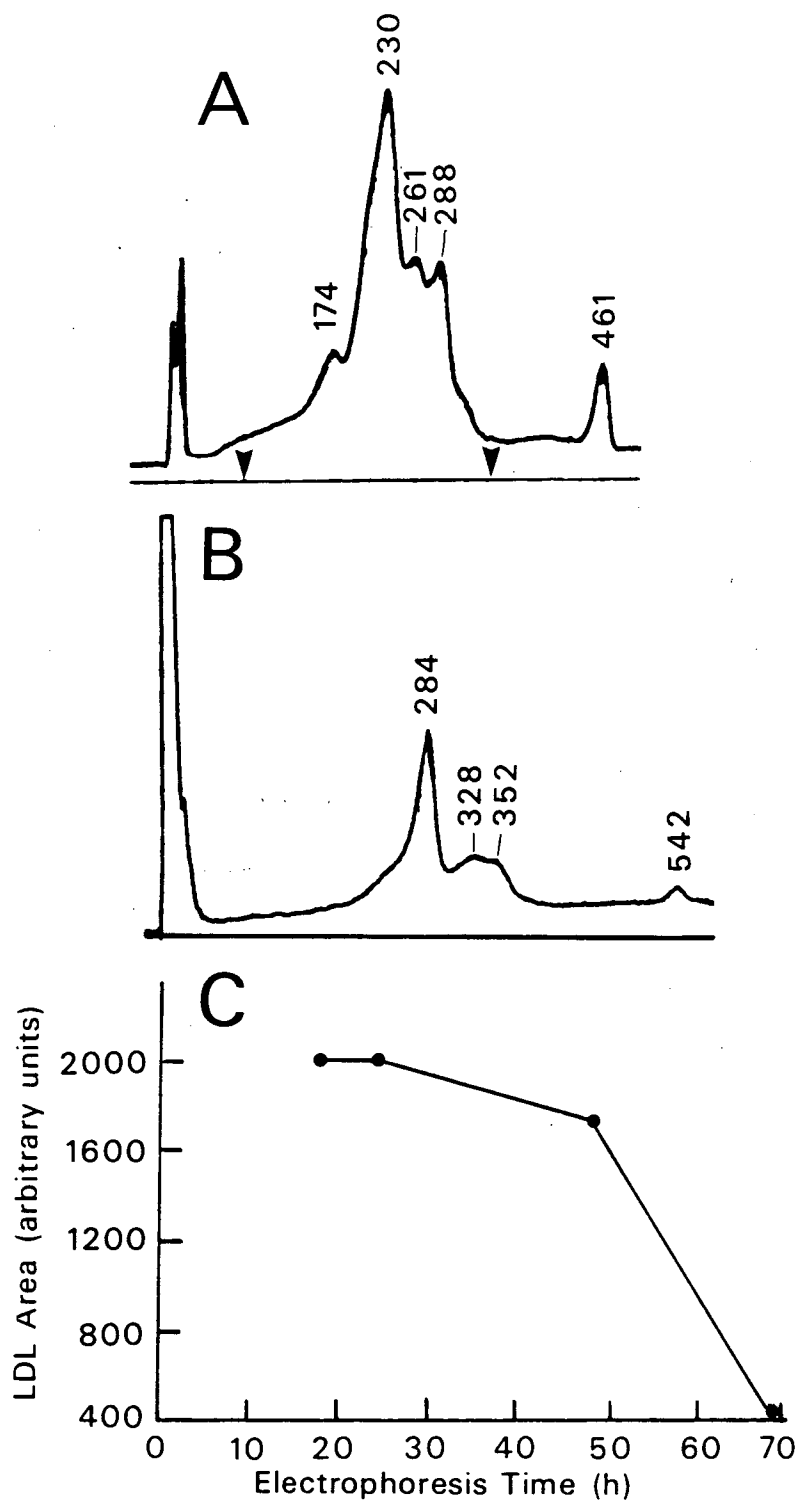
XBL 848-7869

Fig 5. Migration distance (in mu) of native LDL (N—LDL, sub-
ject KP), trypsin-treated LDL (T-LDL, subject BG; see
Methods, section J for method of preparation), and calibra-
tion proteins as a function of electrophoresis time. Elec-
trophoresis was performed on 2-16% gels.
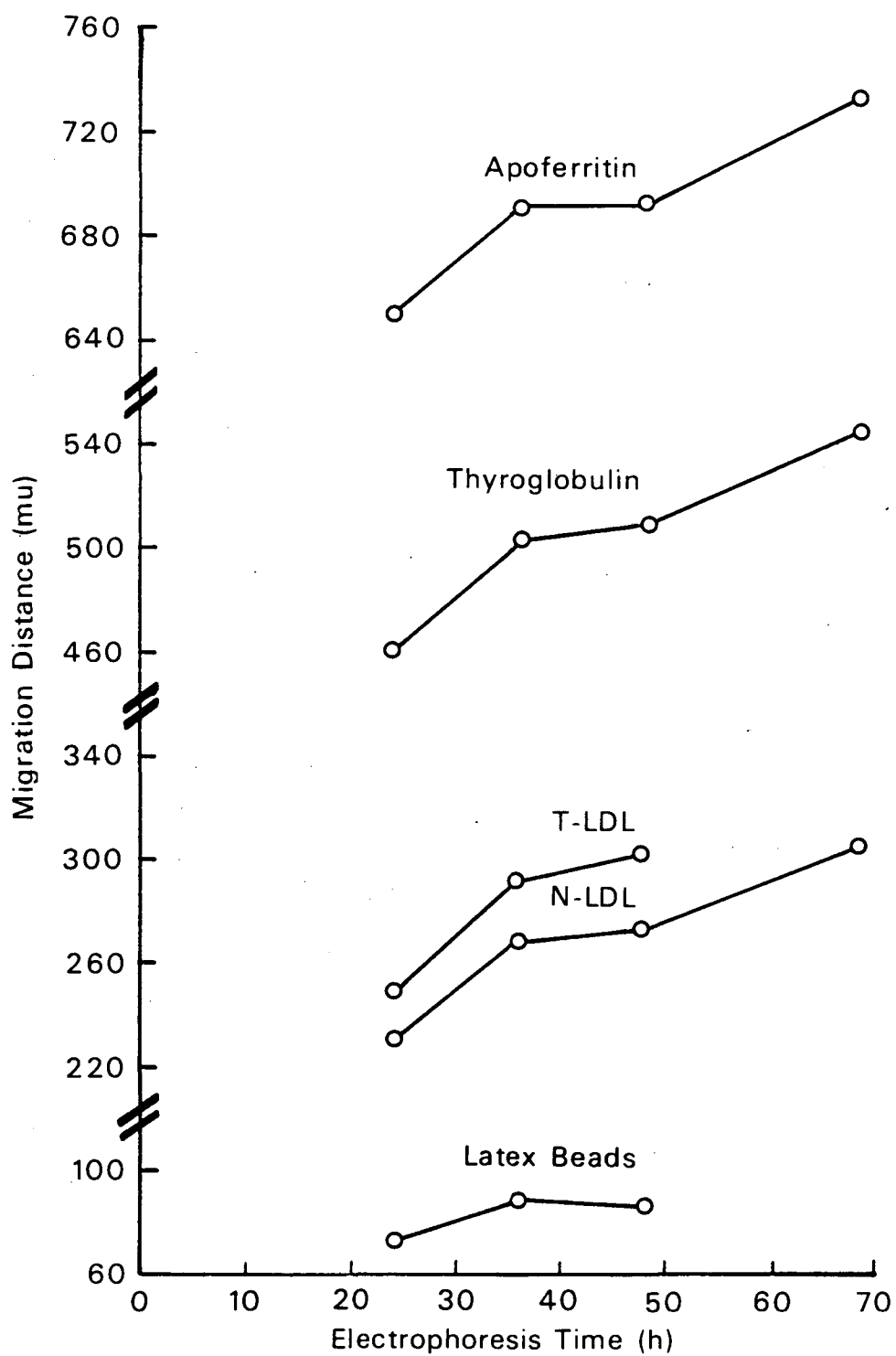
particle size for subsequent studies. Even when LDL were modified by trypsin (37°C, 1h, 5:1 LDL:enzyme weight ratio) with a reduction of about 25% of their protein content (50,123) and an increase in their negative charge, the rate of change in migration distance (between 24h and 36h) was similar to that of untreated LDL (3.250 mu per h). Thus, our choice for electrophoresis time (24h) appeared valid for estimation of particle sizes not only for untreated LDL and other globular proteins, but for modified LDL as well.

2. Particle Size Measurement

Once the electrophoresis time was chosen, studies were conducted to develop a procedure for determination of particle size, using protein and latex bead calibration standards of known size. Figure 6 shows a typical GGE pattern of a reference calibration mixture. One major and several minor peaks were noted for latex beads. The mean particle diameter of latex beads (379), measured by negative stain electron microscopy, was assigned to the major GGE peak. Of the five reference proteins (thyroglobulin, apoferritin, catalase, lactate dehydrogenase, albumin), in the calibration mixture, the latter two electrophoresed off the gel, and only thyroglobulin (mean diameter,[†] 170A) and apoferritin (mean diameter, 122A) could be used for LDL particle size measurements.

[†]Particle diameters of globular proteins were calculated from values of their diffusion coefficient and by use of the Stokes-Einstein equation.

Fig 6. Gradient gel electrophoresis (GGE; 2-16% gel) of a particle size calibration protein mixture. In this and subsequent GGE studies, electrophoresis was carried out for 24h. The ordinate is migration distance and the abscissa is absorbance at 603 nm (protein stain).

XBL 848-7879

Migration Distance

Absorbance (603 nm)

Catalase

Apoferritin

Thyroglobulin

Latex Beads
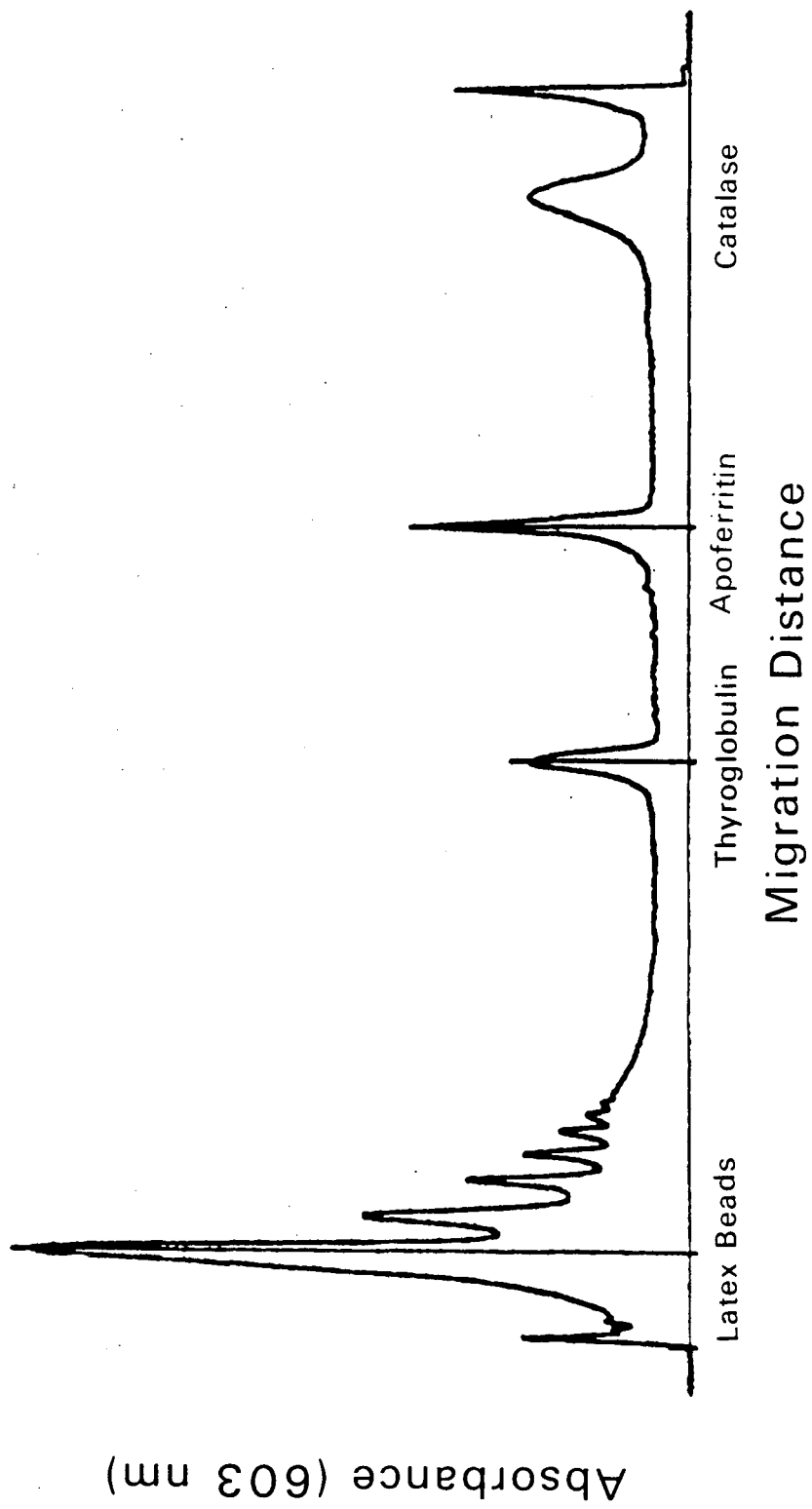
Whereas apoferritin and thyroglobulin showed little variability in the absolute value of migration distances (1981-82, [††] 619+2% mu and 438+3% mu; 1983-84, 682+3% and 489+3%, respectively), considerable variation in migration distance was noted for latex beads (average migration distance of major component, 1981-82, 60+27%; 1983-84, 78+19%). This variation may have been due to the variability from gel to gel in the low acrylamide concentration region at the top of the gel. In occasional cases where deviations in migration distance greater than 20 mu occurred relative to the average value, the average value was used for calibration purposes.

Variation in migration distance and hence particle size was observed for the same major component when applied to different regions of the gel. Those samples applied at the edges of the gel migrated less than those at the middle, possibly because of better heat dissipation at the edges than in the middle. A characteristic U-shaped pattern was observed in going across the gel (from side to side). The pattern of migration as a function of position on the gel did not affect particle size determination when the difference in the mu value (designated rmu) of the LDL component

[††]The variation in mu from 1981-82 to 1983-84 may have been due to (a) the higher temperature of the bath during electrophoresis in later years (15°C instead of 10°C), (b) possible changes in the properties of gels bought from the manufacturer, and (c) difference in sample buffers (buffer A, 1982-82 and buffer B, 1983-84; see Methods, section A for buffer characteristics).

relative to thyroglobulin (applied to each sample lane as internal standard) was used. Similarly, rmu values for the reference proteins were used for constructing calibration curves. A linear calibration curve (slope, 0.002 ± 0.001; intercept, 5.159 ± 0.012; Fig 7) and consistent size measurements ($\pm4A$, standard error) were thus obtained between gels, for the same LDL preparation.

Particle size measurements using the above calibration method were checked against particle size obtained by electron microscopy (EM). The standard error of the mean particle diameter using EM ($\pm 13A$) was larger than that ($\pm 4A$) by GGE, even when a large number of particles (n=500) were sized. Nevertheless, a significant correlation (r=0.95) was found between the average sizes measured via these methods, both in our present studies and in previous reports (88), indicating that for the most part, GGE is a valid technique for determination of particle size of untreated LDL. It should be noted that particle sizes obtained by negative stain electron microscopy were generally smaller (by about 10A to 30A) than those measured by GGE.

3. Applied Sample Concentration

The effect of LDL concentration on GGE profile was also evaluated. A range of suitable sample concentrations was determined at which consistent GGE patterns could be obtained. For this purpose, the number and rmu values of components within an LDL pattern (subject MB, Fig 8) were examined at various applied sample concentrations. At the

Fig 7. Gradient gel electophoresis calibration curve for particle size determination. Difference in migration distances of calibration proteins relative to thyroglobulin (rmu) were determined from patterns of the calibration mixture. The calibration curve in this figure was constructed from the means of rmu values obtained from 18 separate patterns (see Fig 6 for a typical pattern). The normal LDL size range (218-278A) corresponded to the rmu range of approximately 130-290.
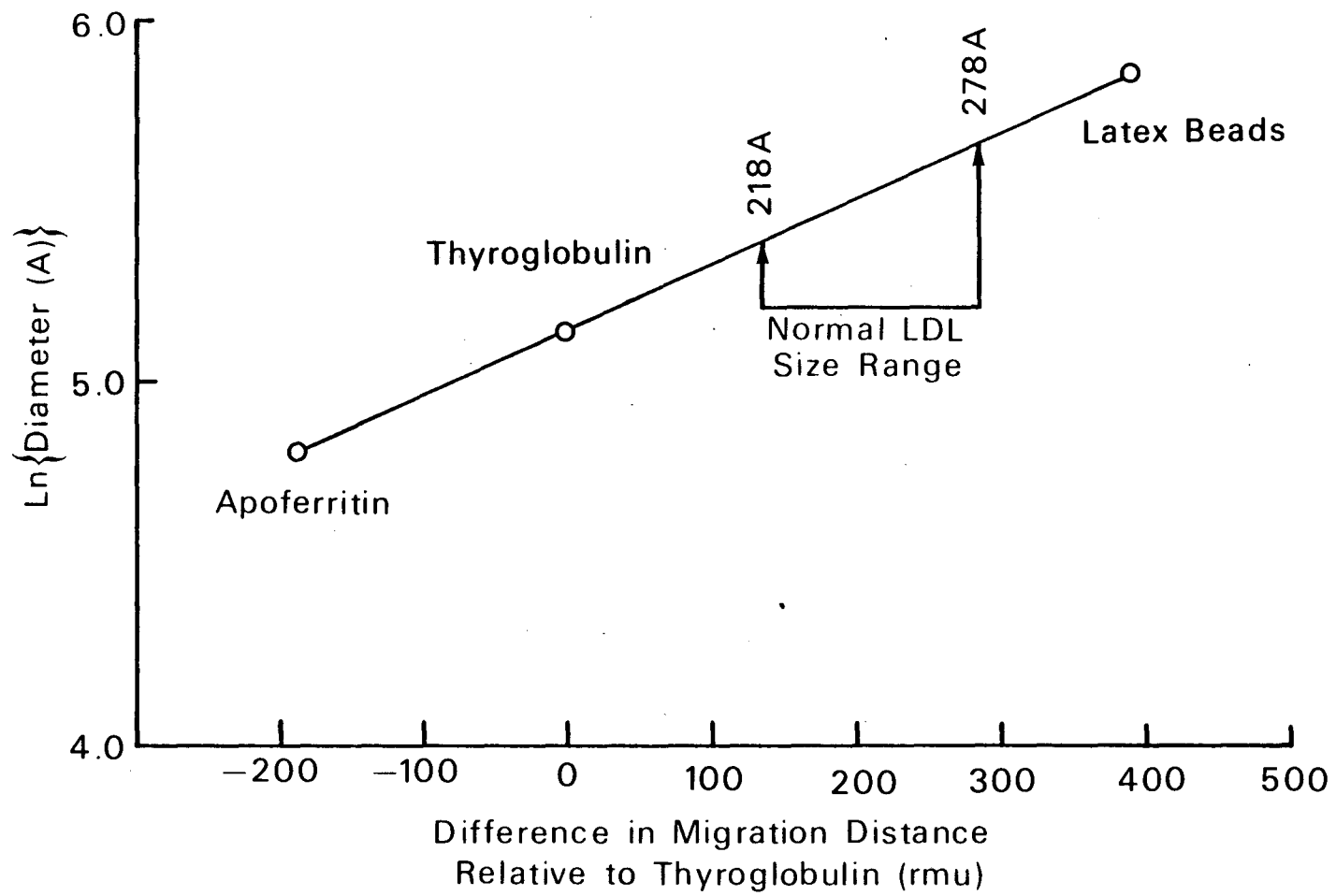
XBL 848-7884

Fig 8. Effect of applied sample concentration on gradient gel electrophoretic patterns of LDL. Aliquots of an LDL preparation (subject MB, plasma d 1.019-1.063 g/ml fraction; 7.16 mg/ml protein) were diluted with buffer B (see Methods, section A) to provide equal application volumes containing (A) 5.5 µg; (B) 6.9 µg; (C) 13.8 µg; (D) 27.6 µg; (E) 55 µg LDL protein.
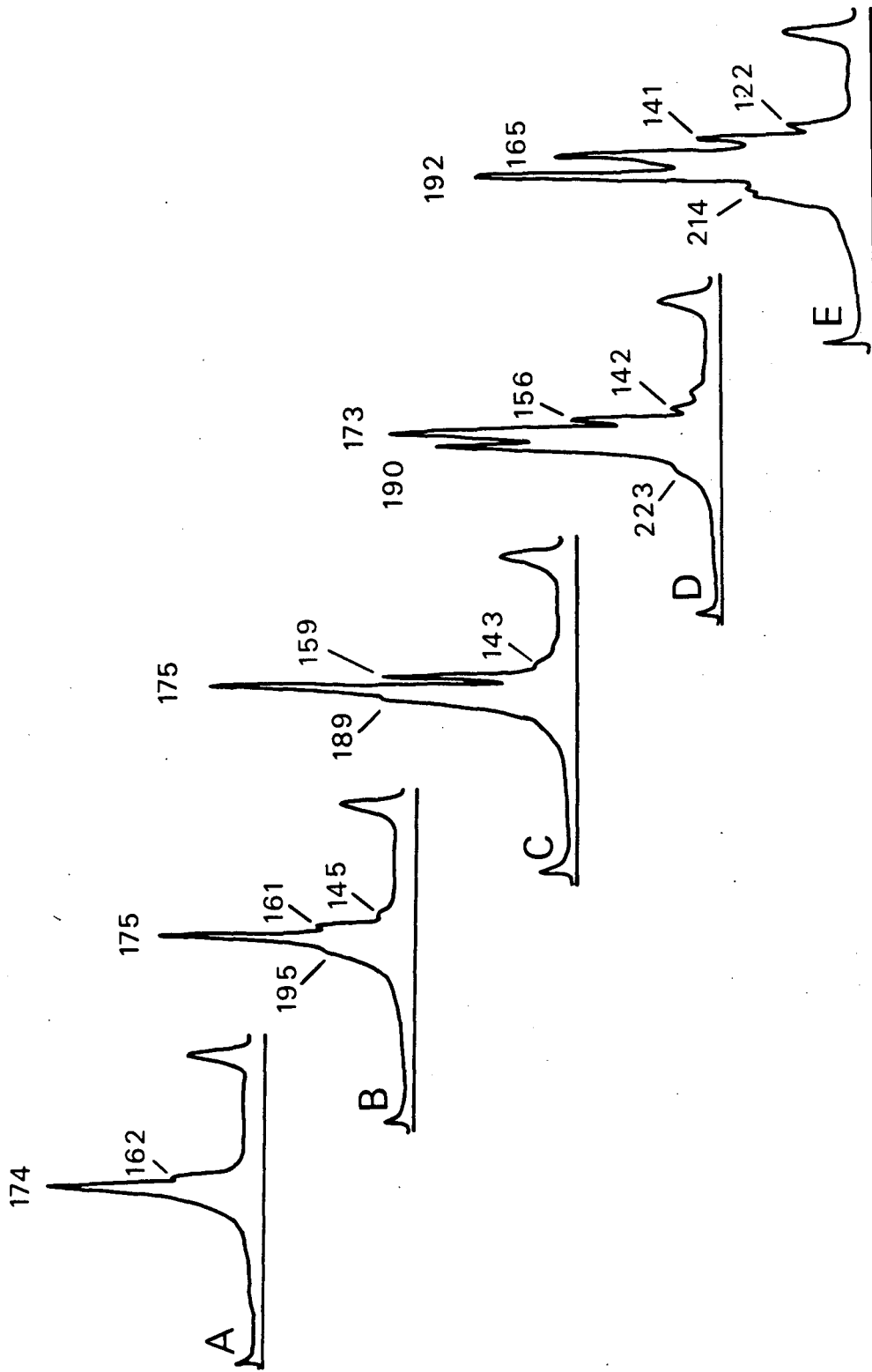
XBL 848-7889

lowest applied sample level (5.5 μgm; Fig 8A), one major peak (rmu, 174) and three minor peaks (rmu, 200, 162, 149) were observed. With increasing applied sample concentration, between 5.5 μg and 13.8 μg, the rmu values of the peaks remained essentially unchanged; and as expected, the areas under them progressively increased (Fig 8B and 8C). However, at 27.6 μg (Fig 8D), the relative contributions of the two major peaks (rmu, 190 and 173) to the LDL pattern were different from those of corresponding peaks (rmu, 189 and 175) at 13.8 μg.

To check whether the areas under the LDL peaks obtained by densitometry of gels (previously stained for protein or lipid) could be used for estimation of the content of LDL components in GGE patterns, areas under the LDL peaks (Fig 9) were plotted against applied LDL-protein concentration. A linear curve was obtained up to approximately 14 μg protein Above 24 μg protein, a plateau was reached which coincided with the appearance of an entirely different pattern (Fig 8D and 8E). Thus, sample concentrations in the range of 5-24 μg were used in all subsequent work, which insured both adequate detection of LDL peaks during densitometry and consistency of GGE patterns.

Fig 9. Area under gradient gel electrophoretic peaks of LDL as a function of applied sample concentration. Aliquots of LDL (d<1.063 g/ml fractions; subject MB, circles; subject BG, triangles) were diluted with buffer B (Methods, section A) prior to application to the gel. Densitometric scans of gels stained for either protein (solid circles), or lipid (empty symbols), were used for area determination.
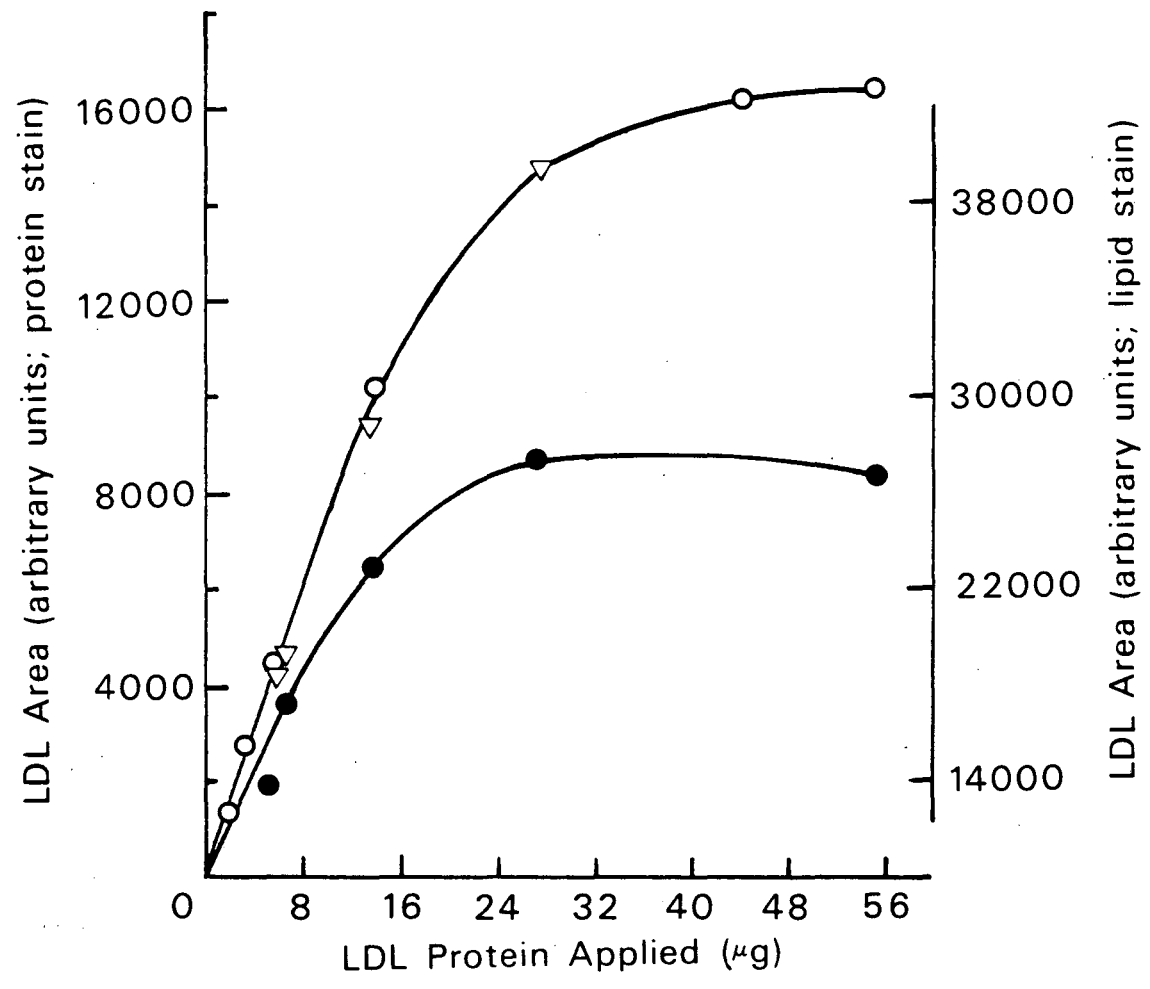
XBL 848-7865

B. Effect of Whole Plasma Incubation on Properties of Lipoproteins

Our first studies investigating interaction of LDL with analogs of surface-derived products were performed with whole plasma. Control studies investigating the effects of whole plasma incubations on LDL, in the absence of model surface products, were conducted to evaluate the contribution of factors in plasma, such as LCAT, lipid transfer proteins (LTPs) and other lipoproteins (e.g., HDL). During incubation of plasma, LCAT utilizes the PL and UC located on the surface of the major lipoprotein classes to greater or lesser degree (63,80). The CE formed by the action of LCAT is rapidly found in HDL, but with longer incubation time it also appears in LDL and VLDL (81). Interconversion from small, more dense to large, less dense HDL species has been observed during plasma incubation (82-84). This interconversion was initially explained as primarily due to the build up of LCAT-derived CE in HDL (83). However, complete inhibition of LCAT activity did not completely inhibit the interconversions (82,84). Consistent shifts in HDL distribution towards larger, less dense species was still observed but to a lesser degree in the presence of an inhibitor. The basis for this residual shift in HDL particle size and density still remains unknown, but may relate to the reciprocal exchange of CE and TG between VLDL and HDL (62,85,86), or transfer of PL among lipoprotein subclasses (85,86), facilitated by plasma LTPs.

VLDL and LDL also provide LCAT substrates and are in fact the major acceptors of LCAT-derived CE during longer term (>1h) plasma incubation (81). Thus some interconversion in their particle size and density distribution might occur, similar to that observed for HDL. In addition, it is possible that plasma factor(s) such as LTPs also contribute to interconversion among VLDL and LDL subpopulations by virtue of the transfer of LCAT product (CE) to LDL and VLDL, and the reciprocal exchange of CE in LDL for TG for VLDL. Due to the slow gradual nature of TG transfer, possible interconversions resulting from core modifications are expected to be detectable at longer (>6h) incubation times. The studies which examined the effects of plasma incubation on HDL size and density distribution did not investigate the effects, if any, on LDL physical properties. Our control studies on whole plasma incubation examined the effects of LCAT activity as well as lipid transfer by lipid transfer proteins on LDL particle size distribution.

1. Apparent Particle Size Distribution of LDL Following Whole Plasma Incubation

To study the effect of whole plasma incubation on the LDL particle size distribution, GGE pattern (Fig 10, lipid stain) were obtained on plasma from a normolipidemic human female (GL). The profile of LDL in nonicubated plasma (Fig 10A) contained a major peak (278A), at the upper bound of normal plasma LDL size range (218-278A), and three minor peaks (266A, 252A, 234A) within the LDL size range. Larger

Fig 10. Effect of whole plasma incubation ($37^{O}C$, 6h) on the particle size distribution (using 2-16% gels; ~~lipid~~ stain) of LDL (subject GL). (A) nonincubated plasma; (B) plasma incubated in the presence (dashed curve) or absence (solid curve) of an LCAT inhibitor (dithiobis-(2-nitrobenzoic acid); 2 mM).
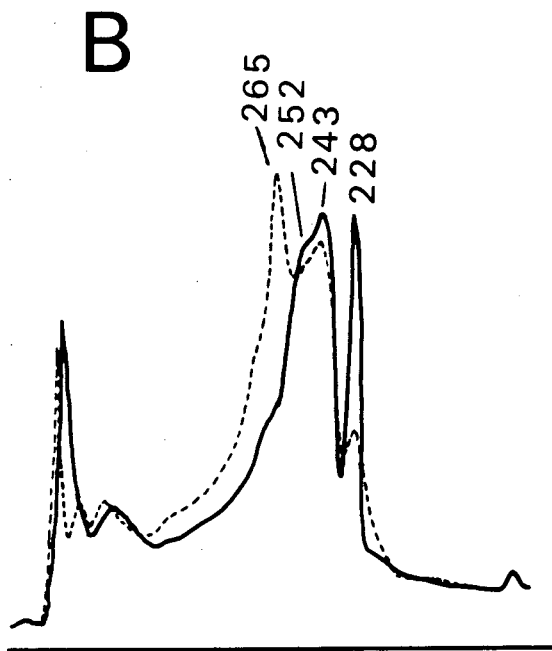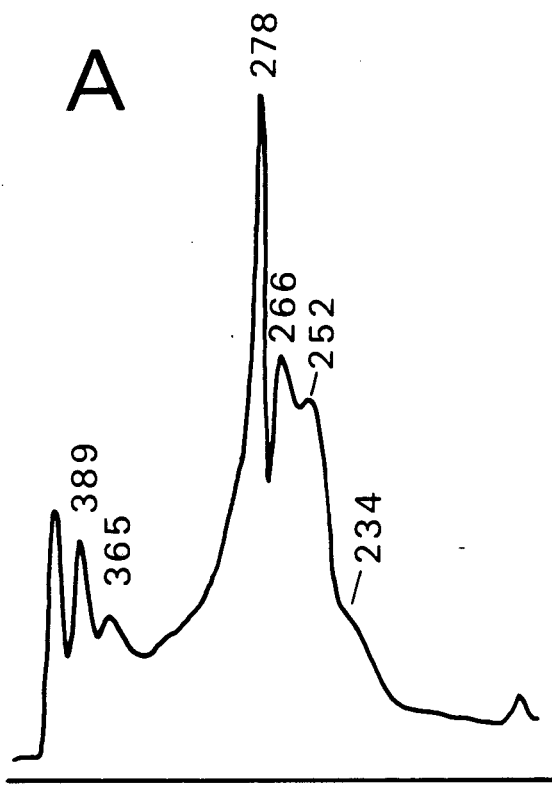
XBL 848-7870

components near the gel top (>365A) corresponded to VLDL species.

Incubation ($37^{\circ}C$, 6h) of GL's plasma resulted in a considerable change in the LDL pattern. Without an LCAT inhibitor, a marked decrease in the area (lipid stain) under the larger components (278A and 266A; Fig 10B) occurred, together with an increase in the area under the smallest component (228A). In the presence of an LCAT inhibitor, DTNB[*] similar changes in GGE pattern were observed except that the decrease in area under the larger components as well as the increase in area under the smaller components were markedly attenuated. These data suggested that interconversion of large (278-252A), major components to smaller species was primarily associated with LCAT activity. Such interconversion was probably due to loss of LDL surface components (PC, UC). With inhibition of LCAT activity, no major loss of LDL surface components occurs and less interconversion to smaller species would be expected. The interconversion noticed in GL's pattern, when plasma was incubated in the presence of DTNB, may have been due some residual LCAT activity.[†]

If the interconversion to smaller species were primarily due to LCAT-induced loss of surface components, less

---

[*]DTNB is a sulfhydryl group blocker that does not interfere with the activity of CE-TG transfer protein.
[†]The extent of LCAT inhibition was not checked in this orienting study.

change in LDL patterns might be expected in plasma which provides a higher amount of substrate PC and UC available as VLDL instead of LDL. To study the effect of VLDL level on changes in LDL properties during plasma incubation, plasma was obtained from three individuals (RM, CB, EB) with a range of TG levels. Incubations were performed using a relatively short time period (6h) to minimize changes due to TG transfer to LDL. Also, to further substantiate the GGE observations on LDL in whole plasma using lipid staining, we performed GGE on the isolated LDL (within the d<1.063 g/ml plasma fraction) and the gels were stained for protein. The lipid and lipoprotein concentrations of plasma from the three individuals used in this experiment are listed in Table 4. Plasma TG level and VLDL/(LDL+HDL) weight ratios increased in the order of RM, CB, EB. RM and CB's LDL by GGE each consisted of a large, major (RM: 268A, Fig 11, top; CB: 261A, Fig 11, middle) and a smaller minor (RM: 255A; CB, 251A) component. EB's pattern (Fig 11, bottom) had a small, major (248A) and a larger minor (260A) component.

Upon incubation ($37^{o}C$, 6h) of plasma from RM and CB, a substantial increase in the area (protein stain) under the smaller minor components occurred (RM, Fig 11, top; CB, Fig 11, middle) in conjunction with a decrease in area under the larger major peak. The small, minor (251-255A) LDL components appeared to arise from the larger major (256-268A) species. The particle size of RM's major component decreased, but that of CB's major component did not change.

Table 4 -Plasma lipid and lipoprotein concentrations (mg/dl) in subjects RM, CB, and EB.

	subject		
	RM	CB	EB
triglyceride	109	130	198
VLDL (calculated)[*]	128	173	301
LDL (ANUC)[**]	253	175	155
HDL (ANUC)[**]	351	352	163
VLDL/(LDL+HDL)[*]	0.21	0.33	0.95

[*] VLDL level was deduced from plasma triglyceride level, assuming that VLDL is 60%, LDL is 7%, and HDL is 4% triglyceride.

[**] ANUC, analytical ultracentrifugation.

Fig 11. Effect of whole plasma incubation (6h, middle column; 24h, right column) on the particle size distribution of LDL (subjects RM, top row; CB, middle row; EB, bottom row). Particle diameters of the major and minor components are marked in the patterns.

noninc   inc (6h)   inc (24h)

subject RM

271   270   268
254   250   250

subject CB

261   262   269
251   250   255

subject EB

248   248   256
260   262   265
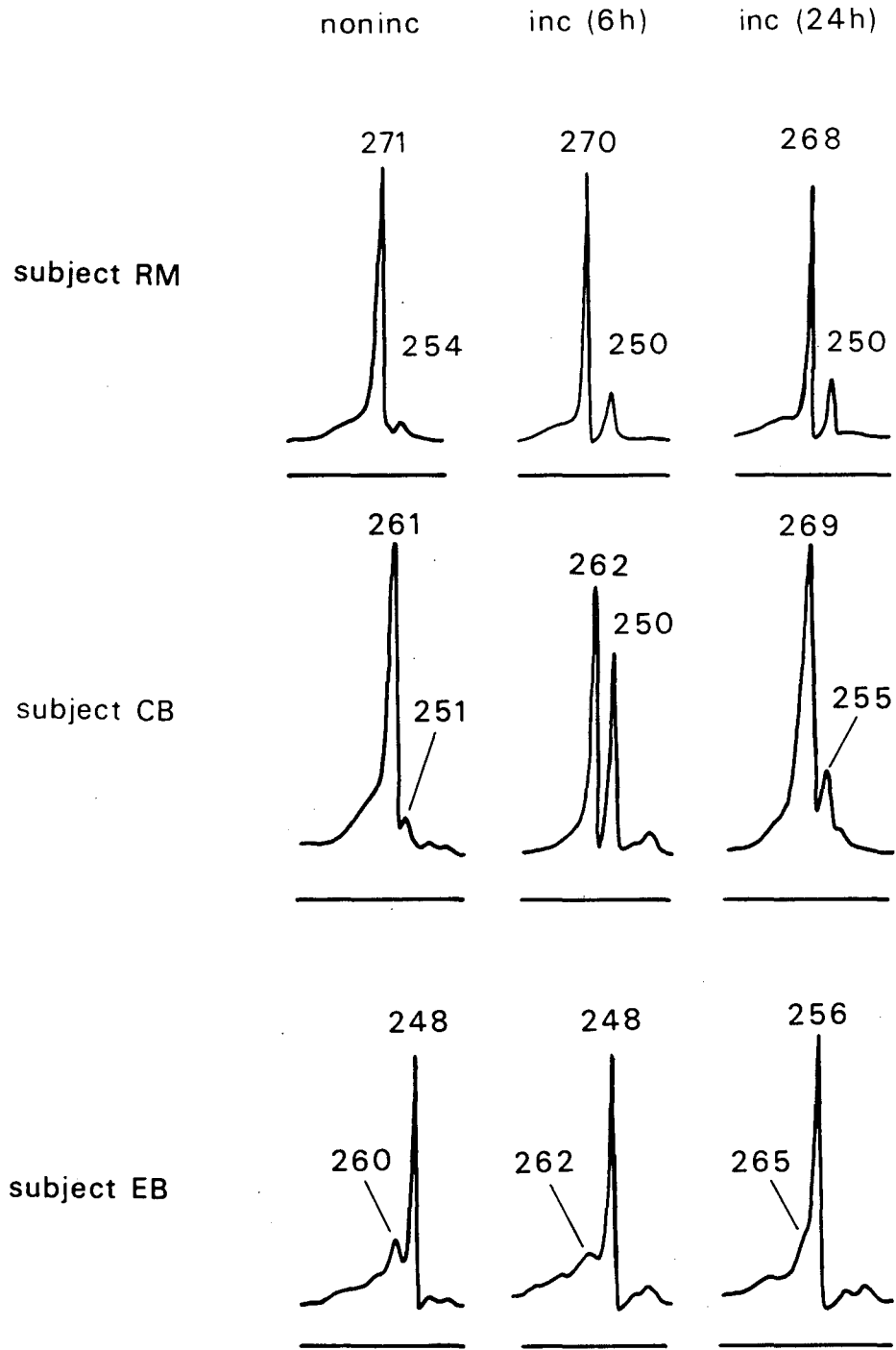
XBL 848-7875

Both the formation of the small, minor species (RM and CB) and the decrease in particle size of the large, major species (RM) were prevented when LCAT and TG transfer activities were simultaneously inhibited by PCMPS (not shown). Incubation of EB's plasma, which contained the highest TG level, showed no formation of small components in the presence of LCAT activity (Fig 11, bottom). In addition, the particle size of EB's major LDL component did not decrease at 6h as observed for CB. Thus, a trend towards more extensive change (i.e., decrease) in particle size of the major LDL component with decreasing plasma VLDL level was observed. This relationship was probably due to a more extensive depletion of LDL surface components when VLDL level and its PL and UC contribution is low. It is interesting that new, small minor components (251-255A) were formed only in plasma (GL, RM, CB) with an initially large (261-278A) major LDL component.

2. Effect of Incubation Time on Particle Size Distribution of LDL

Previous reports (81) have indicated that LCAT-dependent cholesterol esterification (associated with utilization of surface components) occurs linearly with time during the first 1h and reaches about 50% maximal level by 6h. On the other hand, exchange of TG (in the d<1.006 g/ml plasma fraction) with CE (in LDL and HDL fractions) via plasma LTPs is most apparent at longer incubation times (between 6h and 24h). Core enrichment and surface depletion

are expected to have opposing effects on LDL particle size and the LDL profile may depend on the time of plasma incubation.

To study the effect of incubation time on LDL profiles, plasma from the three subject (RM, CB, and EB) were incubated (LCAT active) for 24h. As shown in the previous section (section Bl) an increase in area (protein stain) under the small, minor component occurred at 6h. At 24h, the area under this small, minor LDL component was less in these two plasmas than that at 6h (see Fig 11). The particle size of the major component at 24h either did not change relative to that at 6h (RM, Fig 11, top), or increased (CB, Fig 11, middle). Like the LDL in CB's plasma, the major component of EB's LDL (Fig 11, bottom) also increased at 24h (256A versus 248A, nonincubated). Thus, the reduction in particle size due to surface (PL, UC) depletion at 6h is apparently compensated for, or actually overridden (depending on plasma VLDL levels), by the effect of core (CE and TG) accumulation at 24h. Prevention of both LCAT[*] and TG transfer activity by PCMPS, markedly attenuated the particle size increase at 24h (EB, not shown).

3. Particle Size Distribution of HDL Following Whole Plasma Incubation

---

[*]In these studies, we confirmed the inhibition of LCAT activity by PCMPS by showing that cholesterol esterification was less than 2% up to 24h.

Changes in LDL particle size distribution were also associated with changes in HDL size distribution during whole plasma incubation (15min to 24h). Analysis (see Methods section for method of GGE analysis) by GGE of RM's HDL distribution in nonincubated plasma (Fig 12,top) showed it to consist of 31% $(HDL_{2b})_{gge}$ (major peak at 103A), 22% $(HDL_{2a})_{gge}$ (84A), 27% $(HDL_{3a})_{gge}$ (79A), and the rest as smaller HDL species. E⁻'s HDL (Fig 13, top) consisted mainly of $(HDL_{3a})_{gge}$ (30%; 83A) and $(HDL_{3b})_{gge}$ (24%; 78A). During incubation (1h-24h) of plasma in the absence of an LCAT inhibitor, interconversion of the small HDL_3 species to the large $(HDL_{2a})_{gge}$ species occurred between 3h-6h (i.e. somewhat earlier than the time when changes in LDL patterns (not shown) were observed) which and leveled off at about 16h (RM, Fig 12, left column; EB, Fig 13, left column).

In the presence of an LCAT inhibitor (PCMPS), conversion of $(HDL_{3a})_{gge}$ to $(HDL_{2a})_{gge}$ was reduced but not prevented in RM's plasma (Fig 12, right column). In EB's plasma (Fig 13, right column), interconversion was not attenuated by PCMPS (even when full inhibition of LCAT activity was shown). Thus, major changes in HDL distribution occurred in the absence of changes in LDL distribution during incubation (3h-24h) of plasma with PCMPS, suggesting that factors other than LCAT and TG transfer protein (inhibited by PCMPS) can alter HDL patterns. Similar shifts (in the absence of LCAT activity) in the HDL distribution towards larger species have recently been reported (84) and

Fig 12. Effect of whole plasma incubation on the particle size distribution of HDL (subject RM). Gradient gel electrophoresis (4-30% gel; protein stain) was performed on HDL (plasma d 1.063-1.20 g/ml fraction) following incubation ($37^{O}C$; 3h, second row; 6h, third row; 24h, fourth row) of whole plasma either in the absence (-PCMPS, left column) or presence (+PCMPS, right column) of an LCAT inhibitor (p-choloromercuriphenyl sulfonic acid, PCMPS, 2 mM). The pattern of nonincubated HDL (first row) is also shown. Migration intervals of human plasma HDL subpopulations (HDL_{2b}, HDL_{2a}, HDL_{3a}, HDL_{3b}, HDL_{3c} (71)) are indicated.

noninc
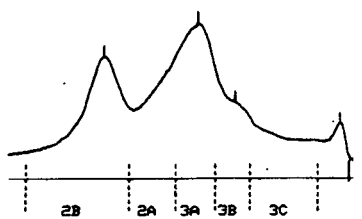
−PCMPS　　　　　　+PCMPS
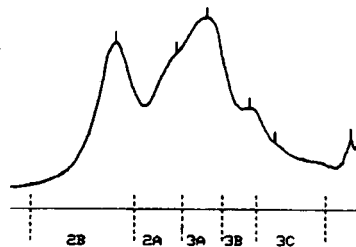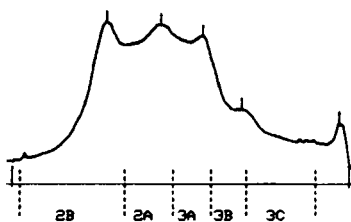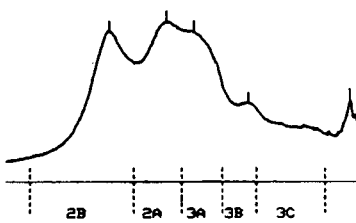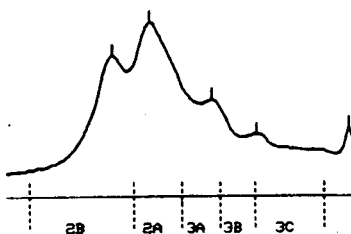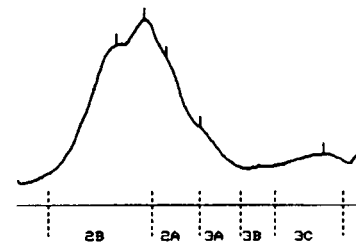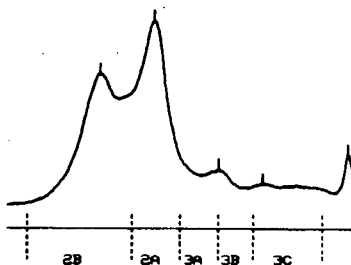
inc (3h)

inc (6h)

inc (24h)

XBL 848-7880

Fig 13. Effect of whole plasma incubation on the particle size distribution of HDL (subject EB). See legend to Fig 12 for details.

noninc
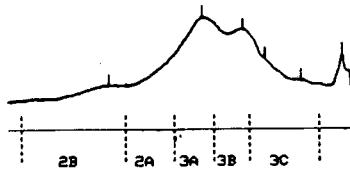
−PCMPS   +PCMPS

inc (3h)
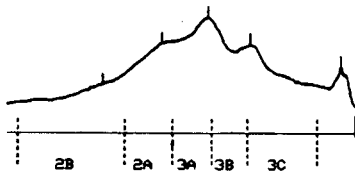
inc (6h)
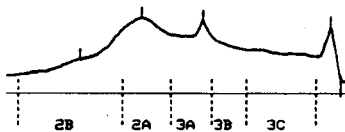
inc (24h)
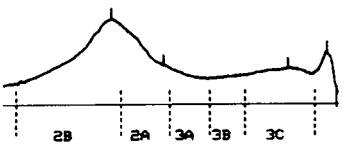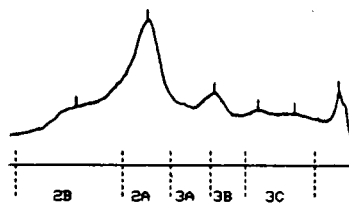
XBL 848-7885

linked to the action of a heat-labile protein in plasma. In another report (86) it has been shown that PL transfer protein (PLTP) of plasma is the only heat-labile LTP which also accelerates HDL transformation to larger, less dense species. Therefore, PLTP may be involved in alterations observed in HDL particle size distribution during incubation of plasma with PCMPS. If this assumption is correct, it is interesting that such an interaction (with PLTP) seemingly had no effect on LDL size distribution.

4. Isolation and Chemical Characterization of LDL Following Whole Plasma Incubation

We next evaluated whether the changes in LDL particle size distribution during plasma incubation were associated with changes in other LDL properties, such as hydrated density. We investigated LDL after 6h plasma incubation during which the TG-transfer effect on the LDL pattern was minimal. Isopycnic density gradient ultracentrifugation (Z-grad; see Methods, section E1) was performed directly on plasma from subject GK, who had a large (272A), major LDL component (Fig 14A). Minor components (264A, 256A, 248A) were also present in the GGE pattern of GK's LDL. Incubation (37°C, 6h) of this plasma resulted in a profile with one major (267A) and three minor (257A, 251A, 238A, Fig 14B) components. As expected, an increase in area (protein stain) under a small (251A) minor component occurred and the particle size of the major component decreased following plasma incubation. Inhibition of LCAT (but not LTPs) by PX prevented these

Fig 14. Effect of whole plasma incubation on the particle size distribution (2-16% gel; protein stain) of LDL (plasma d<1.063 g/ml fraction; subject GK). Gradient gel electrophoretic patterns are for (A) nonincubated plasma; (B) incubated (6h) plasma.

XBL 848-7890
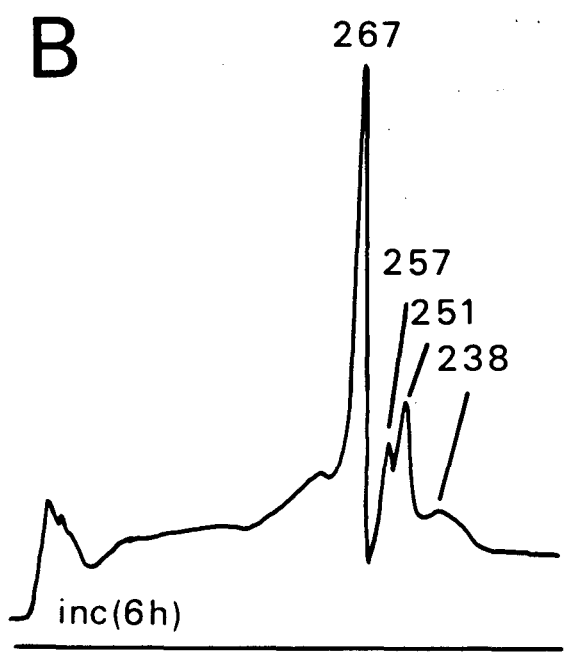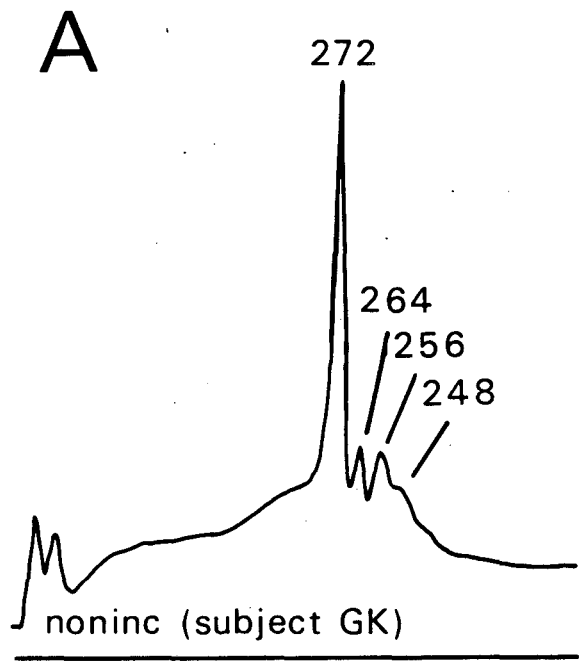
shifts in LDL pattern (not shown), supporting our notion that changes in LDL pattern at 6h are for the most part due to LCAT reaction in plasma with low TG levels.

Densitometric scans (455 nm; Fig 15, top) of the ultra-centrifugal tubes indicated a marked shift in LDL distribution towards higher densities when plasma was incubated (6h) in the absence of an LCAT inhibitor. The observations with densitometric scans were confirmed by demonstration of simi-lar shifts in protein mass measured chemically (Table 5). Thus, a decrease in protein mass within the d 1.029 frac-tion, containing large (280A) species, was associated with an increase in protein within the d 1.030 to 1.039 frac-tions, containing the newly-formed small (249A; see Table at the bottom of Fig 15), minor components. Also, the particle size of the major components (see Table at the bottom of Fig 15) within ultracentrifugal fractions was smaller for the sample from incubated plasma, consistent with the shifts observed in the pattern of the unfractionated sample. In the presence of PX, no shifts in mass distribution of pro-tein across the density gradient (Table 5) or particle size distribution of LDL were noticed.

Results of analysis of both GGE (see Table at the bot-tom of Fig 15) and compositional data (Table 5) were con-sistent with interconversion of the large (280A), major to the small (248-250A), minor components. This interconver-sion was associated mainly with a decrease in LDL surface components (PL and UC) resulting from LCAT acitivity. An

Fig 15. Densitometric scans (455 nm) of tubes containing nonincubated (solid curve) and incubated (dashed curve) plasma (subject GK). Plasma was layered beneath a linear density gradient and isopycnic density gradient ultracentrifugation was performed according to Methods, section E1. One ml aliquots were removed. The density of corresponding fractions of a background salt solution and particle diameters of the major and minor components within the gradient gel electrophoretic (GGE) pattern of each ultracentrifugal fraction are shown in the table below the scans. The GGE patterns of unfractionated LDL for this subject are shown in Fig 14. The densitometric scans of the tube containing plasma incubated in the presence of an LCAT inhibitor (paraoxon, 2 mM) and the corresponding GGE patterns of each ultracentrifugal fraction (data not shown) were similar to those of nonincubated plasma.
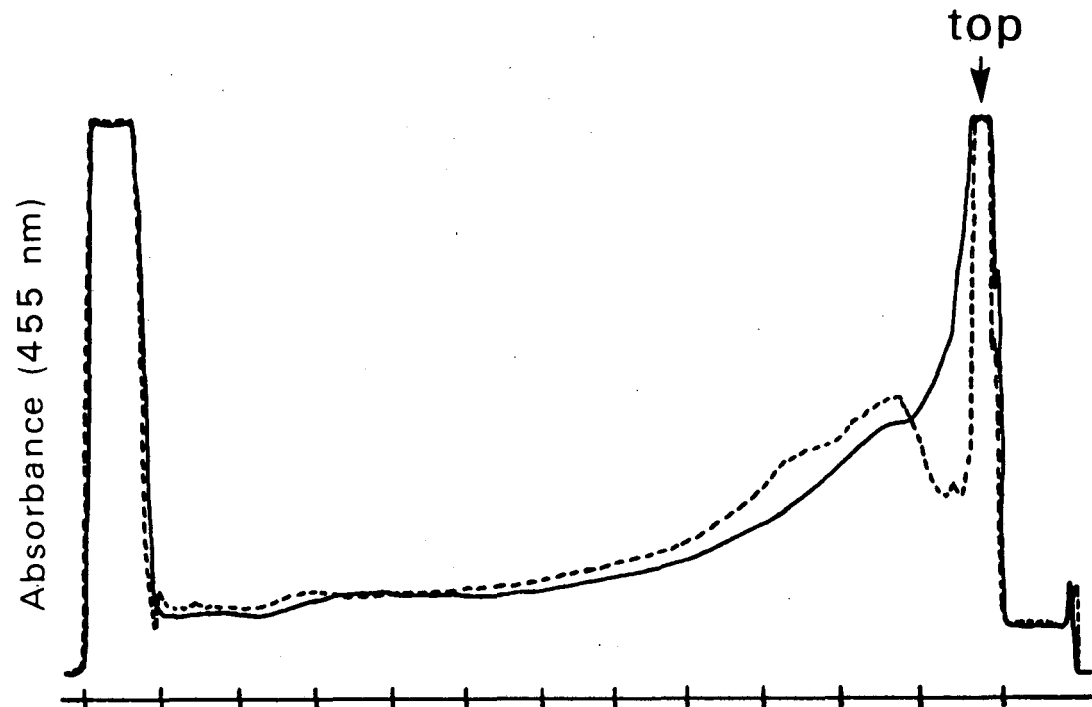
fraction	12	11	10	9	8	7	6	5	4	3	2	1	
density (g/ml)	1.075	1.067	1.058	1.050	1.046	1.043	1.040	1.038	1.036	1.033	1.030	1.029	
LDL components — major noninc	---	---	---	---	---	245	255	260	263	267	270	280	
LDL components — major inc	---	---	---	---	---	242	250	260	263	267	270	277	
LDL components — minor noninc	---	---	---	---	---	---	---	---	---	---	---	---	
LDL components — minor inc	---	---	---	---	---	---	---	---	248	249	---	---	

XBL 848-7866

Table 5 -Ultracentrifugal fractions[*]: distribution of protein (μg)

and chemical composition (weight ratios).[**]

fraction	mean density		protein	CE/P	TG/P	UC/P	PL/P
1	1.029	noninc	291.9	1.72	0.35	0.43	0.88
		inc [†]	200.1	1.85	0.40	0.34	0.88
		inc+PX	275.7	----[††]	----	----	----
2	1.030	noninc	141.4	1.50	0.12	0.45	0.88
		inc	156.2	1.68	0.14	0.35	0.75
		inc+PX	145.0	----	----	----	----
3-4	1.034	noninc	117.0	1.35	0.15	0.47	0.95
		inc	187.8	1.48	0.17	0.33	0.81
		inc+PX	142.6	----	----	----	----
5-6	1.039	noninc	46.8	1.09	0.28	0.39	1.06
		inc	63.1	1.18	0.22	0.26	0.80
		inc+PX	53.5	----	----	----	----

[*]see Fig 15 for description of the conditions. Chemical data are presented for the sum of fractions 3-4 and fractions 5-6. Fractions 7-12 contained little protein.

[**]weight ratios of cholesteryl ester/protein (CE/P), triglyceride/protein (TG/P), unesterified cholesterol/protein (UC/P), and phospholipid/protein (PL/P).

[†]PX, paraoxon, an inhibitor of lecithin:cholesterol acyltransferase.

[††]analysis not performed.

increase in content of core components of LDL in incubated plasma was apparently not sufficient to compensate for the surface loss, the size decrease, and the density increase.

It should be pointed out that even the use of a density gradient as shallow as the Z-grad did not enable isolation of the small, minor LDL products of plasma incubation from the large, major LDL component. This was unexpected in view of the size versus density relationship of nonincubated LDL components. For example, untreated LDL components larger (255-260A) than the minor (245-250A) LDL products appeared in a more dense fraction (d 1.038-1.040 g/ml versus d 1.033-1.036 g/ml; see Table at the bottom of Fig 15). Also, other particles similar in size to these minor LDL products appeared in a considerably more dense (d 1.043 g/ml) fraction. A similar observation was made when plasma from two other individuals with large, major LDL components were studied under identical conditions. Thus, these minor components of plasma incubation unexpectedly appear at a density (d 1.033-1.036 g/ml) similar to that where the bulk of the major LDL component floats, giving rise to increased size versus density polydispersity in LDL.

5. Ultracentrifugal Flotation Properties of LDL Following Whole Plasma Incubation

In view of the changes in particle size and density of LDL following plasma incubation, we checked possible alterations in their flotation rate at d 1.20 g/ml.[*] Using an empirically-derived equation[†] (unpublished data), peak S^o_f rates were calculated. LDL from plasma incubated for 6h showed a decrease in peak S^o_f (RM: 6.81, 6h, 7.40, noninc; EB: 4.76, 6h, 4.90, noninc), confirming our expectations based on decreased particle size and increased density. At 24h, RM's LDL showed a decrease (6.82) and EB's LDL showed an increase (5.58) in peak S^o_f value compared to the corresponding nonincubated LDL (RM, 7.40; EB, 4.90). These observations were consistent with the decrease (RM) and increase (EB) in particle sizes of the major LDL components that were related to plasma TG level and associated with TG transfer.

6. Molecular Weight Distribution of Apoprotein B Following Whole Plasma Incubation

The susceptibility of LDL protein to proteolysis or lipid and protein oxidation (24) has been frequently reported. Proteolysis or oxidation might occur during incubation of plasma. The consequent degradative changes in apo

---

[*]Since plasma samples were routinely fractionated at d 1.20 g/ml to analyse both LDL and HDL , analytical ultracentrifugation was performed at d 1.20 instead of the usual d 1.063 used for studying LDL.
[†]peak S^o_f = (peak $F^o_{1.20}$)(0.4815) − (7.2386)

B might result in alterations in LDL particle size. To check the integrity of LDL apoprotein (apo B) following plasma incubation, SDS-PAGE was performed on ultracentrifugally-isolated (from Z-grad) fraction containing GK's LDL. A representative SDS-PAGE pattern is shown in Fig 16 for the d 1.033 g/ml fraction. Similar patterns were obtained for nonincubated and incubated samples. A major high molecular weight species (peak MW value, 422 Kd) and some minor bands (GK, 169, 98, 74 Kd) could be seen in the pattern of fractions from both nonincubated (Fig 16, lane 1) and incubated (Fig 16, lane 2) plasma. The smaller faint bands may have resulted from proteolysis of LDL in the original plasma but this would have been of very low order. In addition, when plasma was incubated in the presence either of a protease inhibitor (phenylmethysulfonyl fluoride) or a disulfide reducing agent[*] (reduced glutathione), identical GGE patterns were obtained (data not shown) as those in the absence of these agents. This would indicate that changes in LDL particle size distribution during plasma incubation are not due to alterations in its apoprotein moiety induced by proteolysis or oxidative degradation of protein.

---

[*]The sulfhydryl groups of apo B are highly implicated in the process of oxidative degradation of LDL (30).

Fig 16. ELectrophoretic analysis of apo B within the ultra-centrifugal fraction (d 1.033) containing LDL from nonincubated (lane 1) and incubated (lane 2) plasma (subject GK). For details of ultracentrifugal fractionation see legend to Fig 15. SDS-polyacrylamide gel electrophoresis was performed on approximately 30 µg protein (see Methods, section G3 for delipidation and preparation conditions) using 4% polyacrylamide tube gels. Lane 3 contains high molecular weight standard protein mixture.

1　　**2**　　**3**

< **330 Kd**
< **220 Kd**

< **67 Kd**
< **60 Kd**
< **36 Kd**

< **18.5 Kd**
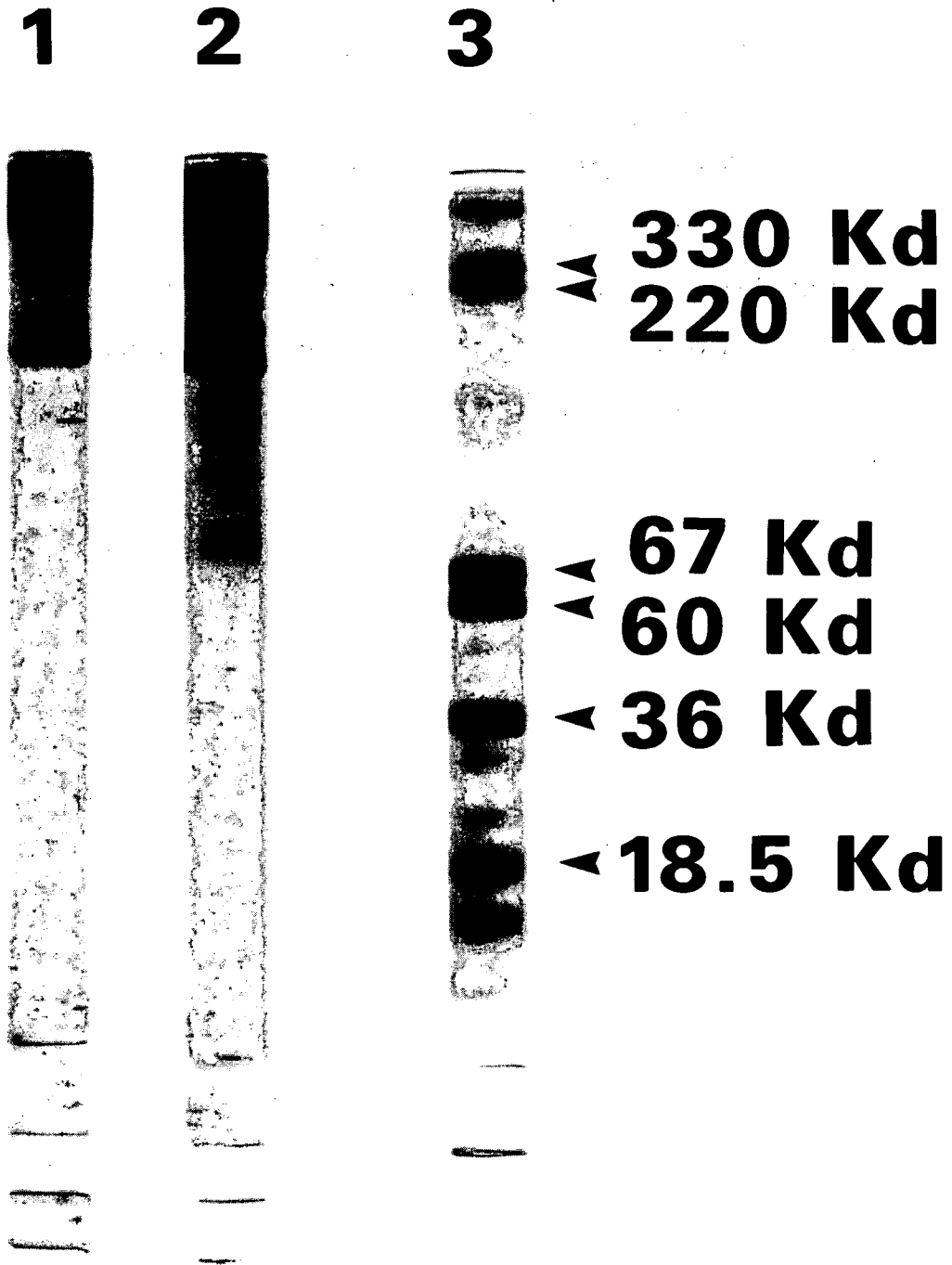
XBB 849-6740

7. Summary of Whole Plasma Incubation Studies

Plasma incubation studies elucidated the complex nature of the effect of surface and/or core modifications on LDL particle size and density distribution. At 6h, the extent of change in particle size (0-8A) of the large, major LDL components towards smaller species depended on plasma VLDL levels. The formation of the small, minor components (251-255A) occurred only in plasma with an initially large, major LDL component. These effects were associated with LCAT-related reduction in both surface components (PL, UC) at 6h. Core enrichment due to the activities of both LCAT and LTPs at longer incubation time (24h) resulted in an increase (about 9A) in LDL particle size, a process also dependent on plasma VLDL levels. Changes in LDL particle size were accompanied by changes, in the expected directions, in hydrated density and peak S^o_f rate. However, the small, minor components formed at 6h unexpectedly had a density similar to the large, major component.

In summary, the changes in LDL properties during plasma incubation depended on incubation time, plasma TG level, and the activity of LCAT and LTPs. On the basis of the information obtained from these control studies we proceeded to examine the effect on LDL properties of PL addition to plasma.

C. Incubations of LDL with PC Vesicles with or without Plasma Components

1. Changes in Apparent Particle Size Distribution of LDL Following Incubation of Whole Plasma with PCV: Effects I, II, III, and Aggregate Formation

The effect of incubation of whole plasma with PCV on LDL properties was evaluated in plasma obtained from four subjects, two of whom had high plasma TG levels (JG, 550; RM, 198 mg/dl) and two with low plasma TG levels (RM, 109; BG, 120 mg/dl). Incubations were carried out for 6h to minimize LDL size increase via TG enrichment of LDL by LTPs. Some decrease, however, in particle size of the LDL from subjects with low TG level (as described for whole plasma in the previous section) was expected. The two plasmas with high TG levels each had a small, major LDL component (EB, 248A, Fig 17A; JG, 243A, Fig 17B) and the two with low plasma TG levels each had a large, major LDL component (RM, 268A, Fig 17C; BG, 262A, Fig 17D).

Incubation (37°C, 6h) of plasma containing small, major LDL components (subjects EB and JG with high TG levels) alone produced little change in the size of the major species (EB, see Fig 11, bottom, section B1; JG, not shown). Incubation of these plasmas in the presence of increasing PL concentrations (in the form of PC vesicles) resulted in a characteristic sequence of changes in LDL properties (Fig 18). The first effect was that of no change in LDL apparent particle diameter (APD) up to a threshold PC level (0.2

Fig 17. Particle size distribution (2-16% gel) of LDL iso-
lated from nonincubated plasma. (A) subject EB; (B) subject
JG; (C) subject RM; (D) subject BG.
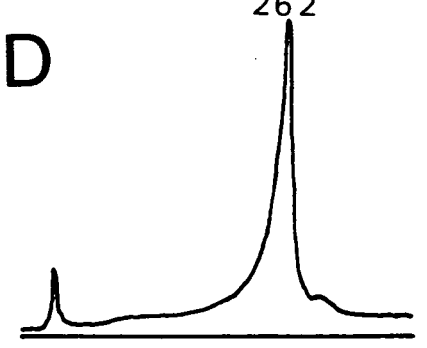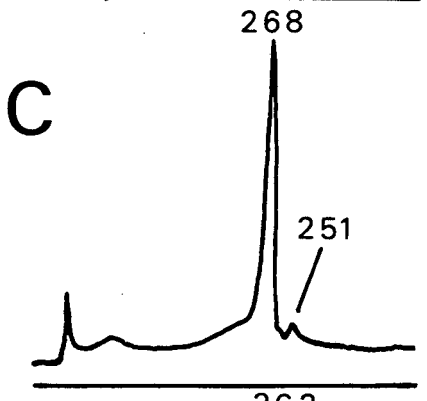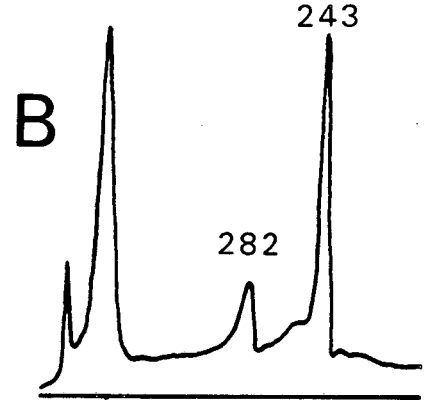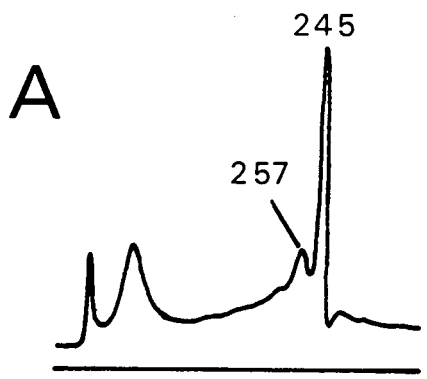
XBL 848-7871

Fig 18A. Change in apparent particle diameter (APD) of LDL (subject EB) as a function of added PC concentration. Plasma was incubated (6h) with PC and gradient gel electrphoresis (GGE; 2-16% gel) was performed on the d<1.20 g/ml fraction. Lower inset: GGE pattern (2-16% gel) of LDL from nonincubated plasma; upper inset: GGE pattern of LDL from plasma incubated with 2.13 mg/ml PC. An additional minor peak (329A, class II product) is observed at this PC level.

Fig 18B. Change in APD of LDL (subject JG) as a function of added PC concentration. Plasma (circles) and the d<1.20 g/ml fraction (triangles) were separately incubated (6h) with PC vesicles. Lower inset: GGE pattern of LDL from nonincubated LDL; upper inset: GGE pattern of LDL from plasma incubated with 2.0 g/ml PC. The component with APD 282A (probably Lp(a), lower inset) also increased in size with increasing PC level (see example in upper inset). Thin arrows in both (A) and (B) indicate threshold PC concentrations for Effect I.
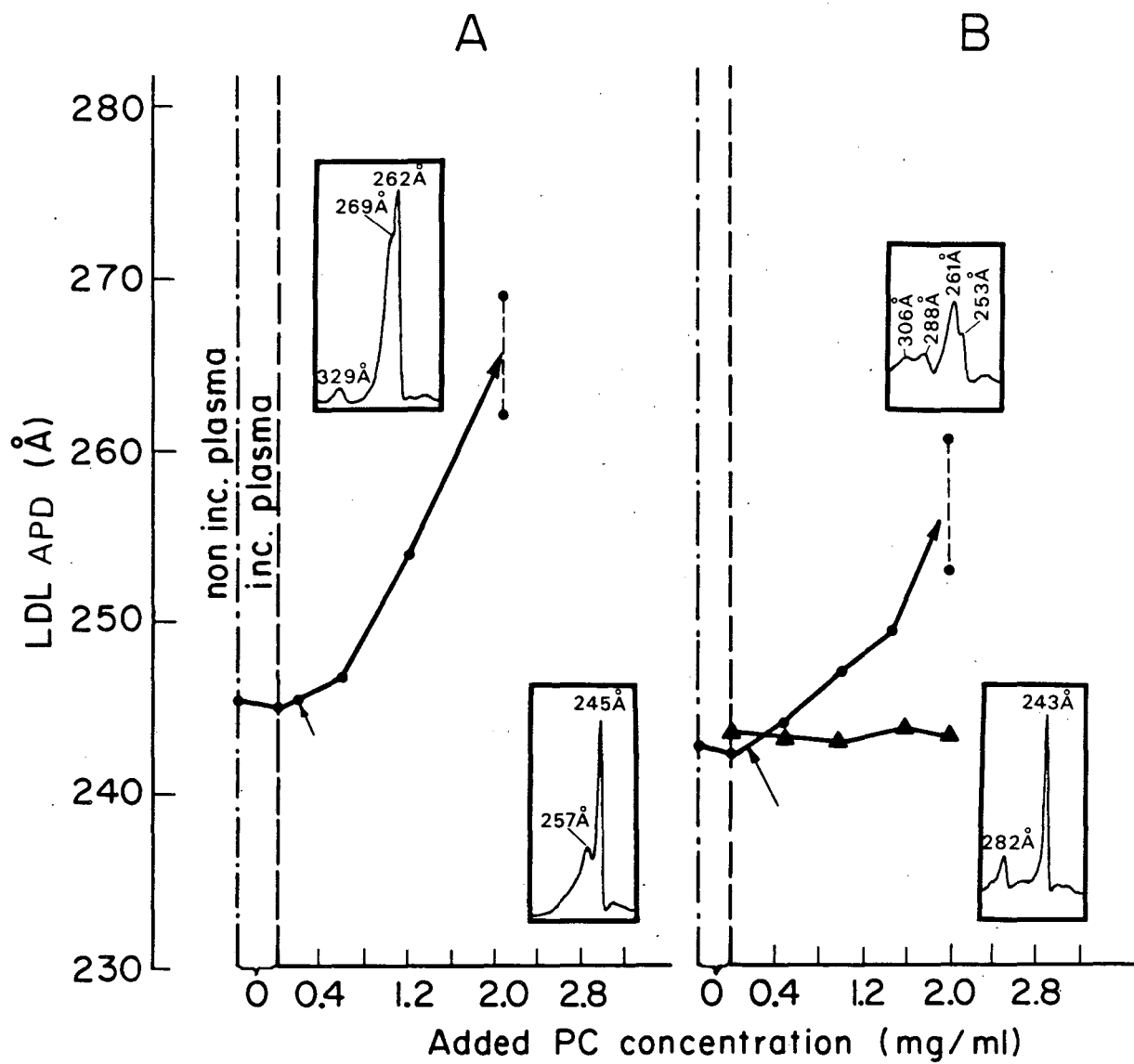
XBL 828-10912A

mg/ml, EB; 0.17 mg/ml, JG). This effect was designated Effect I. In the PC range of 0.2-1.2 mg/ml (EB) and 0.17-1.5 mg/ml (JG), a progressive increase in LDL APD occurred, which we designated Effect II. A bimodal LDL pattern was observed at higher PC concentrations in both EB (2.2 mg/ml PC; Fig 18A) and JG (2.0 mg/ml PC, Fig 18B). Whereas the component of smaller APD was the major contributor to the bimodal distribution of EB's LDL, the component with larger APD was the major contributor to the bimodal pattern of JG's LDL. At still higher PC levels (2.4 mg/ml) the bimodal pattern of EB's LDL became a pattern with a single peak (272A). The formation of a bimodal LDL pattern upon incubation of plasma plus PCV, and the transformation of this bimodal pattern to a single-peak pattern at higher PCV levels, was designated as Effect III. At E III additional minor components, larger in APD than LDL (329A, EB; 306A, JG) were observed. The LDL products remaining within the LDL size range were termed class I components and the additional minor components appearing beyond the LDL size range (290-330A) were designated class II products.

We next studied plasmas from subjects RM and BG in order to investigate whether the PCV-induced effects on the initially small, major LDL species would be observed for large, major LDL species as well. The GGE pattern of the d<1.20 g/ml fraction from subject RM's plasma (incubated (37°C, 6h) without PCV) showed an increase in area (protein stain) under the small minor components (see Fig 11, top;

section Bl), and a shift of both LDL subpopulations to smaller size (major component: 268A, nonincubated, 261A, PCV-exposed; minor components: 251A, nonincubated, 243A, PCV-exposed). The shift to smaller size was expected because of (1) the low VLDL level, and (2) the large, major LDL in RM's plasma. The decrease in size became progressively less with addition of PC to the extent that it was completely prevented at a threshold PC level of approximately 1.5 mg/ml (Fig 19A, arrow). In addition to attenuation of the particle size decrease, the area under the small, minor component decreased with increasing PCV levels. This component could no longer be observed above 1.5 mg/ml PC. The effects which comprised of either no change in LDL APD (e.g., such as those in plasma of EB and JG) or a decrease in LDL APD (e.g., such as that in plasma of RM), were both designated Effect I. Above the threshold PCV level for Effect I (RM, 1.5 mg/ml PC), a characteristic transformation of the GGE pattern was observed similar to that noted in EB and JG. Thus, in the range between 1.5 mg/ml and 2.0 mg/ml PC, LDL APD value of both the major and minor components of RM's LDL increased. This effect was similar to Effect II observed for EB and JG's LDL. With increasing PC levels (>2.0 mg/ml), a bimodal pattern was generated, apparently as part of a conversion sequence (RM, Fig 19B; BG, Fig 20). First, a shoulder developed on the major LDL peak (RM, Fig 19B, top); this was followed by build-up of the shoulder, leading to a clearly bimodal

Fig 19A. Change in apparent particle diameter (APD) of LDL (subject RM) as a function of added PC concentration. Plasma was incubated with PC vesicles and LDL (within the d<1.20 g/ml fraction) was analysed by gradient gel electro-phoresis (GGE; 2-16% gel). The thin arrow points to the threshold PC concentration. Inset: GGE pattern of LDL from nonincubated plasma.

Fig 19B. GGE pattern of LDL from plasma incubated with increasing amounts of PC. Upper: 2.0 mg/ml PC; middle: 2.4 mg/ml PC; lower: 3.2 mg/ml PC. Gel top and peak of thyro-globulin standard (added to all samples just prior to GGE) are indicated. Additional components larger in APD value than LDL (class II products) are observed at all of these PC concentrations.
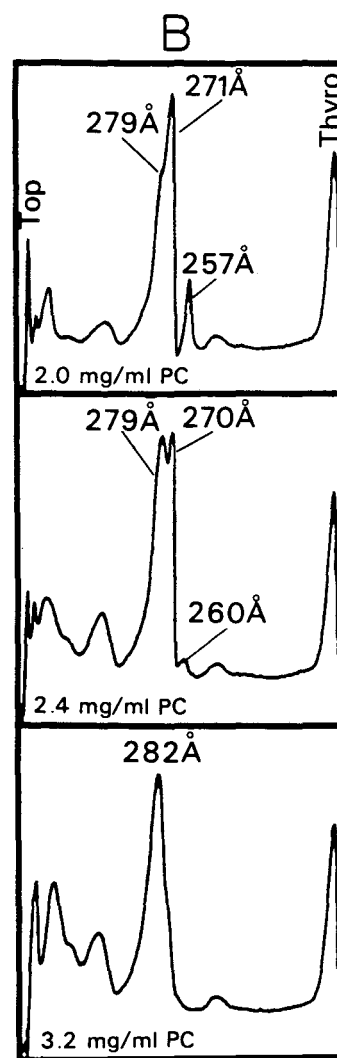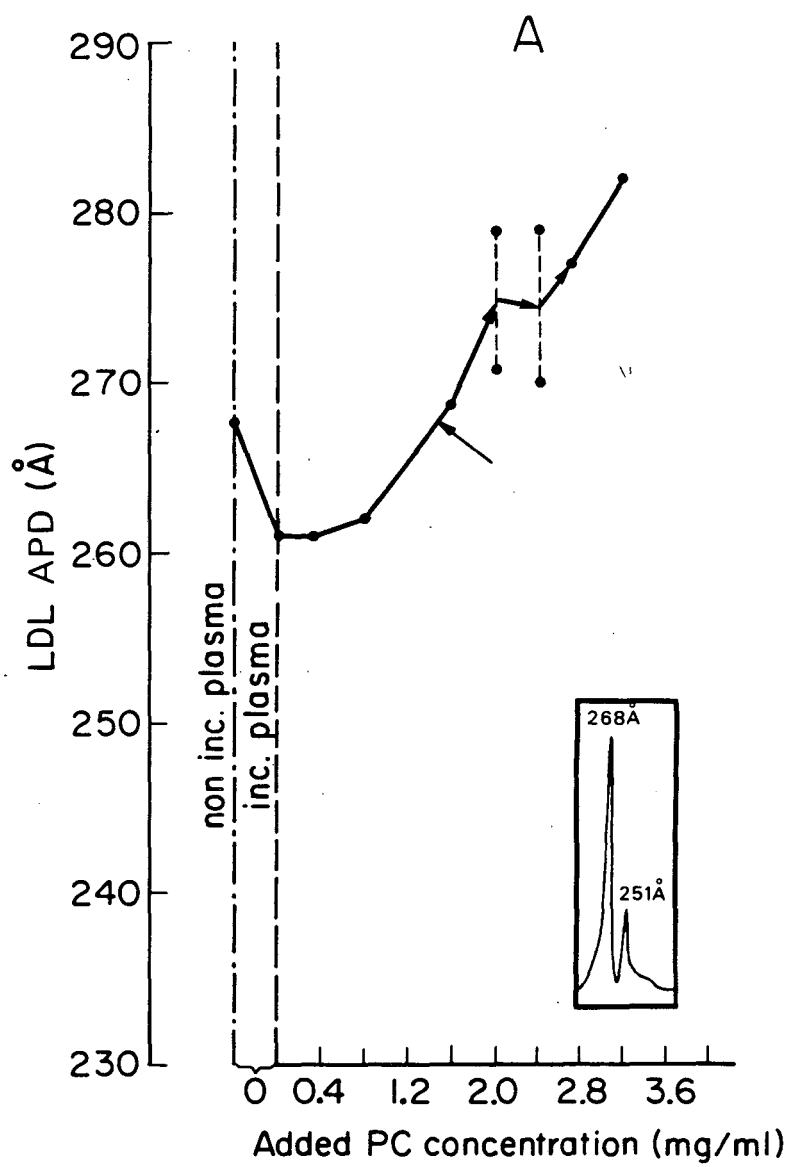
XBL 828-10911A

Fig 20 A-D. Changes in particle size distribution of LDL (within plasma d<1.20 g/ml fraction; subject BG) following incubation (6h) of whole plasma with PC vesicles. (A) nonincubated plasma; plasma incubated with (B) 2.5 mg/ml PC; (C) 3.5 mg/ml PC; (D) 4.5 mg/ml PC. The apparent diameters of components within each pattern are shown.

Fig 20E. Change in area under LDL peaks in above patterns (A-D).
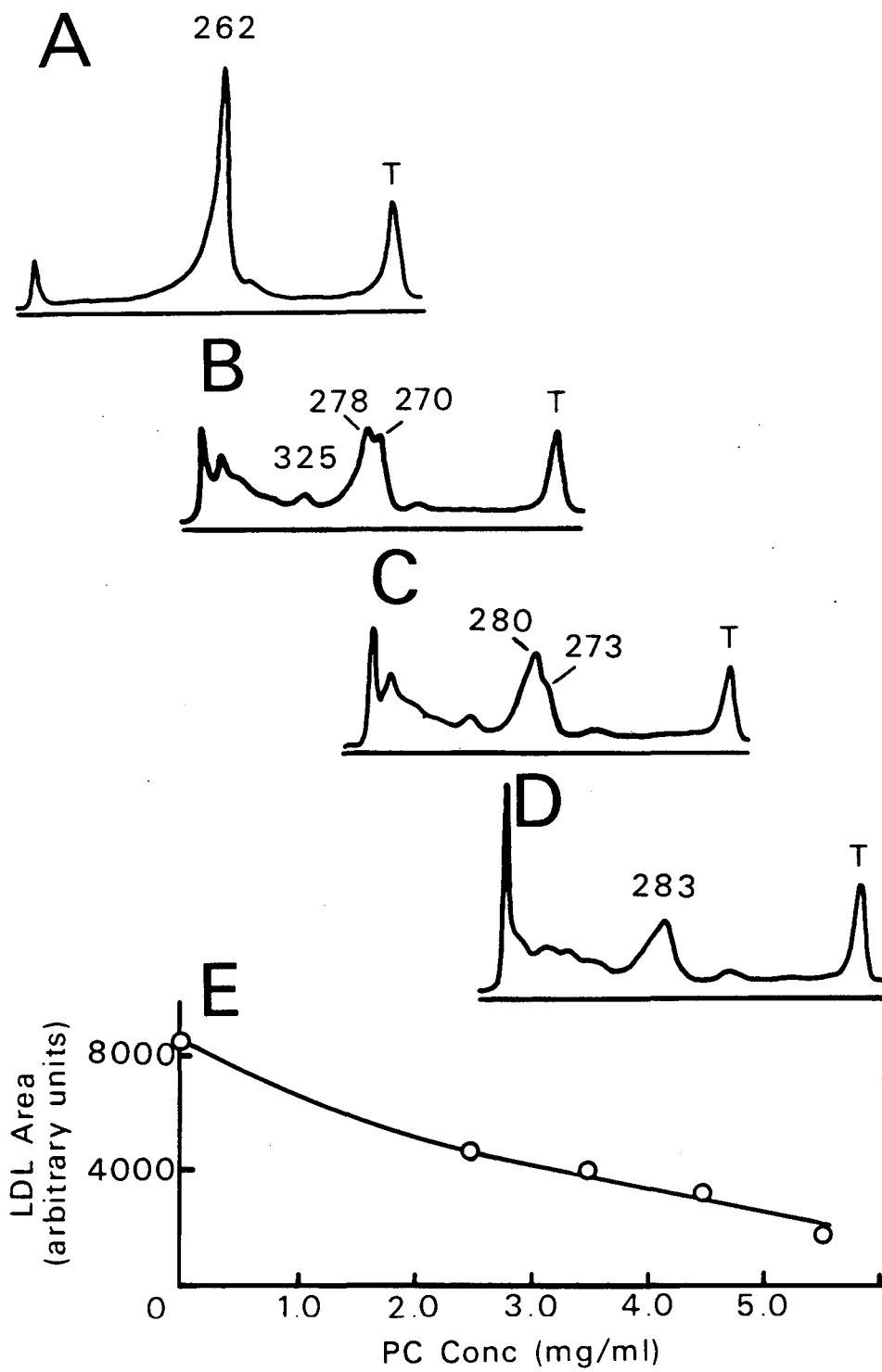
XBL 848-7891

profile (RM, Fig 19B, middle; BG, Fig 20B); then, the area under the component with smaller APD value decreased such that it appeared as a shoulder on the peak with larger APD value (BG, Fig 20C), and lastly, the profile was converted into a single peak pattern (RM, Fig 19B, bottom; BG, Fig 20D). The development of the bimodal pattern and the subsequent transformation was termed Effect III and was observed for EB's and JG's LDL as well.

At PCV levels high enough to induce Effect III, additional peaks (class II products) with larger APD values than LDL were observed. The APD range of class II products (306A to 329A) using plasma of subjects EB and JG, with initially small, major LDL components was shifted towards smaller species compared to the range of values (325-410A) in subjects (RM and BG) with initially large, major LDL components.

In summary, addition of low amounts of PCV to plasma, followed by incubation, produced effects similar to those seen during incubation of plasma alone (i.e., decrease or no change in particle size). As PC concentrations increased LDL APD value decreaed progressively. (Effect II) but the overall pattern did not change significantly. The formation of the bimodal LDL pattern (Effect III) at even higher PCV levels and the appearance of class II products appeared in both plasma with initially large, as well as initially small, major LDL subpopulations (i.e., independent of plasma TG levels). Nevertheless, the extent of increase in LDL APD

(e.g. at 2.0 mg/ml PC) was greater (about 12-20A per 6h) in plasma with initially small, than with initially large, major LDL component (about 7A per 6h). This reflected a difference in either levels of other plasma lipoproteins (e.g., VLDL, HDL) or reactivities of the large versus the small LDL subpopulations towards PL.

We next investigated the influence of plasma LDL and HDL levels on the specific PCV concentrations that defined the threshold for Effect I and Effect III (Table 6). Although Effect I occurred within a narrow range (0-0.3 mg/ml PC), the threshold value was related to plasma HDL levels. Hence, in subject RM with about a 1.8-fold higher HDL concentration (351 mg/dl) than subject EB (196 mg/dl), a six-fold higher PCV threshold concentration for Effect I (1.8 versus 0.3 mg/ml PC) was observed. However, incubation ($37^{\circ}C$, 6h) of plasma from a subject (RN: major LDL component, 255A; minor LDL component, 249A) with only 10% greater HDL concentration (220 mg/dl) compared to EB and JG resulted in an eight-fold higher Effect I threshold PCV level (2.3 mg/ml PC). This discrepancy could be resolved by considering the higher (about two to three-fold) LDL level in RN's plasma (449 mg/dl versus 270 and 155 mg/dl in JG and EB's plasma, respectively). These differences suggest that the PCV level at which Effect I occurs is a function of both HDL and LDL concentrations present in the incubation mixtures. Several previous studies have demonstrated PL uptake by HDL, and our present data suggest PL uptake by LDL.

Table 6 -Lipoprotein levels* (mg/dl) and threshold PC** concentrations (mg/ml) for Effects I and III.

	subjects			
	EB	JG	RM	RN
LDL (ANUC)*	155	270	253	449
HDL (ANUC)*	196	200	351	220
Effect I PC** threshold	0.3	0.3	1.8	2.3
LDL+HDL*	351	470	604	669
Effect III PC threshold	2.0	2.0	2.5	3.0

*Lipoprotein levels were measured from areas within schlieren patterns of LDL (d 1.063) and HDL (d 1.20) using analytical ultracentrifugation (ANUC).

**PC, phosphatidylcholine.

The PCV level at which Effect III occurred could only be approximated, due to the small number of data points taken. It was apparent, however, that higher PCV levels were required for the occurrence of Effect III in individuals who had high LDL and/or HDL levels (Table 6).

In addition to Effects I, II, and III, we noted major changes in overall pattern areas. Thus, incubation (37°C, 6h) of plasma (subject BG), with PCV (2.5 to 4.5 mg/ml PC), at high enough concentrations to induce Effect III (Fig 20B-D), resulted in a considerable reduction in area under the LDL peaks (Fig 20E). This decrease occurred in conjunction with the appearance of protein staining material on top of the gel (APD value > 400A), and was presumably due to formation of aggregated complexes of LDL and PCV as discussed in the next section.

The above studies indicated that relative levels of LDL, HDL, and PCV were important in determining the observed effects designated as Effects I, II, III, and aggregate formation. Although the influence of plasma VLDL levels on these effects was not assessed directly, it did not seem to be significant (except at Effect I). In order to delineate more clearly the role of the various plasma components in the above changes, reconstitution experiments were carried out at concentrations (Co) corresponding to plasma levels (designated as 1 Co). Reconstitution studies were done starting from the simplest system of LDL and PCV.

2. Apparent Particle Size Distribution of LDL Following Incubation of LDL with PC Vesicles: Aggregate Formation

The occurrence of each of the effects (Effects I, II, III, or aggregate formation) was checked in the simple incubation system of LDL plus PCV. To evaluate possible differences in reactivity towards PL of the large, versus the small, major LDL components, incubations were carried out using LDL preparations (the plasma d 1.019-1.063 g/ml fraction) from two subjects (JG and DR) with a small, major LDL component (JG, 243A, see Fig 17B; DR, 240A and 229A, Fig 21A), and two subjects (BG and DJ) with a large, major LDL components (BG, 262A, see Fig 17D; DJ, 268A and 260A; Fig 23A). Incubation (37°C, 6h) of LDL (JG, 0.6 mg/ml protein) without or with PCV (range, 0.2-1.2 mg/ml PC) did not result in any change in LDL particle size (Fig 23A, empty circles). Instead, as PCV levels increased, the area under LDL peak decreased progressively (Fig 23B, empty circles). This occurred together with the appearance of protein staining material at the top of the gel and was consistent with our previous observation (87) of aggregation of LDL and PCV under conditions similar to present studies.

Similar to the observations on JG's LDL following interaction with PCV, we found no change in APD values of the large, major LDL components of BG (0.6 mg/ml protein) or DJ (0.3 mg/ml protein) upon incubation (37°C, 6h) without or with PCV (BG, 1.5 mg/ml PC, not shown; DJ, 0.8 mg/ml PC, Fig 22B). A decrease in area under LDL peaks associated with

Fig 21. Effect of incubation (6h) of LDL (subject DR) with or without PC vesicles on the particle size distribution (2-16% gel) of LDL. LDL was isolated by gel filtration (using 6% agarose beads; see Methods, section G2 for details) of the plasma d<1.20 g/ml fraction. (A) nonincubated LDL; (B) LDL incubated with PC vesicles (0.8 mg/ml PC); protein staining material (aggregates of LDL and PC vesicles) appeared at the top of the gel; (C) LDL incubated alone.
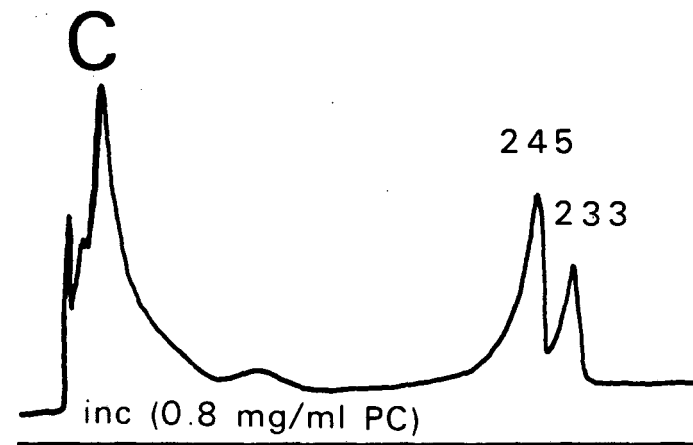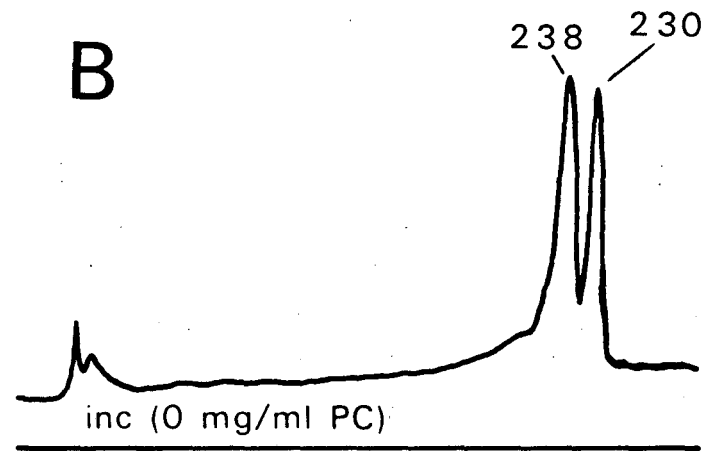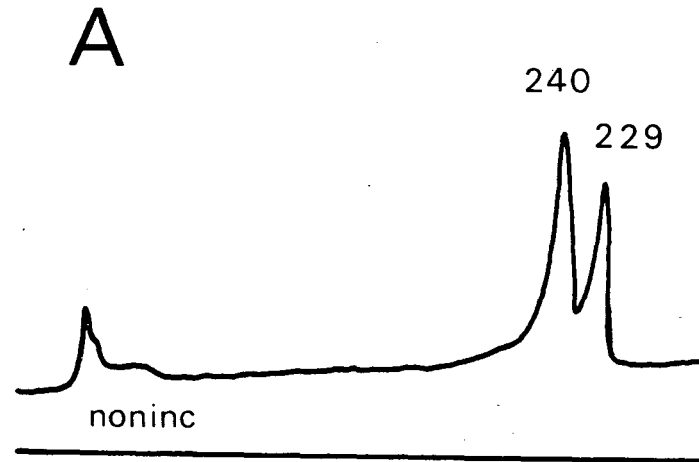
Fig 22. Particle size distribution (2-16% gel) of LDL (subject DJ; 0.3 mg/ml protein). (A) nonincubated LDL, or (B) incubated LDL (6h) with PC vesicles (0.8 mg/ml PC).

A

266

noninc

262

255

245

B

266

inc (0.8mg/ml PC)
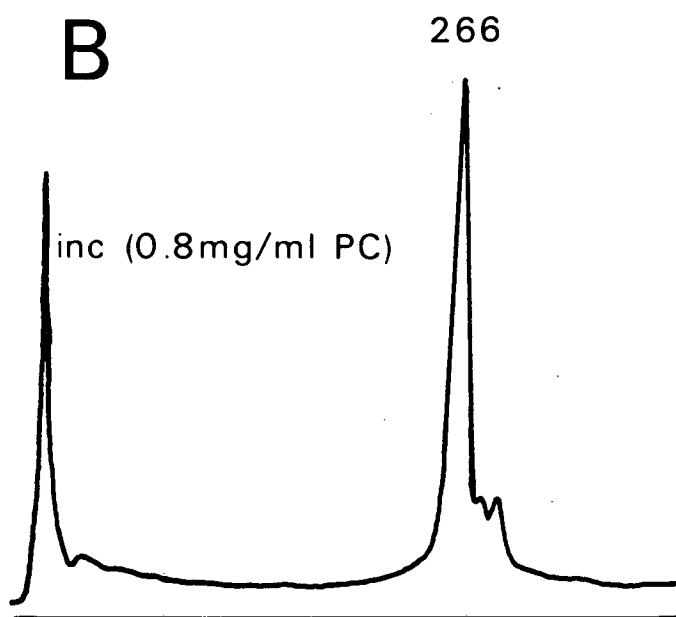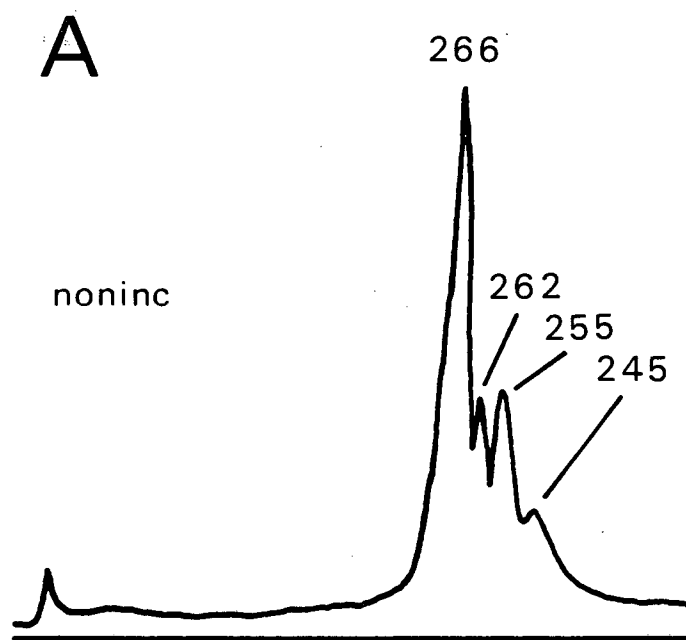
XBL 848-7876

Fig 23. PC vesicle-induced changes in: (A) LDL apparent par-
ticle diameter, and (B) area under LDL peaks. Each incuba-
tion (6h) mixture contained LDL (subject JG; approximately
0.6 mg/ml protein), PC vesicles (0.1 to 1.2 mg/ml PC),
either alone (empty circles), or in the presence of plasma
d>1.20 g/ml fraction (BF, 1 Co; solid circles), BF and HDL
(0.5 mg/ml protein, empty diamonds), BF (1 Co) and HDL (1.0
mg/ml protein, solid diamonds).
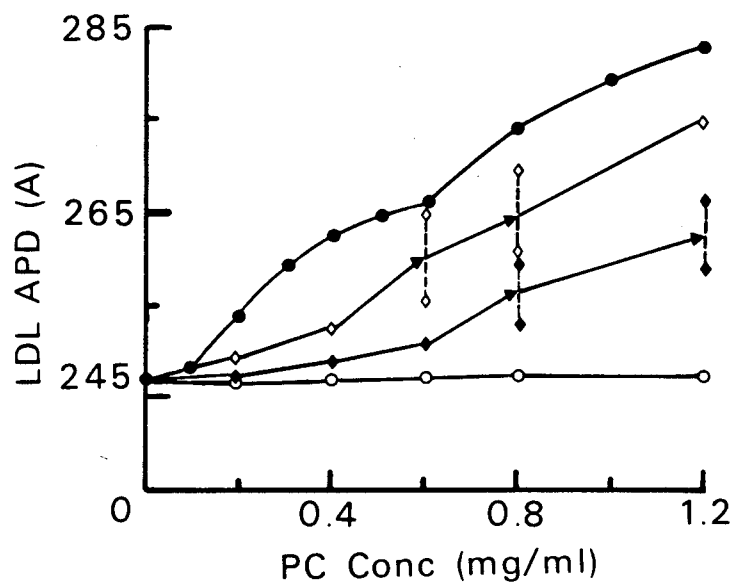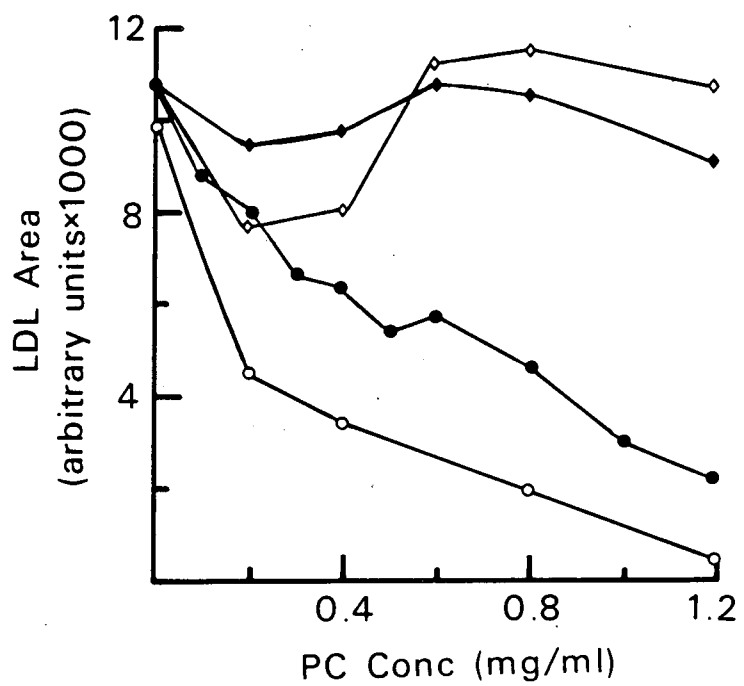
XBL 848-7881

protein staining material at the top of the gel was again observed.

In contrast to the findings on the LDL of these sub-jects incubation with PCV of LDL from the fourth subject (subject DR) resulted in a small increase in LDL APD values (nonincubated, 240A, 229A; plus PCV, 245A, 233A, Fig 22C). Since such changes were not noticed upon incubation of LDL alone (238A, 230A; Fig 22B), the changes in LDL APD values were apparently due to interaction with PCV. It should be pointed out that these changes were markedly less than those later noticed for Effect II for DR (see Table 7, section C3).

Thus, only in one (DR) out of four subjects was any PCV-induced increase in LDL APD value observed. Subject DR was severely hypertriglyceridemic (plasma TG>1000 mg/dl) and had the smallest initial LDL components (229A, 240A). The reactivity of such small LDL species towards PCV may arise from their altered composition.

3. Increase in LDL Apparent Particle Diameter Following Incubation with PC Vesicles in the Presence of Plasma d>1.20 g/ml Fraction: Effect II

Since PCV-induced changes in LDL pattern characteristic of Effect II and Effect III in plasma were not observed dur-ing interaction of PCV with LDL alone, the effect of other plasma components on the LDL pattern was evaluated. Previ-ous studies (67) on the incubation of HDL with PCV under

similar conditions showed conversion of HDL to larger, less dense species. This conversion was increased in the presence of the d>1.20 g/ml plasma fraction (bottom fraction, BF). In the present study, we examined whether BF might also induce changes in LDL pattern upon incubation of LDL with PCV and BF. We used LDL from the same subjects (BG, DJ, JG, and DR) who provided LDL for incubation studies with PCV alone.

Addition of BF to incubation (37°C, 6h) mixtures containing LDL (JG) and PCV (0.1-1.2 mg/ml PC) produced changes we have designated Effect II (Fig 23A, solid circles, and Fig 24). The increase in LDL APD as a function of PCV level (0.1-1.2 mg/ml PC) occurred in an apparent two-step manner: first, an increase in APD occurred which reached a plateau at 0.5-0.6 mg/ml PC. Further increase in PC (up to 1.2 mg/ml PC) resulted in additional increase in APD (up to 284A); this increase appeared to level off but did not reach an actual plateau. Such two-step APD increase was not seen during Effect II of whole plasma incubated with PCC. It is possible that the number of added PCV levels investigated in this incubation experiment was insufficient to resolve the steps. The mechanisms responsible for the two-step change in LDL APD was not investigated further but might involve reorganization of LDL structure at the plateau of the first step. Since the major LDL components at all added PCV levels were still within the usual LDL size range, these components were designated class I products.

At PC levels above 0.5 mg/ml, an additional minor component (308A, presumably a class II product) beyond LDL size range appeared, and a progressive increase in APD value of this product occurred with increasing PCV levels. At no PCV level was a bimodal pattern transformation characteristic of Effect III observed.

With increasing PCV levels (0.1-1.2 mg/ml PC) in the presence of BF a progressive decrease in area under LDL peak occurred (Fig 23B, solid circles), associated with increased protein staining at the top of the gel (Fig 24). However, the decrease at each PCV level was much less than that in the absence of BF (Fig 23B, empty circles).

Similar studies utilizing LDL from the other three subjects (DJ, BG, DR) clearly showed that BF is either required (BG and DJ), or considerably enhances (DR) the increase in APD value upon interaction of the LDL with PCV (Table 7). For the same LDL-PL/PCV-PL weight ratio, the extent of APD increase of a small, major LDL component (e.g., DR, 25A) was more than that (e.g., BG, 6A; DJ, 8A) of a large, major LDL component.

Thus, our data on LDL incubation with PCV and BF indicate that BF facilitates APD increase resulting in Effect II and decreases LDL aggregation with PCV. However, no transformation to a bimodal pattern (Effect III) occurs in the presence of BF and relatively high PCV levels.

Fig 24. Gradient gel electrophoresis (2-16% gel; protein stain) of incubation mixtures containing LDL (subject JG), PC vesicles (0.1-1.2 mg/ml PC), and plasma d>1.20 g/ml fraction (1 Co). The increase in APD, the decrease in staining of LDL bands, and the appearance of protein staining material at the top of the gel can be seen in this figure. Lane 1, nonincubated LDL. LDL incubated with the following amounts of PC: lane 2, 0 mg/ml; lane 3, 0.1 mg/ml; lane 4, 0.2 mg/ml; lane 5, 0.3 mg/ml; lane 6, 0.4 mg/ml; lane 7, 0.5 mg/ml; lane 8, 0.6 mg/ml; lane 9, 0.9 mg/ml; lane 10, 1.0 mg/ml; lane 11, 1.2 mg/ml PC. Lane 12, particle size calibration protein mixture: latex beads (L), thyroglobulin (T), and apoferritin (A).
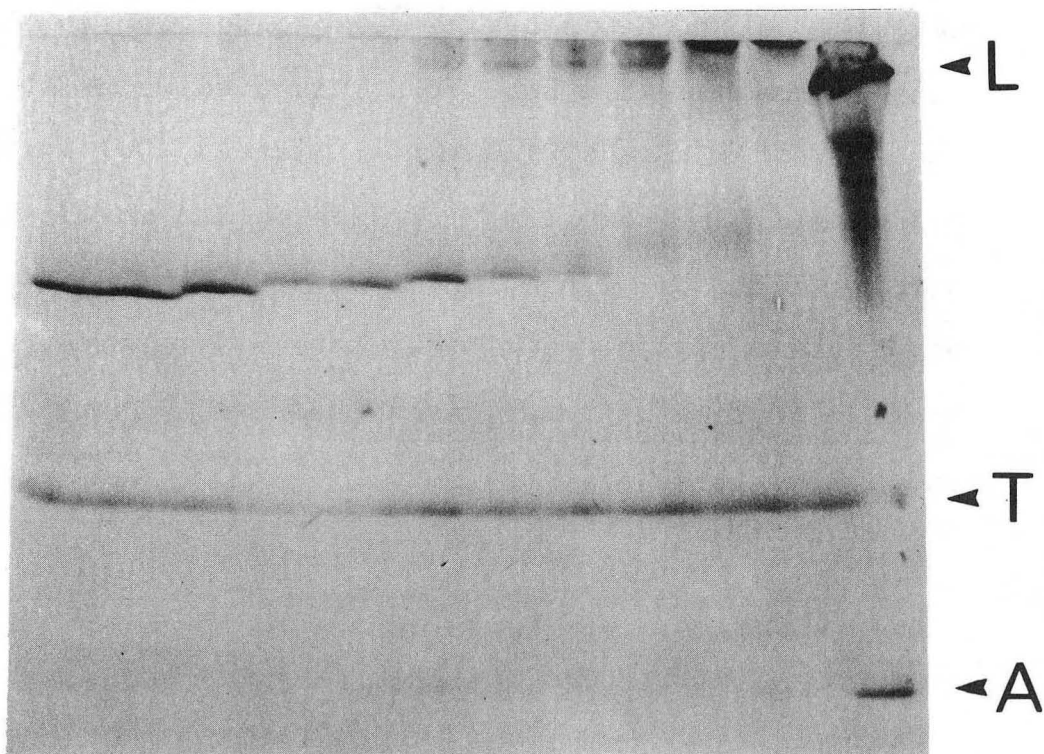
XBB 849-6739

Table 7 -Effect of incubation (37°C, 6h) of LDL*, PC vesicles (PCV)**,

with or without plasma d>1.20 g/ml fraction (BF, 1 Co), on

the apparent particle diameter (Å) of the major LDL components.

	subjects		
	DJ	BG	DR
noninc	268,262	262	240,229
inc (+PCV)	268	262	245,233
inc (+PCV+BF)	273	268	260

*The LDL concentrations were 0.3 mg/ml
protein (subjects DJ and DR), 0.6 mg/ml
protein (subject BG).

**The PC concentrations were 0.8 mg/ml
(subjects DJ and DR); 1.5 mg/ml (subject
BG).

4. Transformation of the Electrophoretic Pattern of LDL Following Incubation with PCV in the Presence of the Plasma d>1.20 g/ml Fraction and HDL: Effect III

To examine whether the absence of Effect III was due to lack of other plasma components such as HDL in the incubation mixtures, incubations (37°C, 6h) were carried out on mixtures of LDL (0.6 mg/ml protein), BF (1 Co), HDL (approximately 1.0 mg/ml protein), and increasing PCV levels (0.2-1.2 mg/ml PCV). In the presence of HDL (Fig 23A, solid diamonds), the increase in LDL APD was much attenuated compared to that in the absence of HDL (Fig 23A, circles). Above a threshold value of 0.8 mg/ml PC, a bimodal pattern transformation characteristic of Effect III occurred and class II products were observed. At a two-fold lower HDL concentration (0.5 mg/ml protein), there was about a 3-fold greater increase in APD value at Effect II and a decrease in threshold PC level (from approximately 0.8 to 0.6 mg/ml PC) for Effect III (Fig 23A, empty diamonds). Also, further progression of bimodal pattern transformation (Effect III) into a single peak pattern (at 1.2 mg/ml PC) occurred at a lower (0.5 mg/ml protein) HDL concentration. Thus, in the presence of HDL both Effects II and III occur.

At both HDL levels used in the above-mentioned experiment, the area under the LDL peak did not change significantly (Fig 23B, diamonds), indicating that the presence of HDL markedly attenuated both the changes in LDL distribution and aggregate formation. This was in accord with our

expectation that, as an acceptor for PL, HDL would decrease the available vesicle concentration in the incubation mixture.

We thus established that the presence of HDL in the incubation mixture containing LDL, PCV, and BF was necessary to induce the Effect III transformation. The specific mechanism for this effect was not clear, but might have been related to the production, and interaction with LDL, of new structures containing PC (e.g., discoidal complexes of apo AI and PC formed during interaction of HDL with PCV). Since new PC-containing structures derived from HDL can appear during interaction of HDL and PCV alone, we assessed the possible occurrence of Effect III when LDL (JG), PCV (0.2 to 1.2 mg/ml PC), and HDL (0.5 and 1.0 mg/ml protein) were incubated (37°C, 6h) alone, in the absence of BF. LDL APD values did not change at PCV levels less than 1.2 mg/ml PC. At the highest PCV (1.2 mg/ml PC) and HDL (1.0 mg/ml protein) levels , a bimodal LDL pattern was seen but the APD values of the two components (246A and 256A) within the bimodal pattern were much less than the corresponding ones which appeared in the presence of BF (254A and 261A). Thus, HDL presence produced a bimodal LDL pattern during interaction of LDL with PCV; but this was not the complete Effect III since addition of BF was necessary to induce (1) a larger increase in APD values of the components within the bimodal pattern and (2) a the transformation from bimodal to single mode pattern.

5. Electron Microscopy of LDL Undergoing Effect II and Effect III

The above studies established that consistent changes occur in LDL apparent particle diameter when LDL were interacted with PCV in the presence of other plasma factors such as BF and HDL. For nonincubated LDL, particle sizes were determined at their exclusion limit in the gradient gels and were based on the assumption that LDL are quite rigid spheres. The relatively good correspondence reported (88) between size measurements by GGE and by EM for native LDL suggests that this assumption is reasonable. However, application of this assumption to LDL modified by agents such as PL may not be valid. Thus, negative stain electron microscopy was performed on LDL undergoing Effect II (subject JG) or Effect III (subject EB).

Nonincubated LDL appeared either as round, free-standing (EB, Fig 25A) or within patches of hexagonally-packed homogeneous particles (JG, Fig 25B). Often, chains of 4-6 deformed, rectangularly-shaped species were seen in nonincubated LDL from both subjects. PCV-exposed (EB, Fig 25C; JG, Fig 25D) LDL consisted of free-standing, round species as well as rectangularly-shaped (156A x 265A) parti-cles. Occasionally observed discoidal species (72 ± 20A x 5 ± 20A) trapped within chains of LDL or alternating with LDL-sized particles could be seen (Fig 25C and D, arrow heads). Hollow vesicular (Fig 9C, arrow) structures with deposits of negative stain on one corner were often noted as

Fig 25. Electron micrographs of nonincubated LDL ((A) sub-ject EB; (B) subject JG) and PC vesicle-exposed LDL ((C) subject EB; (D) subject JG). In (C), the vesicle-exposed LDL (within the d<1.20 g/ml fraction) were obtained from an incubation mixture containing plasma (subject EB) and PC vesicles (3.5 mg/ml PC). In (D), the vesicle-exposed LDL (within the d<1.063 g/ml fraction) were obtained from an incubation mixture containing subject JG's LDL (approximately 0.6 mg/ml protein), PC vesicles (0.4 mg/ml PC), and plasma d>1.20 g/ml fraction (1 Co). The arrowhead in Fig 25C indicates a hollow vesicular structure and the arrow in Fig 25D points to a disc-shaped (72A x 56 A) particle.
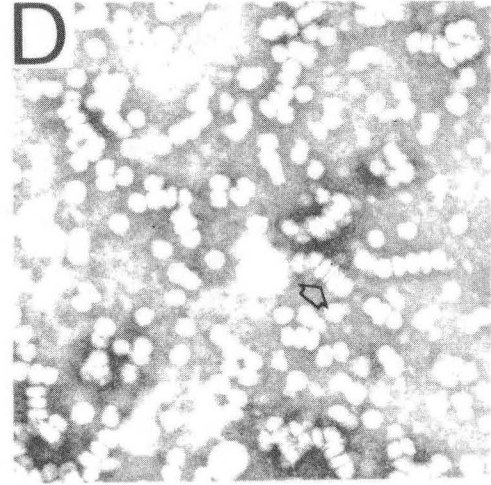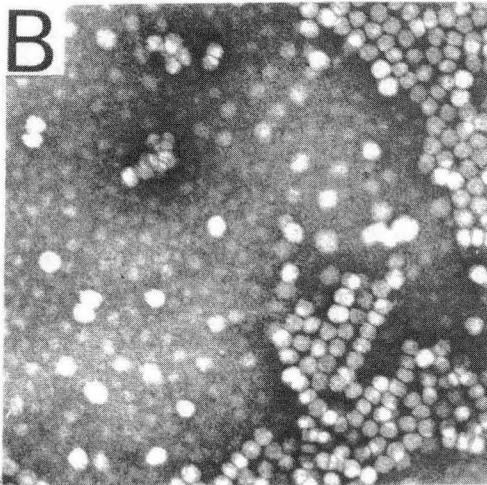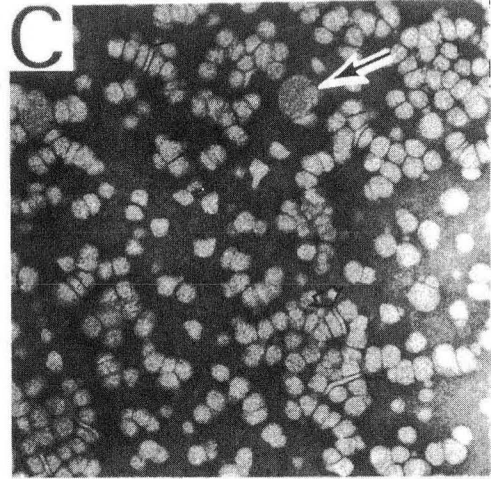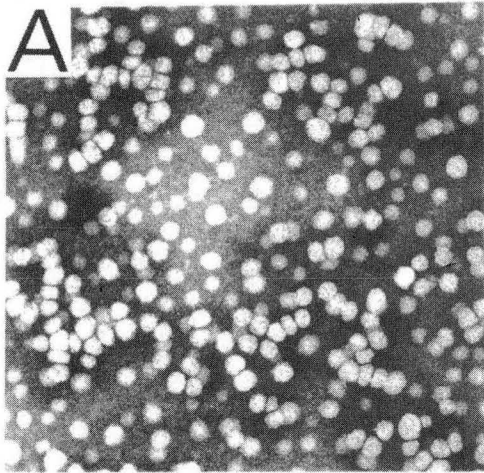
XBB 849-6746

well. Thus, no major changes in the overall shape of the PCV-exposed LDL has occurred during Effects II and III.

We also measured the apparent diameter of round, free-standing species. An increase in mean particle size of the LDL undergoing Effect II (JG, 236+25A, Fig 25D, versus 224+21A, nonincubated LDL, Fig 25C) and Effect III (EB, 251+27A, Fig 25B; 223+32A at 3.5 mg/ml PC (not shown), versus 226+33A nonincubated, Fig 25A) was observed. Hence, at least at PCV concentrations high enough to produce major changes in LDL size (i.e., greater than about 13A)[*] EM observations were consistent with an increase in the particle size of PCV-exposed LDL (class I). The increase in mean particle diameter observed by EM was about 7-16A less than the increase in APD found by GGE. This difference is at the limit of EM resolution.

6. Ultracentrifugal Properties of LDL Undergoing Effect II and Effect III

Based on the above observations, we considered the hypothesis that the PCV-induced changes in the LDL particle size distribution are most likely due to PL uptake by LDL. To test this hypothesis, attempts were made to isolate and directly determine possible compositional changes in the modified LDL. Also, ultracentrifugal properties of PCV-

---

[*]It should be pointed out that 13A is the standard error of particle size measurements by EM and we could not evaluate with certainty smaller changes in size by EM.

exposed LDL, such as flotation rate and hydrated density were assessed.

a. Peak S^O_f Rates of LDL Undergoing Effect II and Effect III

A positive correlation has been found between LDL size and flotation rate (42). Recently an empirical relationship between particle diameter (D) and peak S^O_f rate has been obtained[†] for purified native LDL with a single peak GGE pattern:

$$D \text{ (in Angstrom units)} = (5.13) \, S^O_f + 218$$

To assess any changes in LDL ultracentrifugal flotation properties undergoing Effects II and III, analytical ultracentrifugation was performed at (d 1.20 g/ml)[*] on the total lipoprotein fraction obtained from either whole plasma (subject BG) incubated with PCV (see Fig 20 for experimental conditions and GGE patterns) or the plasma d>1.019 g/ml fraction (subject EB) incubated with PCV (see Fig 27 in the following section for experimental conditions and GGE patterns). Analysis of the schlieren patterns of LDL yielded peak flotation rates at d 1.20 g/ml (peak $F^O_{1.20}$ rate), which were converted to flotation rates at d 1.063 g/ml (peak S^O_f rate) using a relationship[*] also obtained

empirically (unpublished data). The observations can be summarized (Table 8) as follows:

1) The calculated peak S^o_f rate of EB's LDL from nonincubated plasma (S^o_f 5.51) was less than BG's LDL from nonincubated plasma ($S^o_{f\ 6.68}$). Based on the particle size of the major components (EB, 248A; BG, 253A) these S^o_f rates fitted well the empirical equation obtained for native LDL.

2) The S^o_f rate of the LDL undergoing Effect II (EB) and Effect III (BG, only at 4.5 mg/ml PC) were faster than LDL from nonincubated plasma. Although we expected the peak S^o_f rates of LDL undergoing Effect II to increase with increasing APD values, this was not the case (Table 8).

3) With increasing PCV levels, the schlieren peak area contained within Sf range of LDL (S^o_f 0-12, corresponding to $F^o_{1.20}$ 15-40) decreased considerably (BG, Table 8). Concomitant with this decrease, faster floating material (up to S^o_f 400) appeared. We did not explore further the identity of the faster floating material, but speculate that it was either PCV and/or aggregates of LDL and PCV.

Thus, while small changes in peak S^o_f rate of PCV-exposed LDL undergoing Effects II and III were noted, these changes did not follow the size versus S^o_f relationship observed for native LDL subpopulations.

b. Ultracentrifugal Distribution of LDL Undergoing Effect II and Effect III

Table 8 -Peak S_f^o rates[*] of LDL undergoing Effects II[**] and III[**, ‡].

LDL (subject EB)[**]	peak S_f^o	LDL (subject BG)[‡]	peak S_f^o	LDL area[‡]
noninc	5.54	noninc	6.67	264
inc (1.1 mg/ml PC)	6.07	inc (2.5 mg/ml PC)	6.63	163
inc (1.3 mg/ml PC)	5.96	inc (3.5 mg/ml PC)	6.82	148
inc (1.8 mg/ml PC)	5.87	inc (4.5 mg/ml PC)	7.25	110

[*] calculated from an empirical equation:
peak S_f^o = peak $F_{1.20}^o \times$ 0.4815 - 7.2386.

[**] Following incubation (6h) of the plasma d>1.019 g/ml
fraction (subject EB) with PC vesicles (1.1-1.8 mg/ml PC),
anlytical ultracentrifugation (ANUC) was performed on the
d<1.20 g/ml fraction isolated from the incubation mixture.

[‡] The d<1.20 g/ml fraction from BG's plasma incubated (6h)
with 2.5-4.5 mg/ml PC was analysed by ANUC. Areas within
the schlieren patterns ($F_{1.20}^o$ 15-40 or S_f^o 0-12) were measured.

In an attempt to detect changes in the hydrated density of PCV-exposed LDL (during Effects II and III), isopycnic density gradient ultracentrifugation was performed on incubation mixtures using JG's LDL with small, major LDL component. A densitometric scan (455 nm) of the ultracentrifugal tube containing nonincubated LDL (Fig 26) showed that the major part of the LDL was contained within d 1.042 g/ml fraction, as expected in hypertriglyceridemic individuals.

Densitometric scans of the ultracentrifugal tube containing incubation (37°C, 6h) mixtures of LDL, BF, and PCV (0.2, 0.3, 0.4 mg/ml PC) showed a major component between d 1.038-1.048 g/ml and a minor one at about d 1.035 g/ml. The peak of this component was shifted to lower densities (d 1.043 g/ml, at 0.2 mg/ml PC; d 1.041 g/ml at 0.3 or 0.4 mg/ml PC) compared to that (d 1.045 g/ml) of the nonincubated LDL. GGE was not performed on the ultracentrifugal fractions, but from the GGE pattern of the unfractionated samples (APD values: nonincubated, 248A; plus 0.2 PC, 253A; plus 0.3 PC, 260A plus 0.4 PC, 263A), we established an approximate particle size versus hydrated density relationship for LDL at each PCV level. We found a decrease in density (0.002-0.004 mg/ml) of the peak of the LDL mass distribution in the ultracentrifugal tube. This decrease was much less than expected for the APD change (5-15A at various added PC concentrations) when the normal LDL size versus density relationship reported for native LDL was used (38).

Fig 26. Densitometric scans (455 nm) of tubes following ultracentrifugation of incubation mixtures containing LDL (subject JG), plasma d>1.20 g/ml fraction, and PC vesicles (0.2-0.4 mg/ml PC). Isopycnic density gradient ultracentrifugation was performed as described in Methods, section E1. The top of the tube and densities from a separate salt background sample are indicated.

XBL 848-7877
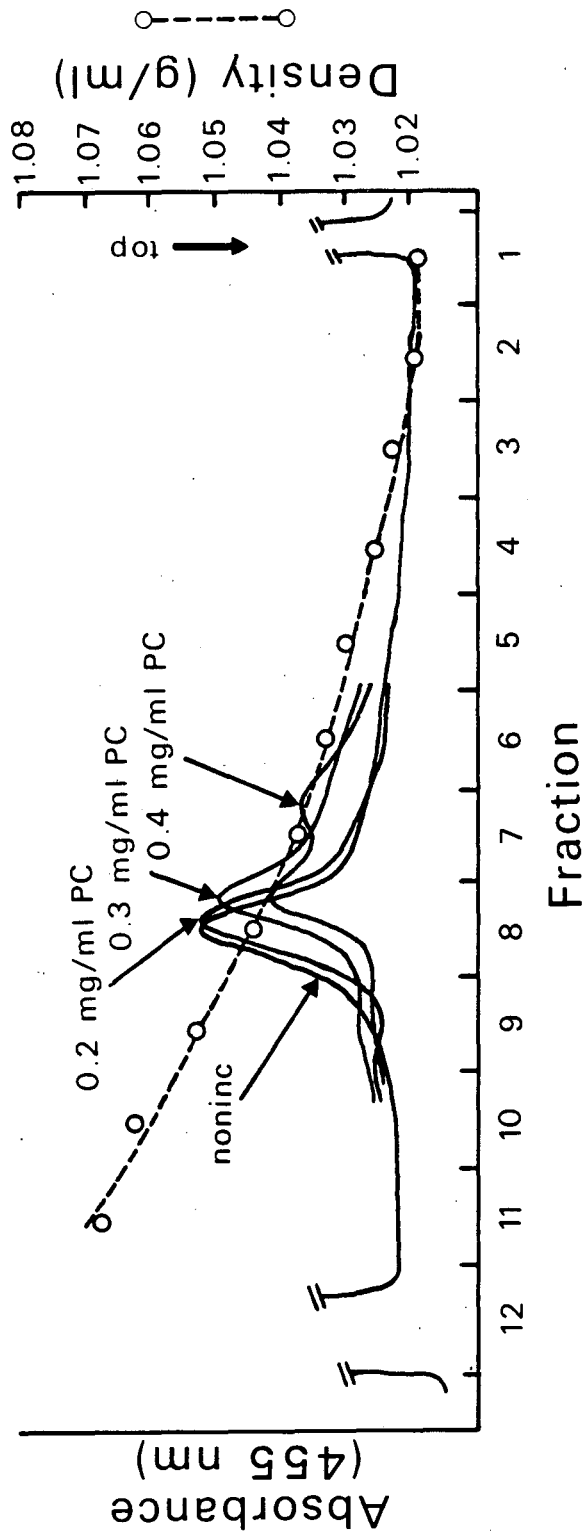
The component at d 1.035 g/ml, which developed as a shoulder in the less dense side of the major ultracentrifugal LDL peak at 0.4 mg/ml PC appeared turbid. Our data suggest that this component may have been aggregated complexes of LDL and PCV. For example, at 0.8 mg/ml PC, a 66% decrease in the area under the GGE peak of unfractionated LDL occurred and was associated with the appearance in the ultracentrifugal tube of an additional component at a lower density (d 1.035 g/ml than the main LDL component. The GGE pattern at 0.8 mg/ml PC showed protein staining material at the top of the gel, which we have considered to be aggregates of LDL and PCV. In addition, when LDL (JG) were incubated (37°C, 6h) with even higher PCV concentrations (1.8 mg/ml PC), GGE patterns showed maximal aggregate formation, and isopycnic density gradient ultracentrifugation showed a shift of the entire LDL density distribution to fractions of markedly lower density (d 1.029 g/ml).

To study changes in LDL hydrated density during Effect III, IDGUC was next performed on incubation mixtures which contained HDL as well as LDL, BF, and PCV. The GGE patterns of unfractionated mixtures indicated an APD increase (Effect II) that occurred between 0.4-0.6 mg/ml PC and the appearance of bimodal LDL patterns (Effect III) between 0.8-1.2 mg/ml PCV 'see Fig 23, section C3). Densitometric scans of the ultracentrifugal tubes (not shown) containing incubation mixtures showing the bimodal pattern indicated only a minor decrease in mean density of the peak of the PCV-exposed LDL

which was comparable to those observed Effect II. It should be pointed out that the shifts in LDL density during Effects II and III were in a direction towards lower values, i.e., opposite in direction to that observed during incubation of plasma in the absence of PCV.

c. Chemical Characterization of LDL Undergoing Effect II and Effect III

In view of the density differential between PCV (d<1.019 g/ml) and LDL (d 1.019-1.063 g/ml), isopycnic density gradient ultracentrifugation was next used to isolate and characterize PCV-exposed LDL produced during Effect II and Effect III. Plasma (subject EB with small major LDL component) ultracentrifugally depleted of VLDL (plasma d>1.019 g/ml fraction) was incubated (37°C, 6h) with increasing PCV levels (0.4-1.8 mg/ml PC). Effect II was produced in the range of 0.4-0.9 mg/ml PC, and Effect III was seen in the range of 1.1-1.8 mg/ml PC (for GGE patterns see inserts at the right side of Fig 27). Following IDGUC, densitometric scans of the tubes (Fig 27) showed shifts in LDL mass towards lower density values, similar to those observed using JG's LDL (see Fig 26). Thus, an approximately 5-25 A increase in LDL APD value, using a range of PCV (0.4-1.8 mg/ml PC), was associated with at most a 0.002-0.004 g/ml density decrease.

Chemical analysis of the LDL within each ultracentrifugal density fraction (at 0.4-1.8 mg/ml PCV) indicated about 20-46% increase in PL/protein weight ratio and about 19%

Fig 27. Effect of incubation (6h) of the plasma d>1.019 g/ml fraction (subject EB) with PC vesicles (0.4-1.8 mg/ml PC) on the ultracentrifugal distribution of LDL. Isopycnic density gradient ultracentrifugation was performed as described in Methods, section E1. Densitometric scans (455 nm) of tubes are shown for nonincubated LDL (first row); incubated (0.9 mg/ml PC; second row); incubated (1.1 mg/ml PC; third row); incubated (1.3 mg/ml PC; fourth row); incubated (1.8 mg/ml PC; fifth row). The insets to the right of each row show the gradient gel electrophoretic (2-16% gel) patterns of unfractionated LDL from the corresponding incubation mixture. The material appearing within d 1.023-1.031 fractions (between arrows; second row) appeared turbid and probably consisted of LDL-vesicle aggregates and/or PC vesicles. Density distribution of a background salt solution is shown at the bottom of the figure.

XBL 848-7872
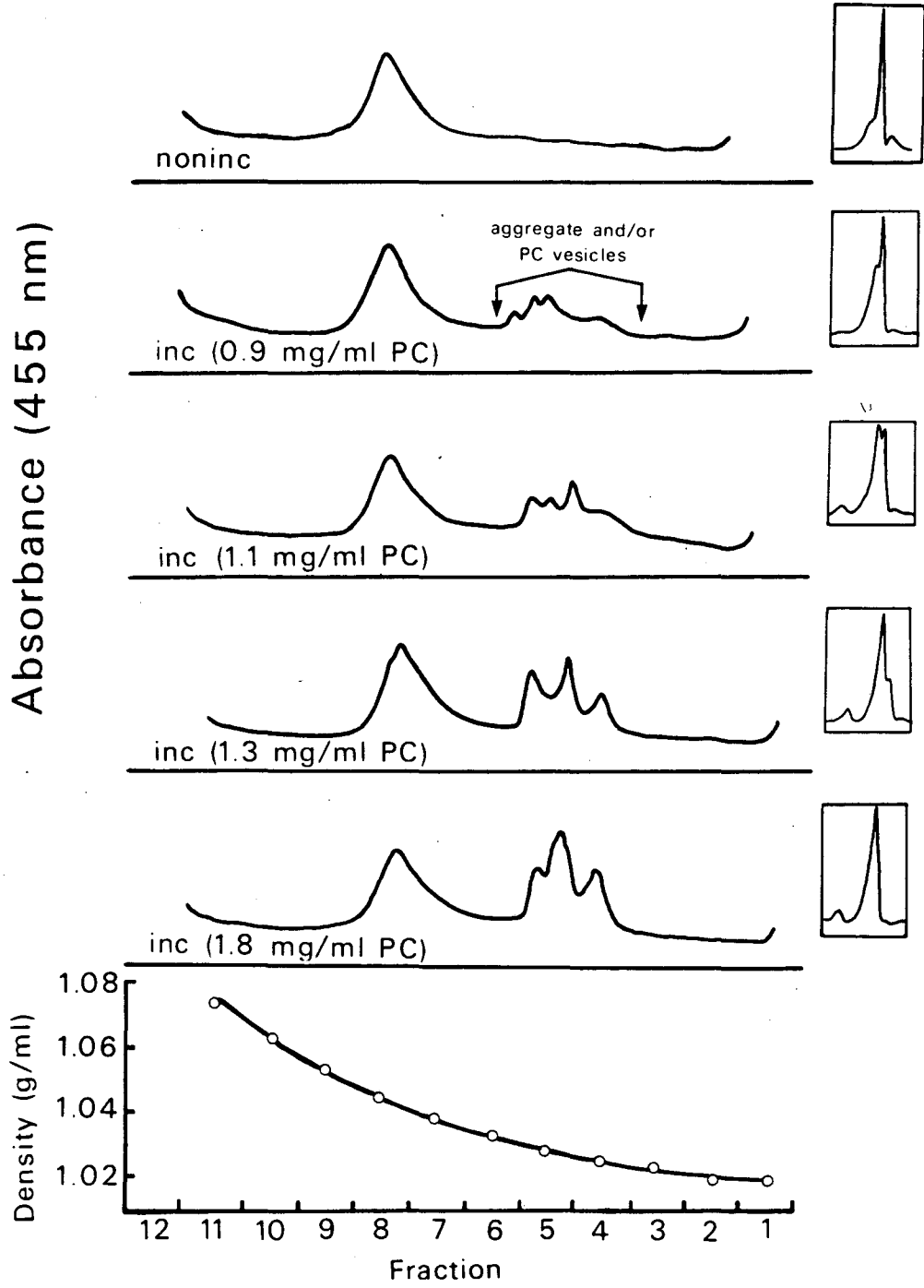
decrease in UC/protein weight ratio. Although the densitometric scans of the ultracentrifugal tubes suggested that the aggregate had separated from the bulk of LDL (i.e., class I products), GGE patterns of material within the major ultracentrifugal peak (d 1.040-1.045 g/ml) showed the presence of species larger than LDL (data not shown). Even a density gradient as shallow as the one used in this study did not provide adequate separation of class I products from class II products and the aggregate. Hence, these fractions were not useful in elucidating the chemical properties of the various forms of PCV-exposed LDL (i.e. class I, class II, and aggregate).

7. Summary of Incubation Studies Using PC Vesicles

Our incubation studies using PCV showed four charac-
teristic PCV concentration-dependent changes in LDL GGE pat-
terns:

[1]   Effect I: Interaction of LDL with PCV in the presence
       of all plasma components (VLDL, LDL, HDL, and BF) gave
       rise to either a decrease (for large, major components)
       or no change (for small, major LDL components) in LDL
       APD value, below a threshold PCV concentration. Simi-
       lar changes occurred without addition of PCV to plasma
       during incubation in the presence of active LCAT.

[2]   Aggregation: In the absence of other plasma components,
       interaction of LDL and PCV leads to the formation of
       large (>400A) complexes between LDL and PCV. This
       occurred without any change in the APD value of unag-
       gregated LDL (except for the smallest (229-240A) LDL
       components from severely hypertriglyceridemic individu-
       als).

[3]   Effect II: Above a threshold PCV concentration an
       increase in LDL APD value occurred during plasma incu-
       bation with PCV. The addition of BF to an incubation
       mixture comprised of LDL and PCV also produced such an
       LDL APD increase. The addition of components capable
       of PC uptake (e.g., HDL) modulated the extent of LDL
       APD increase. Unlike the changes in LDL properties
       during incubation of plasma alone (i.e., LCAT-dependent

and towards formation of smaller, more dense species),
the changes during Effect II did not depend on LCAT
activity (not shown) and were towards formation of
larger and slightly less dense species.

[4]   Effect III: With increasing PCV concentrations, bimodal
      LDL pattern transformations occurred during incubation
      of plasma with PCV. Both HDL and BF (and PCV, of
      course) were required for transformation of the pattern
      first to a bimodal and subsequently to a single peak
      pattern.   In the course of this transformation an
      increase in APD value of each component within the
      bimodal pattern was observed when both HDL and BF were
      present. Both HDL and LDL levels modulated the PCV
      concentration at which this effect, Effect III,
      occurred.

During Effects II and III, in addition to the com-
ponents within the usual LDL size range, additional com-
ponents (class II) with APD values beyond the usual LDL size
range (>290A) appeared when LDL, PCV, and BF were incubated,
with or without HDL

Changes in LDL APD during Effects II and III were con-
firmed by EM; however, changes in shape could not be con-
sistently demonstrated.

Although compositional changes during Effects II and
III were consistent with PL uptake by LDL products, the
extent to which such changes reflected those occurring in

LDL alone could not be determined since contaminants could not be adequately removed by the ultracentrifugal procedures used. Thus, the chemical bases for the PCV-induced changes in LDL GGE patterns (i.e., Effect II and Effect III) could not be determined unambiguously by the approaches used and hence were investigated by utilizing a different source of PC and by different fractionation procedures.

D. Incubations of LDL with Discoidal Complexes Comprised of Apo AI and PC

Post-meal lipolysis of TG-rich lipoproteins results in the release of excess surface components in forms other than vesicular structures. A heterogeneous mixture of discoidal structures containing PC, UC, and apoproteins (A, E, and C) appears transiently both in post-heparin plasma (89)* and during in vitro lipolysis of VLDL (11). Our next investigation of the role of phospholipid-containing structures on LDL interconversions in plasma was directed to characterization of LDL after interaction with model discoidal structures containing PC and apo AI (DC). Following the approach used in our reconstitution experiments using PCV, we first studied interaction of LDL with DC, and subsequently tested the effects of addition of other plasma components to the incubation mixtures. Based on our observations using PCV, we did not expect changes in LDL APD when LDL and DC were incubated alone. To our surprise, an increase in LDL APD occurred, which was characteristic of Effect II. Also, preliminary studies indicated that no Effect III was observed using DC at PC concentrations which were high enough to produce Effect III, using PCV. Thus, our initial studies focused on the properties of LDL undergoing Effect II during interaction of LDL with DC.

*Heparin releases LPL from capillary walls into plasma and thereby initiates lipolytic activity in plasma.

1. Apparent Particle Size Distribution of Major LDL Components Following Incubation with Discoidal Complexes: Formation of Class I and Class II Products

Plasma incubation studies, both with and without PCV, indicated differences in the extent of APD change between the small versus the large, major LDL components. Although these differences were in part due to PCV interaction with other plasma components, such as VLDL and HDL, the nature of the LDL used also contributed to the observed differences. In our investigation of LDL interaction with discoidal complexes, we used plasma LDL preparations that exhibited major components of significantly different initial particle size. The particle size of components in GGE patterns of isolated nonincubated LDL (Fig 28, left column) obtained from two normolipidemic human subjects (DJ and AP) and three hypertriglyceridemic subjects (TI, LS, DR) used in this study, are summarized in Table 9. The GGE pattern of subject DJ's LDL exhibited four components, two large, major (mean diameter, 269A and 262A) and two small, minor (255A and 245A). The pattern of LDL obtained from subject AP's plasma showed two large,major components (260A and 253A). LDL from the three hypertriglyceridemic subjects (TI, LS, DR), each consisted of two small, major components (241A and 230A; 240A and 231A; 240A and 229A, respectively); all of these were smaller than the major LDL components of the normolipidemic subjects.

Fig 28. Time course of change in particle size distribution (2-16% gel) of LDL (0.3 mg/ml protein; subjects DJ, first row; AP, second row; TI, third row; LS, fourth row; DR, fifth row), either nonincubated (left column), or incubated (37°C; 6h, middle column; 24h, right column) with discoidal complexes (0.4 mg/ml PC).
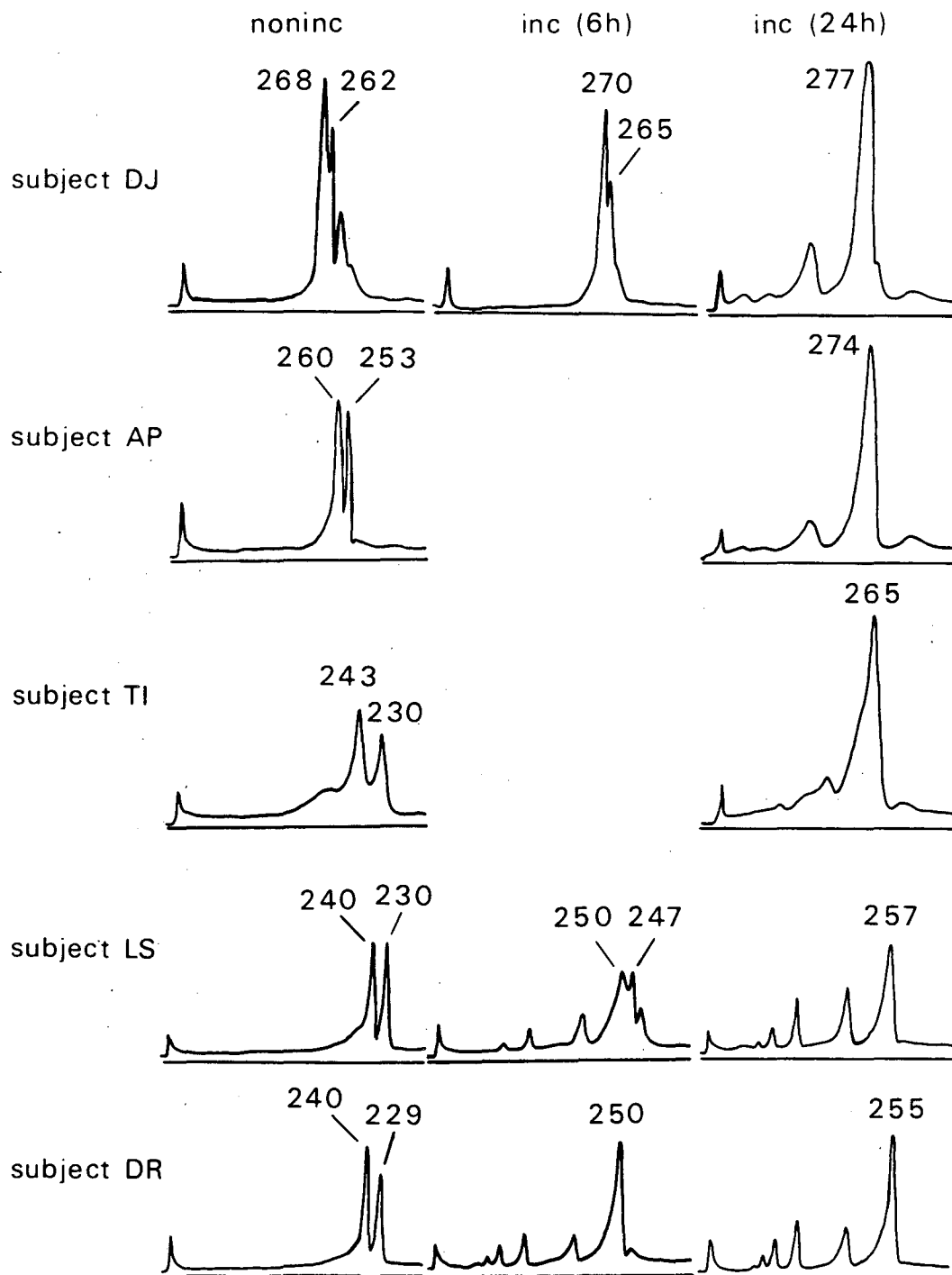
XBL 848-7867

Table 9 -Summary of the apparent particle diameter (APD, Å) of nonincubated and discoidal complex-exposed* LDL.

		DJ	AP	TI	LS	DR
noninc	no. of components	4	2	2	2	2
	LDL diameter	268,262,255,245**	260,253	243,230	240,230	240,229
inc (1h)	no. of components	3 (I)‡	1 (I)	2 (I)	---	---
	APD of class I products	267,260,253	256	245,231	---	---
inc (6h)	no. of components	2 (I)	---	---	3 (I); 3 (II)‡	1 (I); 4 (II)
	APD of class I products	270,265	---	---	250,247,240	250
	APD of class II products	---	---	---	371,344,290	390,333,340,290
inc (24h)	no. of components	1 (I); 1 (II)	1(I);1(II)	1(I);1(II)	1 (I); 4 (II)	1 (I); 4 (II)
	APD of class I products	277	274	265	257	255
	APD of class II products	412,382,327	336	305	384,379,344,294	395,386,345,295

*For details of incubation conditions, see legend to Fig 28.

**Major LDL components within the patterns are underlined.

‡Roman numerals in paranthesis designate class of products.

Marked changes in the GGE patterns (Fig 29, middle and left columns; Table 9) were observed upon incubation (37°C) of LDL (0.3 mg/ml protein) with DC (0.4 mg/ml PC)[*] over time periods of 1h, 6h, and 24h. During the course of the incubation, there was a shift in APD values of components within each LDL pattern towards larger values; the smaller the initial LDL size, the greater the extent of shift towards larger APD values at each incubation time. For example, the extent of shift (15 to 23A; subjects TI, LS, DR) towards larger APD values at 24h was more for the small initial LDL components than that (6 to 9A; subjects DJ, AP) for large initial LDL components. By 24h, the LDL pattern for each subject was transformed from one containing two or more well-resolved peaks to one with a single, relatively broad peak. The APD of the single, broad peaks were either slightly (DJ, 277A), or considerably (AP, 260A versus 274A; TI, 241A versus 265A; LS, 240A versus 257A; DR, 240A versus 255A) larger than the APD of the major LDL components in corresponding patterns of untreated LDL. The range of APD values (255-277A) in the GGE patterns (24h) of these transformation products was smaller than the particle size range of the corresponding initial major LDL components (229-268A). Since they still remained within the usual

---

[*]The concentration of both the discoidal complexes and LDL were such that the LDL-PL/DC-PL weight ratio (1.3) was within the range of LDL-PL/PCV-PL (0.7-2.0) that gave rise to E II during incubation of LDL, PCV, and BF.

particle size range of human plasma LDL (218-278A), we designated them as class I products, conforming to the designation used in the PCV incubation system.

In four out of five subjects, the transformation to a single peak pattern appeared to proceed in time via, either a progressive decrease (DJ), or no change (DR), in the number of components within the size range of plasma LDL. In LS's LDL, however, the transformation involved an increase, at 6h, from two components to three (Fig 29, middle column): two components had larger APD values (255A, 249A) than those observed in the pattern of nonincubated LDL (240A, 231A) and the third component had the same APD value (240A) as the larger component in the nonincubated LDL It is possible that a comparable increase in number of components, particularly in the LDL of the hypertriglyceridemic subjects, might also have occurred, but was not observed because of the different rates of transformation and inappropriate time points selected for sampling.

At 24h, the patterns of all subjects' transformed LDL showed a decrease in total area under all peaks of class I products. This decrease was associated with a consistent appearance of three to four new, relatively minor components with APD values (412-290A, Table 9) substantially beyond the normal LDL size range. We designated such components as class II products in the PCV incubation system. Interestingly, no material appeared at the top of the gel, suggesting that no aggregates of LDL and DC were formed in contrast

to our results using PCV. The formation of class II pro-
ducts occurred earlier (6h versus 24h) in the hypertrigly-
ceridemic subjects and the APD values were smaller (range,
395-290A) than those of similar products (range, 412-327A)
found in GGE patterns of the normolipidemic subjects.

Thus, the effect of LDL interaction (6h) with DC was
similar to Effect II observed during incubation (6h) of LDL,
PCV, and BF, i.e., formation of class I and class II pro-
ducts. Furthermore, the small, major LDL components were
more reactive to DC and APD increase than the large ones.

2. Ultracentrifugal Distribution of Discoidal Complex-
Exposed LDL

To establish further the physical-chemical properties
of class I and class II LDL products formed during interac-
tion of LDL and DC, we next investigated procedures for
their isolation from each other, as well as from DC. Using
LDL with major components of considerably different initial
particle sizes (from subjects DJ, AP. and TI), isopycnic
density gradient ultracentrifugation was performed on
d<1.063 g/ml fractions isolated from separate incubation
(37°C, 24h) mixtures. As indicated previously (Table 9),
the patterns obtained at 24h showed the greatest extent of
APD change, as well as complete transformation to class I
and class II species.

Using GGE, the particle sizes of LDL components within
each ultracentrifugal density fraction (DJ, Fig 29A; AP, Fig

Fig 29. Particle size distribution of nonincubated LDL and discoidal complex-exposed LDL within ultracentrifugal fractions. Two ml of the plasma d 1.019-1.063 g/ml fraction from incubation (6h) mixtures containing LDL (0.3 mg/ml protein) and discoidal complexes (0.4 mg/ml PC) were subjected to isopycnic density gradient ultracentrifugation (method of Shen et al (2)). The top 0.5 ml (fraction 1) and underlying 1 ml fractions were separated for gradient gel electophoresis (GGE; 2-16% gel, protein stain). The patterns of only fractions 1-6 (lanes 1-12, respectively) are shown. LDL within the incubation mixtures were from (A) subject DJ, (B) subject AP, (C) subject TI. Odd-numbered lanes: GGE of LDL in density fractions from nonincubated samples; even-numbered lanes: GGE of LDL in density fractions from incubated samples. Lane 13, calibration standards (latex beads (L), thyroglobulin (T), apoferritin (A)).

1 2 3 4 5 6 7 8 9 10 11 12 13

subject DJ
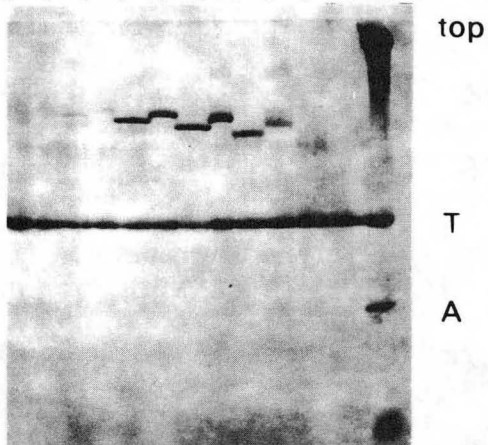
subject AP
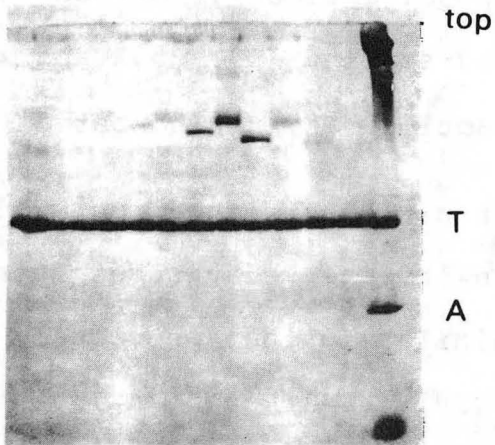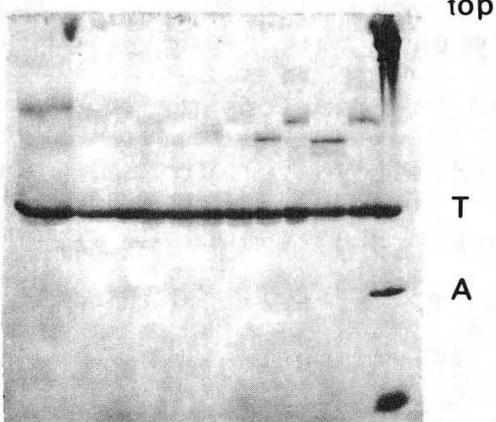
subject TI

XBB 848-6352A

29B; TI, Fig 29C), were determined and are summarized in Table 10. For nonincubated LDL of all subjects, we found that each component observed within the GGE pattern of the separated density fractions (Table 10) had a corresponding component of approximately similar particle size within the pattern of the unfractionated LDL (Table 9). For example, the particle sizes of LDL components found in each of the d 1.036 g/ml (DJ, 265A; AP, 263A) and the d 1.041 g/ml (DJ, 258A and 246A; AP, 253A) fractions corresponded, respectively, quite closely to those of the larger (DJ, 262A; AP, 260A) and smaller (DJ, 255A and 245A; AP, 253A) components of unfractionated, nonincubated LDL.

The ultracentrifugal data on untreated samples indicated an inverse relationship between size and hydrated density, similar to that previously described by Krauss and Burke (38). Although an inverse size versus density relationship also existed for class I products, the latter LDL were spread more widely across the density gradient and detected in fractions more dense than expected from the size versus density relationship observed for nonincubated LDL. For example, the major LDL components (269A and 259A) of subject TI after incubation with DC were found distributed between the d 1.041 g/ml and the d 1.050 g/ml fractions instead of floating in the d 1.036 g/ml fraction.

Changes in distribution of mass across the density gradient were estimated from areas measured under GGE peaks of LDL components within isolated ultracentrifugal density

Table 10 -Ultracentrifugal distribution* of nonincubated and discoidal complex-exposed LDL.

fraction	density (g/ml)	noninc LDL						discoidal complex-exposed LDL					
		subject DJ		subject AP		subject TI		subject DJ		subject AP		subject TI	
		APD**	%area‡	APD	%area	APD	%area	APD	%area	APD	%area	APD	%area
1	1.021												
2	1.026												
3	1.031	274 (264)	34					281	33				
4	1.036	265	34	263	26	242	17	275 [339]	46	275 [337]	73	264	12
5	1.041	258 (246)	33	253	58	243	31	(289) 268 [337]	20	273	22	261 [312]	37
6	1.050			250	16	239 (227)	34					259 [301]	35
7	1.060												

*For details of experimental conditions see legend to Fig 28.

**APD denotes apparent particle diameter (A) of the major and minor (in paranthesis) LDL components. Components with APD values in brackets are class II products.

‡The area (protein stain) under the LDL peak within the gradient gel electrophoresis pattern of each ultracentrifugal fraction (see Fig 29) was estimated from densitometric scans of the gels and the percentage of the LDL area in each density fraction relative to the sum of the LDL areas for fractions with identifiable LDL peaks.

fractions (see Table 10). The distribution of mass of class I LDL across the density gradient was either similar to that of the nonincubated LDL (TI) or shifted (DJ and AP) towards fractions with lower density. The shift in mass of DC-exposed LDL of subjects DJ and AP occurred from the d 1.041 g/ml to the d 1.036 g/ml fraction, where the density gradient was half as steep as the region of the gradient in which TI's LDL floated (the d 1.041 to 1.050 g/ml fractions). The steepness of the density gradient where TI's LDL was located may be responsible for its apparent lack of density shift. In any case, the shift of mass of class I species, if any, to lower density was much less than expected from the increase in APD relative to nonincubated LDL in all three subjects. Moreover, the distribution of mass of class II products along the density gradient was similar to that of class I material in all subjects, in spite of considerably larger APD values.

These data showed striking similarities with those obtained using PCV. In both incubation systems, the shifts in LDL density, if any, were small and towards decreasing density. In both systems, class II products had a density comparable to class I products.

3. Chemical Characterization of Discoidal Complex-Exposed LDL Isolated by Gel Filtration

Since the density differential between class I and class II products produced during interaction of LDL with apo AI-PCDC was insufficient for separation by density

gradient ultracentrifugation, gel filtration was attempted
to take advantage of the size differential identified by GGE
between these products. It should be pointed out that any
discoidal complexes with a size similar to LDL was removed
by gel filtration (see Fig 3 in Methods, section C) from the
disc preparations prior to incubation studies. Fig 30 shows
the elution profiles of total mixtures containing DC-exposed
(24h, top) and nonincubated (bottom) LDL (TI). The position
of the major peak in the elution profile of the former
(fraction 27) was shifted towards lower elution volumes
relative to that of nonincubated LDL (fraction 28), con-
sistent with changes in APD observed in their GGE patterns.
In addition, a shoulder appeared at an elution volume (frac-
tion 21 thru 24) less than that of the major peak (fraction
25 thru 29). GGE patterns of fractions across the elution
profile indicated that this shoulder contained mainly class
II products (295A, 351A; Fig 30, insert) and minor amounts
of class I species (277-251A). Fraction 25 contained both
class I and class II species (Fig 30, insert). GGE patterns
of fractions within the major chromatographic peak (exclud-
ing fraction 25) indicated the presence mainly of class I
species (258-262A; Fig 30, insert). Thus, fractions 26-28
(class I) and 21-24 (class II) of DC-exposed LDL, as well as
fractions 26-30 of nonincubated LDL (241A 230A), were
separately pooled and concentrated.

Chemical analysis of the pool of fractions containing
TI's class I products indicated a 40% increase and a 32%

Fig 30. Elution profiles from gel filtration of incubation mixtures containing LDL and discoidal complexes. Following incubation (37°C, 24h) of LDL (subject TI, 0.3 mg/ml protein) and discoidal complexes (0.4 mg/ml PC), an aliquot was directly applied to a 2.5 x 100 cm column of 6% beaded agarose gels for gel filtration (4°C, 30 ml/h). Samples were eluted (using a 0.01 M Tris-0.15 M NaCl buffer, buffer B, see Methods, section A) and 5 ml fractions collected. (A) nonincubated LDL alone; (B) incubated sample; class I (fractions 26 to 28) and class II products (fractions 21 to 23) were identified by gradient gel electrophoresis (GGE; see inset). The discoidal complexes were eluted in fractions 33-39. Inset: Gradient gel electrophoresis of fractions 20-28 across the elution profile of discoidal complex-exposed LDL.
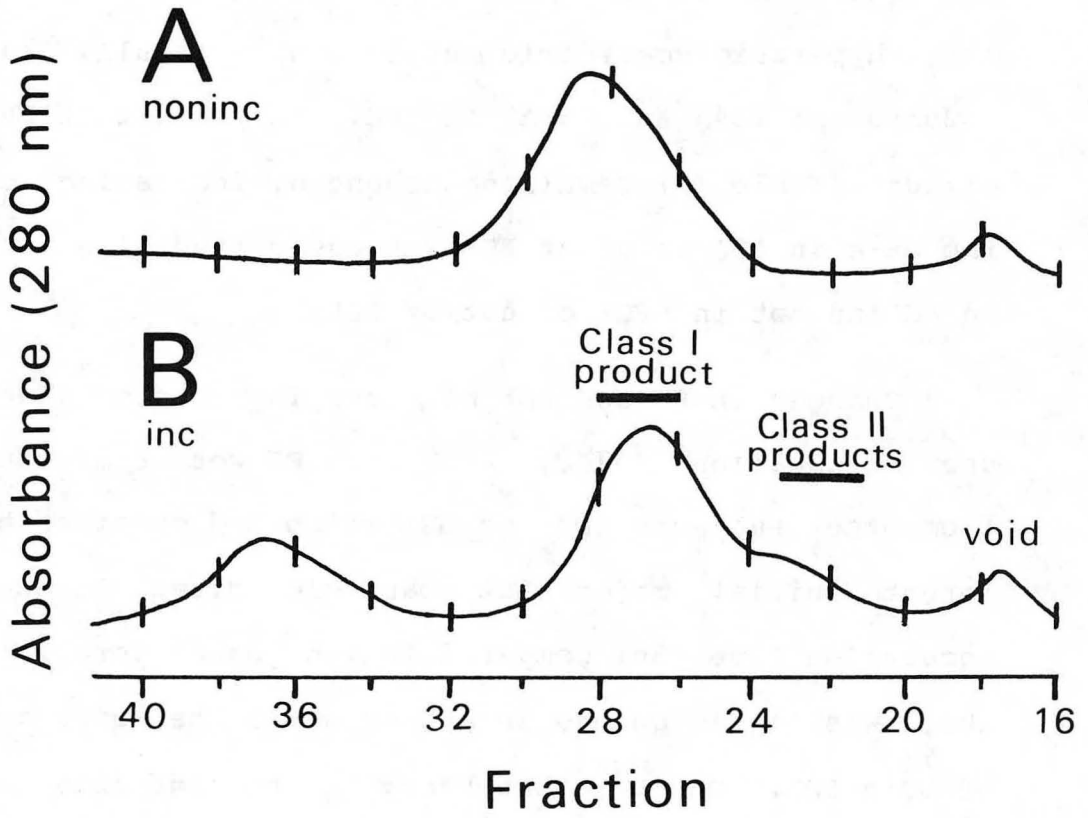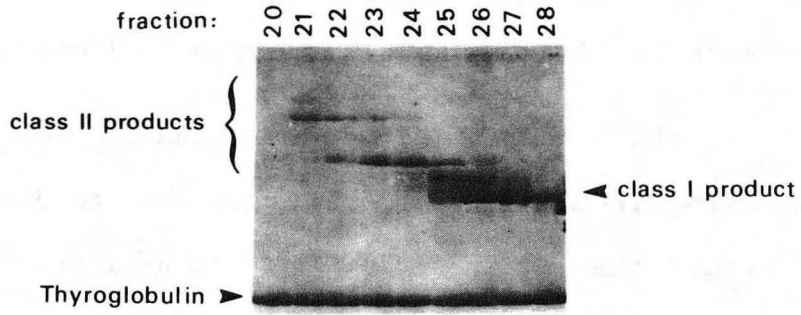
XBB 848-6355A

decrease in PL/protein and UC/protein weight ratio, respectively (see Table 12). By electron microscopy (see Fig 32B, next section) class I species showed negligible amounts of discoidal structures, ruling out the possibility that the increase in PL/protein ratio reflected contamination by DC.

To check that the increased phosphorous levels in LDL following incubation with DC were due to increased levels of PC rather than to degradation products such as LPC, TLC was performed on total incubation mixtures of LDL from subject JB (a hypertriglyceridemic subject with small, major LDL components: 224A and 238A) and DC. The amount of LPC in the mixture (Table 11) remained unchanged, indicating that the increase in APD value of LDL was associated with an increase in PC and not in LPC content of LDL.

Changes in PL content of class I products (Table 12), upon incubation (37^OC, 6h) with DC were evaluated in LDL from other subjects (DJ and LS) which had considerably different initial major LDL particle sizes. At the shorter incubation time (6h, compared to 24h used for TI's LDL), there was little change in APD value of the major components of DJ's LDL. On the other hand, a considerable shift in LS's pattern to larger species (Table 9). Class I species from both incubation mixtures were isolated by gel filtration in a manner similar to that described for TI's LDL. Nonincubated LDL were collected in fractions 25 to 27 (DJ, not shown) and fractions 25 to 28 (LS, Fig 31, top), and DC-exposed LDL were collected in fractions 25 to 27 (DJ, not

Table 11 -Lysolecithin (LPC) content of incubation mixtures.[*]

	total PL (mg/ml)[*]	LPC (mg/ml)[*]	%LPC/total PL
noninc LDL	0.27	0.032	12
inc (6h) LDL	0.30	0.030	10
inc (24h) LDL	0.27	0.038	14
noninc DC	0.38	0.003	--
inc (6h) DC	0.40	0.004	--
inc (24h) DC	0.35	0.003	--
inc (6h) LDL+DC	0.69	0.034	5
inc (24h) LDL+DC	0.72	0.043	6
calculated[**] LDL (6h)+DC (6h)	0.70	0.034	5
claculated LDL (24h)+DC (24h)	0.62	0.041	7

[*] LDL (0.3 mg/ml protein) and discoidal complexes (DC, 0.4 mg/ml PC) were incubated separately and together. Total lipids were extracted from the incubation mixtures by chloroform/methanol and approximately 100 ⅄g PC was used for thin layer chromatography (see Methods, section H). Four spots corresponding to LPC, PC, sphingomylin, and phosphatidylethanolamine were identified. The sum of the latter three spots, as well as the LPC spot, was scraped off for phosphorous measurement. Results are presented as mg phospholipid per 1 ml initial sample.

[**] The sum of LPC contents of LDL and discoidal complexes each incubated (6h, 24h) alone was compared to the LPC content of the incubation mixture containing both LDL and discoidal complexes.

Table 12 -Chemical composition (weight ratios)[*] of nonincubated
LDL and discoidal complex-exposed (class I and class II
products) isolated by gel filtration[**].

| | | subjects | | |
		DJ	LS	TI
noninc LDL	PL/P	0.98	0.94	0.91
	UC/P	0.31	0.20	0.21
	CE/P	1.50	1.41	1.12
class I products	PL/P	1.04	1.22	1.27
	UC/P	0.19	0.13	0.14
	CE/P	1.38	1.12	1.18
class II products	PL/P	----	1.07	1.12
	UC/P	----	0.11	----
	CE/P	----	0.69	----

[*] PL/P, phospholipid/protein; UC/P, unesterified cholesterol/
protein; CE/P, cholesteryl ester/protein weight ratios.

[**] For details see legend to Fig 30 and 31.

Fig 31. Elution profile of LDL (subject LS) obtained from incubation mixtures. The d<1.063 g/ml fractions obtained from mixtures of nonincubated LDL (0.3 mg/ml protein; top), LDL (0.3 mg/ml protein) incubated (6h) with discoidal complexes (0.4 mg/ml PC; middle), and LDL (0.3 mg/ml protein) incubated with discoidal complexes (0.4 mg/ml PC) and albumin (35 mg/ml; bottom) were each subjected to gel filtration (see legend to Fig 30 for details). Class I products (fractions 25-28) and class II products (fractions 21-23) were separately pooled.
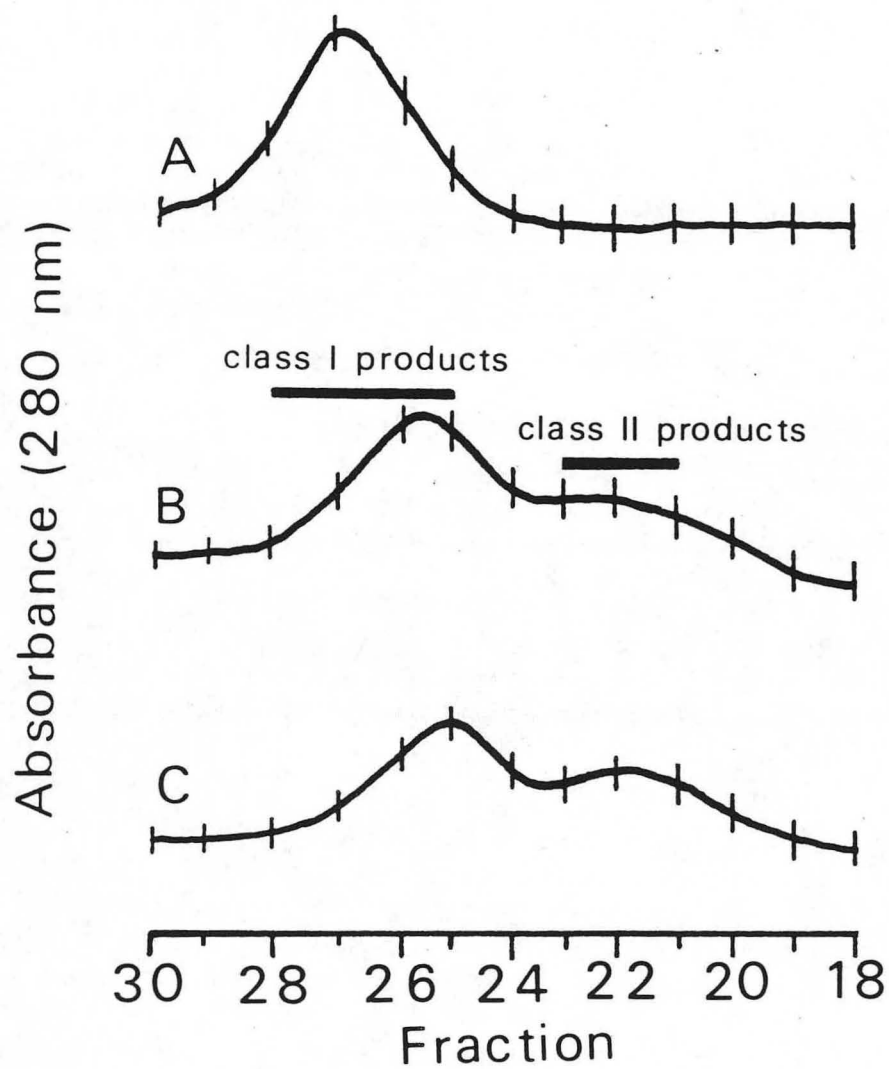
XBL 848-7862

shown) and fractions 25 to 28 (LS, Fig 31, middle). Chemical analysis of the pooled fractions containing class I species from DJ's LDL showed little (6%) change in PL/protein weight ratio (Table 12), and a 30% increase in PL/protein of class I species from LS's LDL. Both DJ and LS's class I products showed 39% and 35% decrease in UC/protein ratio, respectively. Thus, under identical conditions with DC, an initially large, major component showed little PL uptake and little increase in APD whereas an initially small, major LDL component showed a marked increase in PL content and APD value. Also, the size increase in LDL from the hypertriglyceridemic subjects roughly correlated with PL uptake by the LDL. Thus, an about 9-24A size increase (LS, 6h) was associated with 30% PL uptake, and 26A size increase (TI, 24h) was associated with 40% PL uptake.

Chemical analysis of class II products (Table 12) isolated by gel filtration, showed a 45% decrease in UC/protein ratio, similar to that observed for class I products (35%), but a PL/protein weight ratio only slightly greater (14%) than nonincubated LDL (compared to 30% for class I products), suggesting that the increased APD of class II products was not due to a PL uptake comparable to class I products.

4. Electron Microscopy of Discoidal Complex-Exposed LDL

As described above, interaction of LDL with DC resulted in an increase in APD value which was roughly related to the amount of PL uptake. When we calculated[*] the increase in

*Shen model of lipoprotein structure (2).

LDL particle size expected following PC uptake we obtained a value smaller than that observed by GGE. For maximal PL uptake (40% increase in PL/protein weight ratio) by TI's LDL (230A, 240A major components), for example, an increase of 10-14A was calculated. However, by GGE, an apparent increase of 25-35A was obtained. These calculations suggest either a change in LDL shape with DC exposure or shortcomings of the model. As an alternate means of studying LDL shape and/or size change, electron microscopy using negative stain was performed on class I products chromatographically isolated from incubation mixtures of LDL and DC. Representative micrographs are shown for LS's LDL (Fig 32). Both control (Fig 32A) and DC-exposed (Fig 32B) LDL showed round, dispersed particles. Occasionally DC-exposed LDL also showed hexagonal packing as well as chaining of rectangularly-shaped particles. Thus, similar to the results using PCV, no major changes in LDL shape were seen upon interaction of LDL with discoidal complexes.

EM size measurements were made on nonincubated LDL and class I products formed during incubation of LDL with DC. When the particle size distribution (by EM, Fig 32C) of LS's nonincubated LDL was compared with class I products of DC-exposed LDL, a shift to larger particles was seen in the latter without a change in the location of the peak of the distribution. This was in agreement with GGE observations (see Fig 2.8) As shown in the plot of the GGE versus EM mean particle diameter (Fig 33, top) an increase in mean particle

Fig 32. Negative stain electron microscopy on the d<1.063 g/ml fraction from (A) nonincubated LDL (subject LS) and from (B) incubated (6h) mixture of LDL and discoidal complexes. The histogram below the electron micrographs demonstrates particle size distribution of LDL shown in (A) (dashed lines; hashed) and (B) (solid lines). For corresponding patterns see Fig 28 (subject LS).
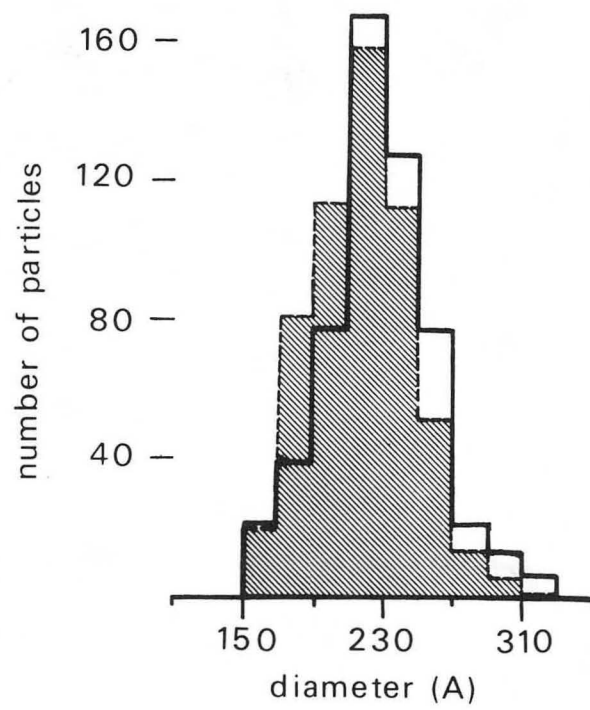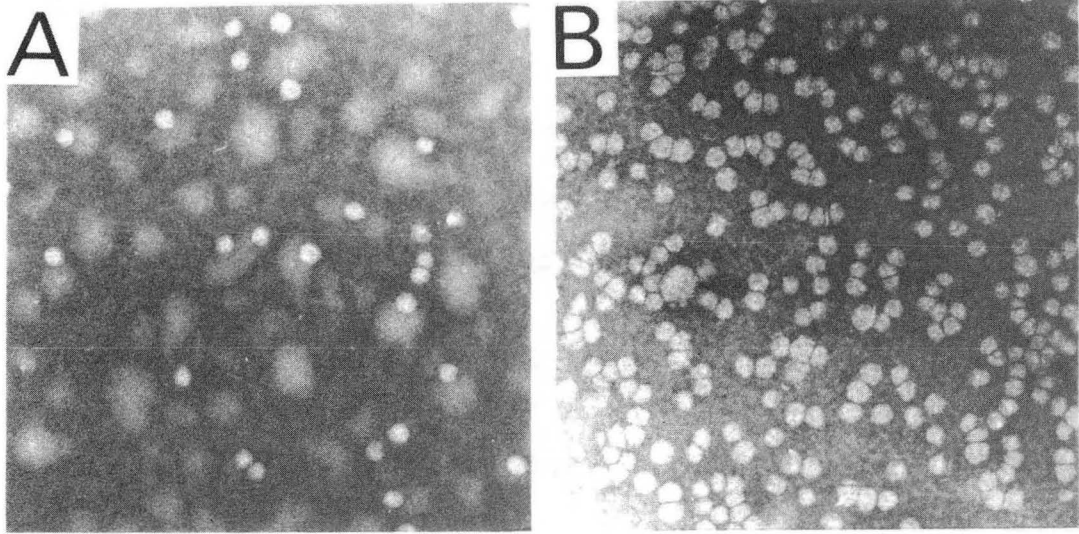
Fig 33. Comparison of the mean apparent particle diameters (APD) of a multicomponent LDL pattern obtained by gradient gel electrphoresis and the mean particle sizes of discoidal complex-exposed LDL (top) and PC vesicle-exposed LDL (bottom) by electron microscopy. Different symbols designate data from different experiments.

discoidal complex-exposed LDL

r=0.89
slope=0.72

PC vesicle-exposed LDL

r=0.93
slope=0.79

EM Size (A)

GGE APD (A)
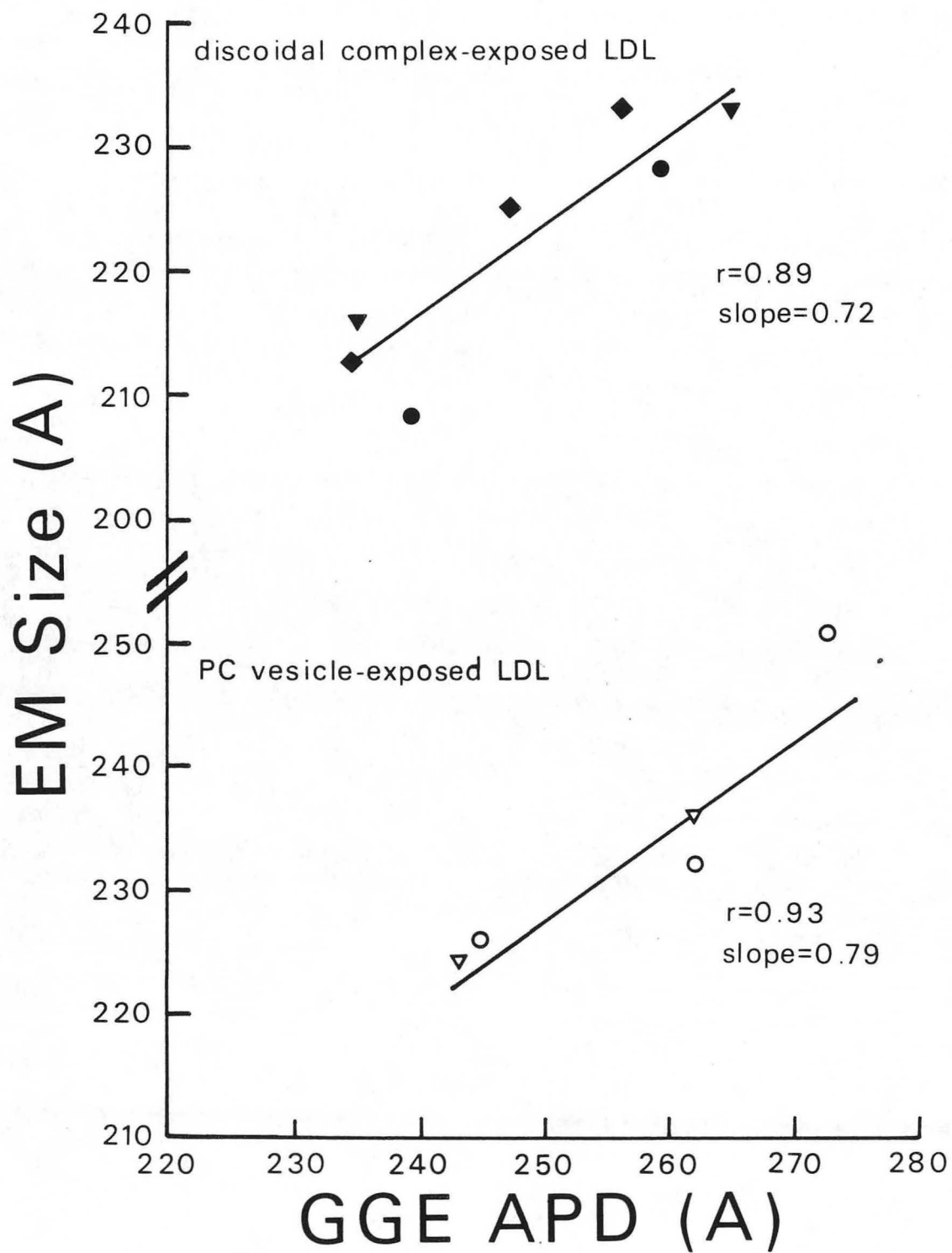
XBL 848-7882

size of the DC-exposed LDL is observed by EM, comparable to that obtained by GGE. Thus, the extent of increase in particle diameter of DC-exposed LDL (by EM or GGE) is more than that predicted by the Shen model. Figure 33, bottom, shows that a good correlation exists between EM particle size and GGE APD value, and that the slope of the regression line using DC-exposed LDL (0.72) is comparable to that (0.79) using PCV-exposed LDL.

5. Susceptibility of the Apoprotein moiety of Discoidal Complex-Exposed LDL to Trypsin

Alterations in size and possibly shape of LDL due to PL uptake may produce alterations in surface properties of LDL. To investigate whether PL uptake by LDL together with the associated changes in APD altered the protein moiety on the surface of intact LDL, the accessibility of apoB to trypsin attack during short term proteolysis was assessed. SDS-PAGE patterns of LDL (isolated by gel filtration; TI), both nonincubated (Fig 34, lane 8) and its class I products (Fig 34, lane 10), showed the presence of a major, broad, high molecular weight (247 Kd) band and two very faint bands (MW, 193 Kd and 136 Kd). Some minor, large MW bands (MW>250 Kd) were also present, which may have been aggregates of apo B formed during delipidation.

Limited tryptic digestion (37°C, 2h, 1:100 enzyme:LDL-protein weight ratio) of LDL not exposed to DC (Fig 34, lane 9) resulted in the disappearance of the major, high MW band and appearance of several bands mainly within MW range of

Fig 34. Changes in susceptibility of discoidal complex-exposed LDL to trypsin attack Nonincubated LDL and discoidal complex-exposed LDL were isolated by gel filtration as described in Results, section D3. Isolated LDL were treated with trypsin (37°C, 2h, 1:100 enzyme:LDL protein weight ratio) and SDS-polyacrylamide gel electrophoresis (4% gel) was performed on 50 µg samples. Lane 2, DJ's nonincubated LDL; lane 3, DJ's LDL treated with trypsin; lane 4, DJ's discoidal complex-exposed LDL; lane 5, DJ's discoidal complex-exposed LDL treated with trypsin; lane 6, DJ's LDL incubated with discoidal complexes and albumin; lane 7, DJ's LDL, first incubated with discoidal complexes and albumin and then treated with trypsin; lane 8, TI's nonincubated LDL; lane 9, TI's LDL treated with trypsin; lane 10, TI's discoidal complex-exposed LDL; lane 11, TI's discoidal complex-exposed LDL treated with trypsin; lanes 1 and 12, molecular weight calibration proteins.

1 2 3 4 5 6 7   8 9 10 11 12

94 Kd ▶
67 Kd ▶
43 Kd ▶
30 Kd ▶
20 Kd ▶
14.4 Kd ▶
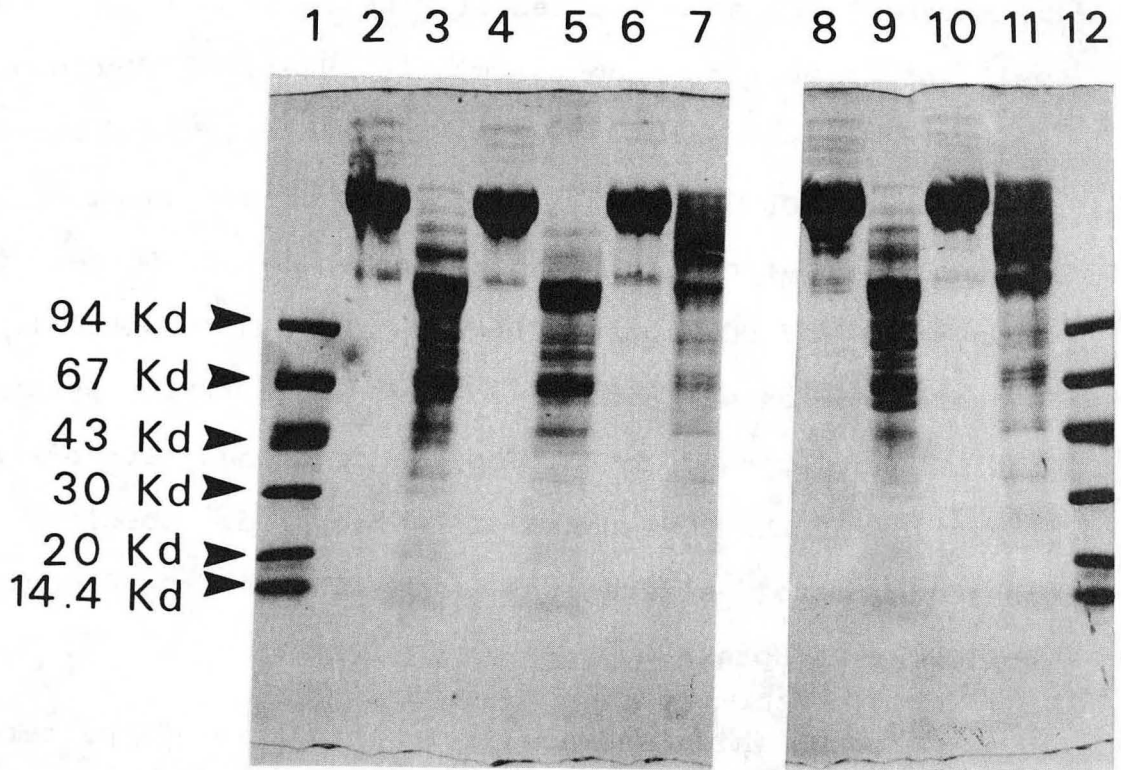
XBB 849-6738

130 Kd to 62 Kd. Proteolysis of class I products, chromatographically-isolated from incubation mixtures of LDL and DC, resulted in a pattern (Fig 34, lane 11) different from that of trypsinized LDL not exposed to DC (Fig 34, lane 9); major bands at MW values of 256-150 Kd and 128 Kd, as well as minor components within 92-67 Kd MW range, were present in the former. Thus, the proteolytic pattern of DC-exposed LDL remained at higher MW values compared to the proteolytic pattern of LDL not exposed to DC. Longer incubation (4h) of DC-exposed LDL with trypsin resulted in a gel pattern (not shown) similar to the proteolytic pattern of the LDL not exposed to DC. Thus, a decreased rate of trypsin digestion of the DC-exposed LDL occurred, possibly as a consequence of alterations in the LDL surface organization following PL uptake.

DJ's LDL which showed little change in GGE pattern when incubated with DC, exhibited little change in the SDS-PAGE pattern (DC-exposed, Fig 34 ,lane 3; not exposed to DC, Fig 34, lane 5) upon exposure to trypsin (37°C, 2h, 1:100 enzyme:LDL-protein weight ratio). SDS-PAGE patterns of non-trypsinized LDL, both the LDL not exposed to DC (Fig 34, lane 2) and DC-exposed LDL (class I products, Fig 34, lane 4), showed the characteristic high MW (247 Kd) major bands, similar to those observed for TI (Fig 34, lanes 8, 10). Thus, when changes in PL content or in APD value of LDL were minimal, as in the case of intially large, major LDL components, no effect on the rate of trypsin attack on apoB was

observed.

6. Further Characterization of Class II Products:

In Results sections C and D, we described the formation of species beyond the LDL size range (APD range, 290-412A), when LDL interacted with either DC or PC vesicles plus BF. Unlike class I products, class II products showed only minor change in PL content. Hence, our first assumption on the structure of class II products was that they may be fusion products of LDL particles whose surface has been altered upon exposure to PL. However, electron microscopy of class II products (Fig 35) showed no particles within the APD range of class II species described by GGE. Instead, particles similar in appearance (shape and packing) and particle size (224±30A) to class I products (mean diameter, 225±28A) were present. Thus, EM observations appeared inconsistent with fusion as the mechanism for formation of class II products.

Based on their APD values, class II products of incubation of LDL with DC could be association complexes of DC (approximate width, 56±20A) and LDL (diameter range, 230-269A). A 1:1 association complex of an LDL of 240A and a discoidal complex of 56A width would have an APD value of 296A, comparable to the APD of the major component of class II products. Since each DC particle contains two apo AI molecules, a 1:1 association complex of DC and LDL would have two apo AI per apo B, or about 36 mg apo AI per mg LDL-protein in an incubation mixture of LDL and DC

Fig 35. Electron micrographs of class II products from discoidal complex-exposed LDL. Class II products were obtained by gel filtration (fractions 21-23, see Fig 31) of incubation mixtures containing LDL (subject LS) and discoidal complexes. Note the overall similarity of packing and shape to class I products shown in Fig 32B.
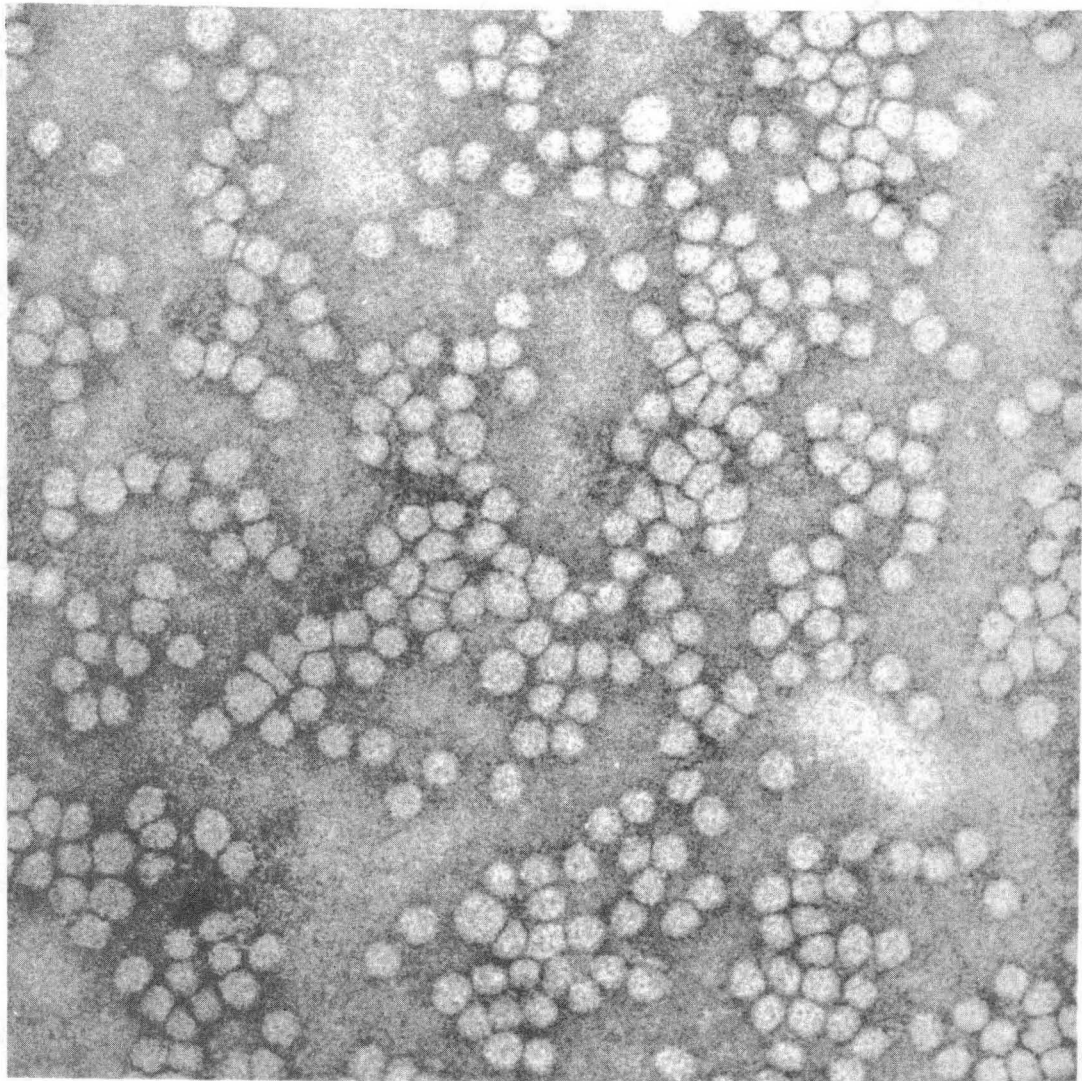
containing only class II products. However, radial immuno-diffusion, using anti-apo AI antibodies, of isolated class II products (from subjects LS and TI; 100 µg protein each), did not indicate any apo AI, under conditions where as much as 1µg apo AI per mg LDL-protein would have been detectable.

It is possible that class II products are association complexes of LDL. Evidence for this possibility derives from our GGE observations (Fig 36) showing that proteolytic digestion (37°C, 1h, 1:5 enzyme:LDL-protein weight ratio) of class II products (LS) resulted in a 90% decrease in the area under the initial peaks of class II products (295A 342A 370A 386A; Fig 36A). This decrease occurred concomitant with the appearance of two GGE components with APD values (242A, 237A; Fig 36B) corresponding to those of nonincubated LDL (LS, 240A and 230A; see Fig 28). One explanation for this observation would be that class II products are complexes of LDL bound together via their apoprotein moieties, and trypsin, by degrading some of the protein, disrupts this binding and releases LDL-sized products. The actual particle size of the particles making up the complexes cannot be unambiguously deduced from the trypsin experiments, because trypsin may alter the particle size of the LDL species (see Appendix B) released from the complex.

Fig 36. Interaction of class II products with trypsin. (A) Particle size distribution of class II products isolated by gel filtration (see legend to Fig 31) of an incubation mixture of LDL (subject LS) and discoidal complexes. (B) Particle size distribution of class II products following treatment with trypsin (37°C, 1h, 1:5 enzyme:LDL protein weight ratio). The sample was directly applied to the gradient gel (2-16%) following trypsin treatment.
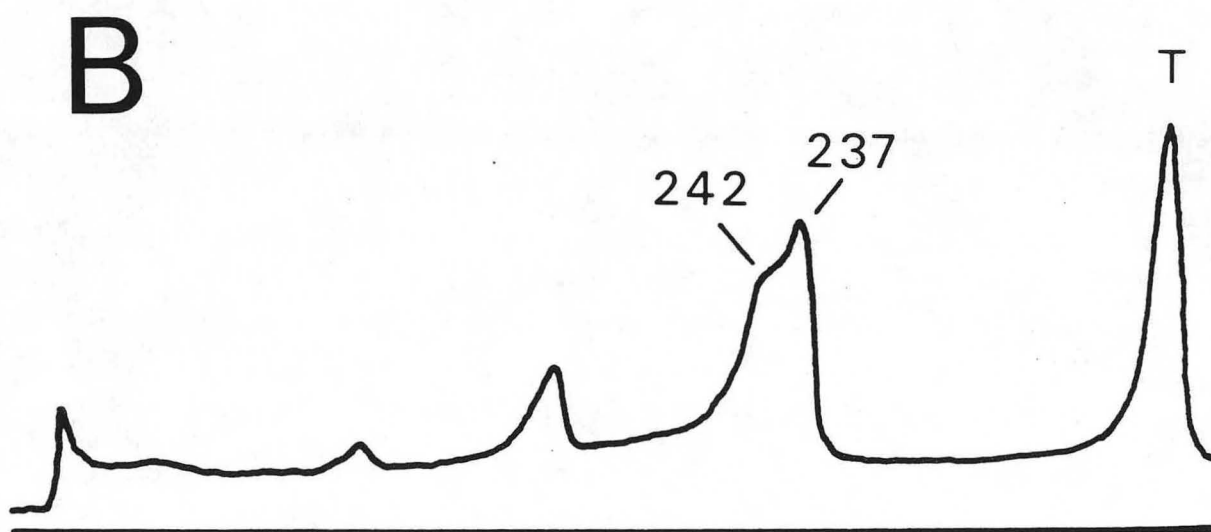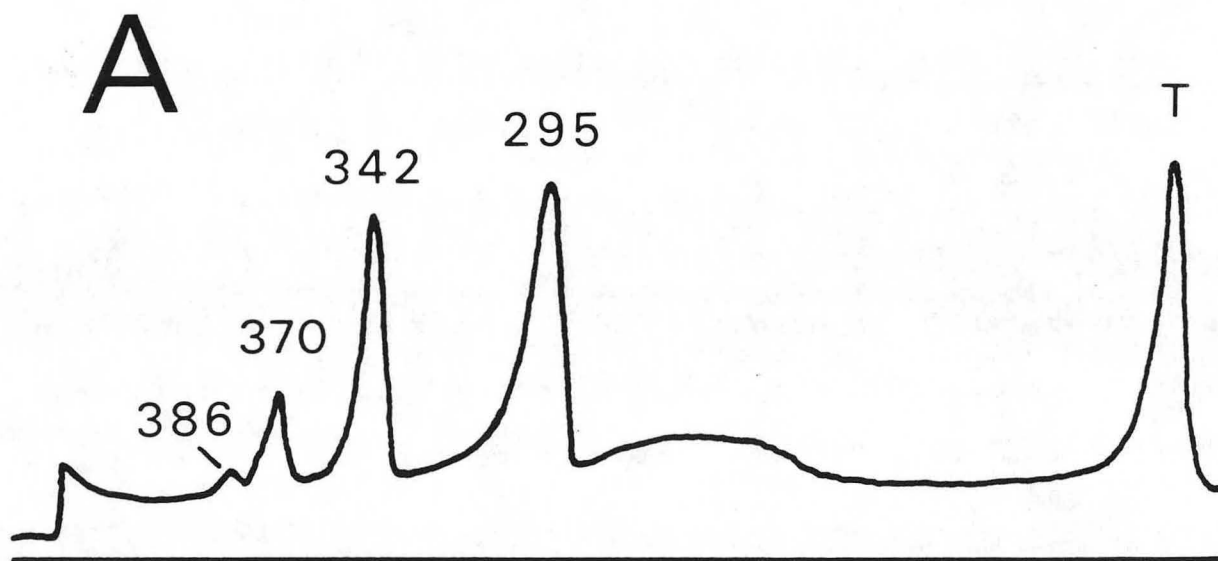
XBL 848-7887

7. Summary of Studies Using Discoidal Complexes and LDL

Discoidal complex-induced changes in LDL properties were strikingly similar to those induced by PC vesicles. During incubation (6h) of LDL with DC, an increase in LDL APD value was observed, similar to that induced by PCV during Effect II. This occurred for LDL-PL/DC-PL weight ratio within the range of LDL-PL/PCV-PL values. The APD increase using either PCV or DC was associated with minor but comparable (between the two systems) changes in hydrated density, morphology, and peak S^o_f rate. In addition to class I products, class II products were formed in both cases. Despite these similarities, however, not all the effects observed using PCV were detected in incubation studies using DC. PL levels high enough to produce Effect III using PCV, for example, did not result in comparable pattern transformations using DC. Also, no aggregates of LDL and PL, as observed with PCV, were noticed. An intriguing difference between the two systems was our observation that LDL incubation with PCV alone did not result in any APD change, whereas DC alone was sufficient to produce APD increase. BF was required for APD increase when using PCV. Studies to ascertain whether an additional increase in LDL APD might occur with DC in the presence of BF were performed and are described in the next section.

E. Incubation of LDL with Discoidal Complexes and Plasma
Components

1. Apparent Particle Size Distribution of LDL Following
Incubation with Discoidal Complexes: Role of the Plasma
d>1.20 g/ml Fraction with or without an Inhibitor of LCAT
Activity

In preliminary studies, LDL (subject ⁻G; 0.6 mg/ml pro-
tein) was incubated (37°C, 1h, 6h, 24h) with DC (1.1 mg/ml
PC) and BF (1 Co). When LCAT activity was inhibited (by
PX), a progressive increase in LDL APD was noticed with
increasing incubation time (nonincubated, 262A; incubated
(6h), 266A; incubated (24h) 270A), and class II products
were detected (24h) by gradient gel electrophoresis. The
APD value was larger in the presence of BF (LCAT inhibited)
than its absence. Thus, BF appeared to play a similar role
in facilitating APD increase in both the PCV and the DC
incubation systems. When no inhibitor of LCAT activity (PX)
was added to the incubation mixture of LDL, DC, and BF, a
progressive decrease in LDL APD value was observed (noninc,
262A; inc (6h), 260A; inc (24h), 256A) and no components
within the particle size range of class II products were
formed. The decrease in LDL APD in this system was similar
to that observed during incubation of plasma (with a large,
major LDL component) either alone (LCAT active, discussed in
Results, section B), or with low PCV levels (Effect I; dis-
cussed in Results, section C). Thus, during incubation of
LDL with DC and BF, Effect I could be seen when LCAT was not

inhibited, whereas Effect II could be seen when LCAT activity was inhibited.

Since an increase in LDL APD during interaction of LDL with DC was shown to be due to PL uptake by LDL, the properties of the BF factors leading to accelerated APD increase might relate to facilitation of PL transfer from discoidal complexes to LDL

2. Particle Size Distribution of Discoidal Complexes Following Interaction with LDL: Role of the Plasma d>1.20 g/ml Fraction with or without an Inhibitor of LCAT Activity

Changes in particle size distribution of DC (Fig 37) were evaluated during interaction of DC with only LDL, and the results were compared to those obtained in the presence of BF as well. The disc preparation consisted of a major (large dimension, 94A class 3) and three minor (125A class 4; 169, class 2; 80A, class 1) components (Fig 37A). Incubation of this disc preparation with LDL (subject BG) alone resulted in a marked decrease in area under the peak of the class 3 component in conjunction with the appearance, at 1h (Fig 37B), of a polydisperse pattern. At 6h, the heterogeneous pattern was transformed into one containing a large, major (109A) and three small, minor (87A, 84A 80A; Fig 37C) components. At 24h, the pattern consisted of one small, major component (79A, Fig 37D) and a large, (107A) minor one. In the presence of BF (LCAT active), the transformation to a large, minor (108A) and a small, major (82A) component occurred rapidly, i.e. at 1h (Fig 37E). Longer

Fig 37. Particle size distribution of discoidal complexes (DC) following interaction with LDL and plasma d>1.20 g/ml fraction (BF). Gradient gel electrphoresis (4-30% gels) was performed (A) on nonincubated DC isolated by gel filtration (see Methods, section C); and (B)-(D), on d 1.063-1.20 g/ml fractions from mixtures comprised of LDL (subject BG, about 0.8 mg/ml protein) and DC (0.4 mg/ml PC) incubated for (B) 1h, (C) 6h, (D) 24h. Mixtures of LDL, DC, and BF (plus paraoxon, 2 mM) were incubated for (E) 1h, (F) 6h, (G) 24h. Mixture of LDL, DC, and BF (without an LCAT inhibitor) were incubated for (H) 1h, (I) 6h, and (J) 24h.
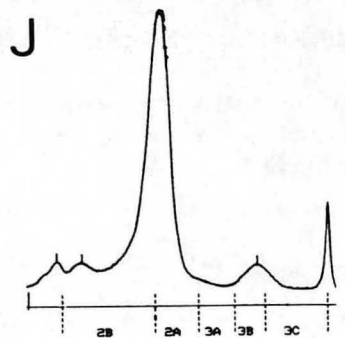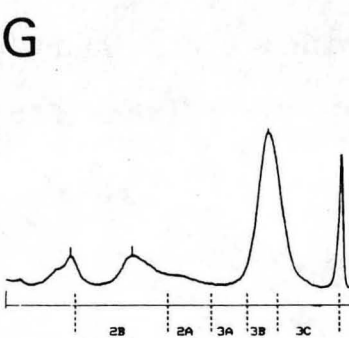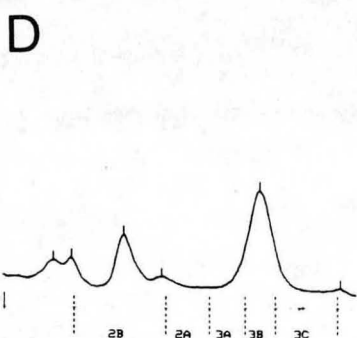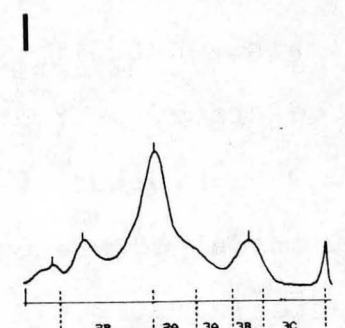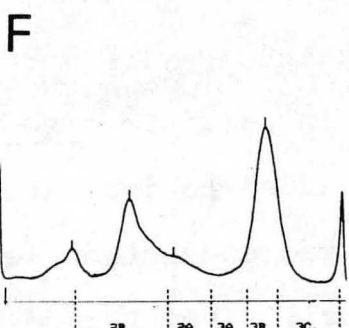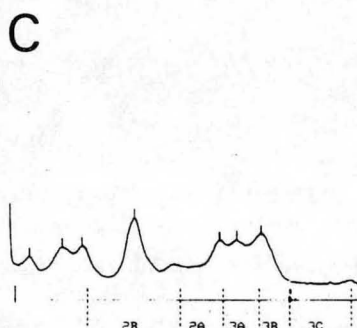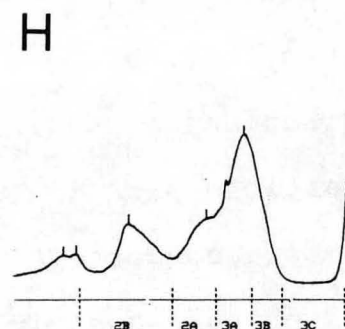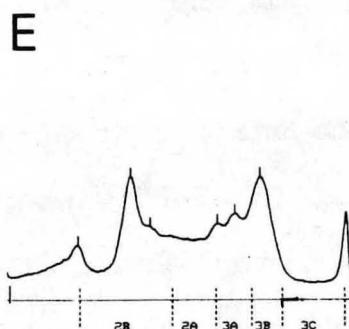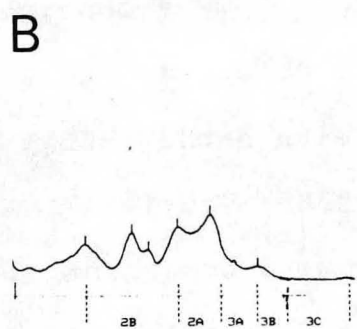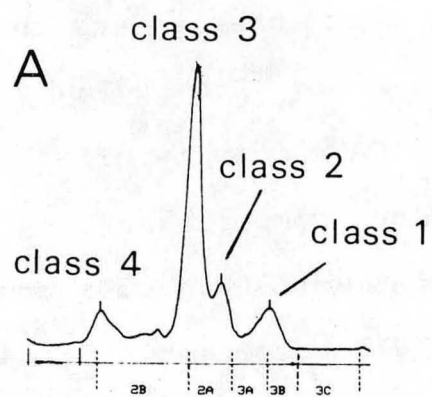
XBL 848-7863

incubation time (6h and 24h) resulted in interconversion of both components to a single peak (6h: 95A, Fig 37F; 24h: 94A, Fig 37G). In the absence of LCAT activity, BF first enhanced conversion of class 3 discoidal complexes mainly to a large, minor (1h: 107A, Fig 37H; 6h: 106A, Fig 37I) and a small major (1h: 86A, 83A 80A; 6h: 78A) component. At 24h, a single small, major component (78A; Fig 37J) was observed. Thus, both LDL and BF (LCAT inhibited) transformed class 3 discoidal complexes to smaller species (within the $(HDL_3)_{gge}$ particle size interval (81.5-87), whereas BF (active LCAT) first converted the complexes to the small component (1h) which subsequently (6h-24h) was transformed to a larger one, within $(HDL_{2a})_{gge}$ particle size interval, 87A to 99A'. The accelerated decrease in particle size of DC when BF (with LCAT inhibitor) was added to incubation mixtures of LDL and discoidal complexes, was consistent with the notion that factor(s) in BF facilitate PL removal from discoidal complexes. We next examined the properties of these factors and made attempts at their identification and purification from BF.

3. Identification of a Facilitation Factor in Plasma d>1.20 g/ml Fraction: Effect of Albumin on the Apparent Particle Diameter of LDL Incubated with Discoidal Complexes

Our assay for facilitation factor activity in BF, evaluated changes in LDL APD value during incubation ($37^{\circ}C$, 6h) of LDL (0.3 mg/ml PC) with PCV (0.8-1.5 mg/ml PC) plus the fraction to be tested. In preliminary studies, the

factor was found to be nondialysable (MW>6000), heat-stable (56°C, 30 min), and not sensitive to either disulfide reagents (e.g. mercaptoethanol or glutathione) or high ionic strength (I=0.64) solutions used for ultracentrifugal separation of BF from lipoproteins. The factor was also stable to at least three consecutive ultracentrifugations (40000 rpm, 24h, each). These observations suggested that the factor is a protein other than LCAT

Preliminary attempts at fractionation of BF were performed by a single-step ultracentrifugation (Sorvall TV-850 rotor, 50000 rpm, 3h, 15°C) of plasma (10 ml) adjusted to d 1.30 and overlaid with d 1.006 NaCl solution (24 ml). The lipoproteins floated away from plasma proteins (BF) into the top 16 ml volume, and separate 2 ml fractions were collected below this volume and assayed for facilitation activity. By evaluating the APD increase during incubation (37°C, 6h) of LDL and PCV, the factor was shown to be present in the 20th ml through 34th ml fractions (not shown), but not the 16th through 20th ml fractions. From the ultracentrifugal distribution of cholesterol (not shown) it was apparent that the 20th ml through the 34th ml fractions contained little cholesterol, indicating that the factor probably was not a lipoprotein (e.g. very high density lipoproteins).

Following a scheme generally used for purification of LTPs in BF (85,86), attempts were next directed to further isolation of the facilitation factor. During fractionation of BF using phenyl-sepharose affinity chromatography, the

facilitation factor appeared in the unbound fraction. This observation ruled out the possibility that LTPs were involved in LDL pattern transformation. In fact, during incubation (37°C, 6h) of LDL (JB, DJ) with either PCV (Table 13, top) or DC (Table 13, bottom) in the presence of partially-purified PL transfer protein (0.27 mg PLTP per mg LDL-protein) the APD values of the major LDL components remained similar to those observed during incubation in the absence of PLTP. Similarly, incubation (37°C, 6h) of LDL (DJ) and DC in the presence of PLTP, did not facilitate transformation of discoidal complexes to smaller species (not shown), in contrast to the effect observed by BF. In contrast, this PLTP preparation (100 µg PLTP per mg HDL protein) enhanced PL transfer to HDL and interconversion of HDL (diameter of nonincubated major component, 86A; Fig 38, lane 1) to larger (90A, Fig 38, lane 3) species (compared to 87A in the absence of PLTP; Fig 38, lane 2) during incubation (37°C, 3h) with PCV.

One of the most abundant proteins in BF which does not bind to phenyl-sepharose (86) and has binding sites for PL (90) is albumin. Thus, we tested the ability of human albumin (fatty-acid free) to induce LDL transformation in the presence of a source of PL (e.g. PCV or DC). Incubation (37°C, 6h) of LDL (DJ, LS, and DR) with either DC or PCV in the presence of albumin (35 mg/ml) resulted in both an increase in APD value (Table 13) and transformation to single peak pattern (Table 13 and Fig 39C). A similar

Table 13 -Apparent particle diameters (Å) of the major components of LDL: Effect of incubation[*] with PC vesicles (top) or discoidal complexes (bottom).

| | subjects | | | |
	JB	DJ	LS	DR
noninc LDL	250,238,224	268,262	240,230	240,229
inc (+PCV)[**]	249,240,228	268	243,233	245,233
inc (+PCV+PLTP)[**]	250,241,228	268	---[‡]	---[‡]
inc (+PCV+HSA)[**]	---[‡]	275	261	256
inc (+DC)[**]	253,243,236	270,265	250,247,240	248,239
inc (+DC+PLTP)	253,242	270,264	---[‡]	---[‡]
inc (+DC+HSA)	---[‡]	281	257	256

[*]Incubation (6h) mixtures contained LDL (0.3 mg/ml protein) in the presence of a combination of the following components: PC vesicles (0.8 mg/ml PC); discoidal complexes (0.4 mg/ml PC); partially-purified phospholipid transfer protein (80 μg/ml); human serum albumin (35 mg/ml).

[**]PCV, PC vesicles; PLTP, partially purified phospholipid transfer protein; HSA, human serum albumin; DC, discoidal complexes.

[‡]not done.

Fig 38. Effect of partially-purified phospholipid or cholesterol ester transfer proteins on particle size distribution (4-30% gel) of HDL. Lane 1, HDL; lane 2, HDL incubated with PC vesicles; lane 3, HDL incubated with PC vesicles and partially-purified PL transfer protein; lane 4, HDL incubated with PC vesicles and partially purified CE transfer protein; lane 5, high molecular weight protein standards. The concentration of components within the incubation (37°C, 3h) mixtures were: HDL, 0.8 mg/ml protein; PC vesicles, 1.3 mg/ml PC; transfer protein, 80 µg/ml. Samples were brought to 1 ml total volume with a Tris buffer (buffer B, Methods, section A).
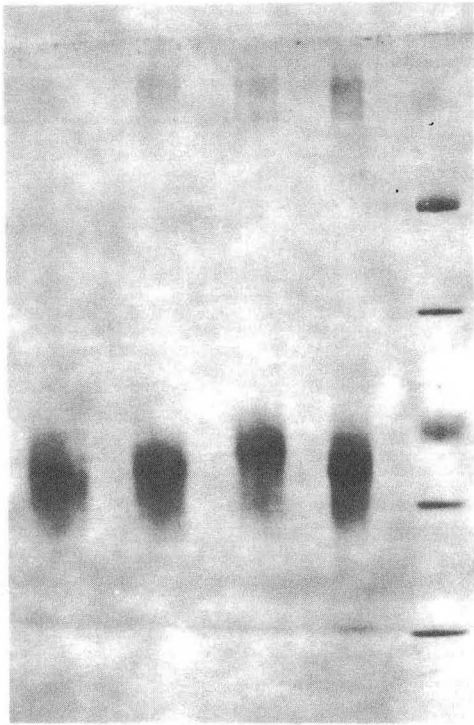
thyroglobulin

apoferritin

catalase

lactate dehydrogenase

bovine serum albumin

XBB 849-6745

Fig 39. Effect of albumin on the particle size distribution (2-16% gel) of LDL (subject LS) following interaction with discoidal complexes. For details of incubation conditions see legend to Table 13.
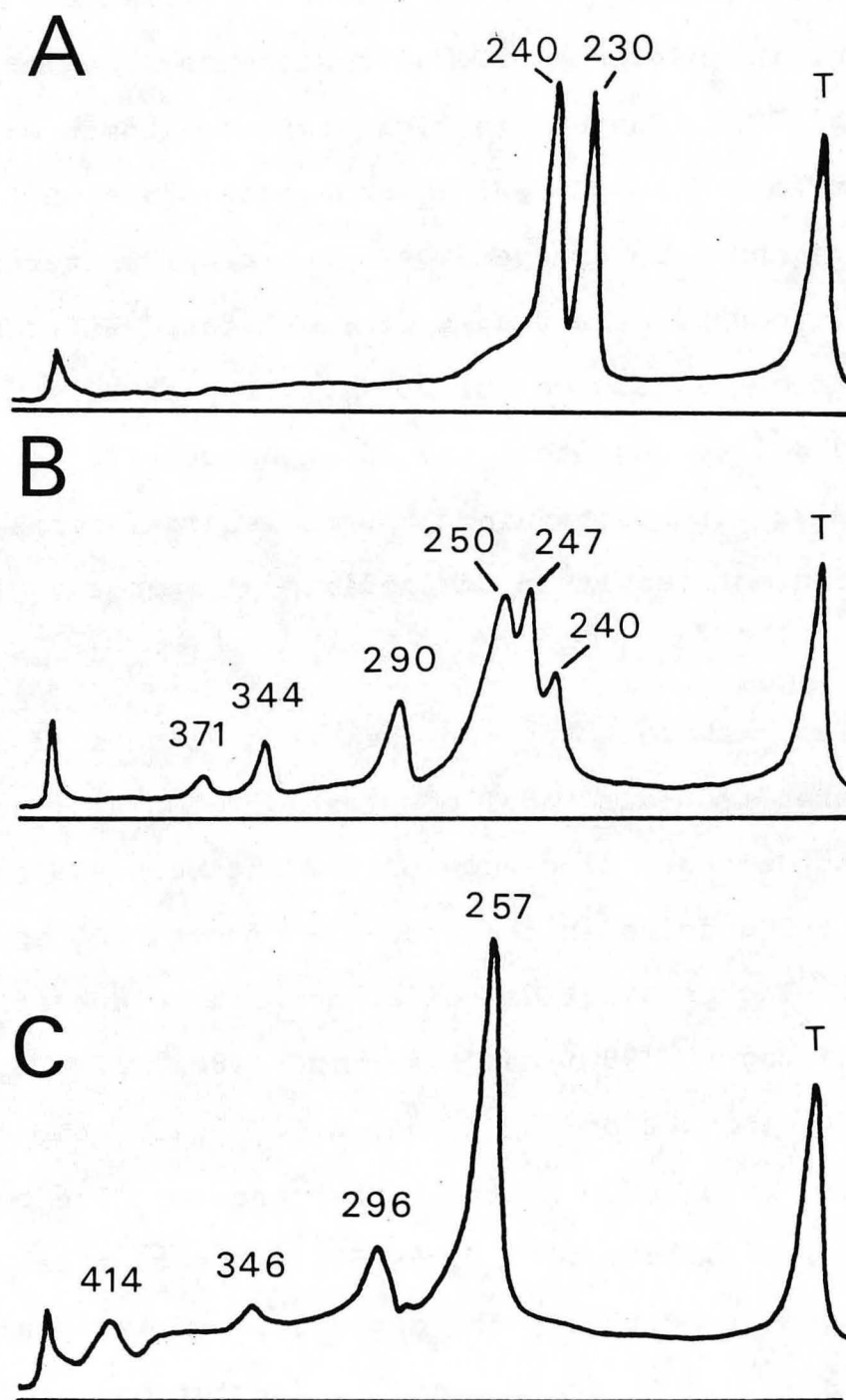
XBL 848-7868

transformation to single-peak pattern occurred during longer term (24h) incubation of LDL with discoidal complexes alone (see Fig 28). These data suggest that albumin may be one of the factors in BF which can accelerate LDL pattern transformation to larger, single peak patterns. This presumably occurs as a result of facilitated PL transfer by albumin from a source of PL (e.g. PCV or DC) to LDL. It should be pointed out that the addition of PLTP to the incubation mixtures containing LDL discoidal complexes, and albumin did not result in any additional change in the patterns.

Indirect support for the idea that albumin facilitates PL transfer from discoidal complexes to LDL derives from an experiment demonstrating accelerated interconversion of DC to smaller species in the presence of both LDL and albumin (Fig 40). The original discoidal complex preparation contained a major (95A) and two minor (88A, 80A) components (Fig 40A). Incubation ($37^{o}C$, 6h) of DC with LDL (subject DJ) alone resulted in the appearance of five components (110A, 94A, 88A, 86A, 81A; Fig 40B). Incubation of DC with albumin alone resulted in the appearance of two small, major components (92A and 86A; Fig 40D). Incubation in the presence of both LDL and albumin (Fig 40C) resulted in conversion to a single major peak (80A) plus a minor component (110A). A similar observation was made when LS's LDL was used (not shown), indicating enhanced transformation of discoidal complexes to smaller species in the presence of

Fig 40. Particle size distribution (4-30% gel) of discoidal complexes following interaction with LDL (subject DJ) and albumin. For incubation conditions see legend to Fig 28. Patterns are for (A) nonincubated discoidal complexes; (B) discoidal complexes incubated (6h) with LDL; (C) discoidal complexes incubated (6h) with LDL and albumin; (D) discoidal complexes incubated with albumin.

A
noninc

B
inc (+LDL)

C
inc (+LDL+albumin)

D
inc (+albumin)

2B   2A   3A   3B   3C
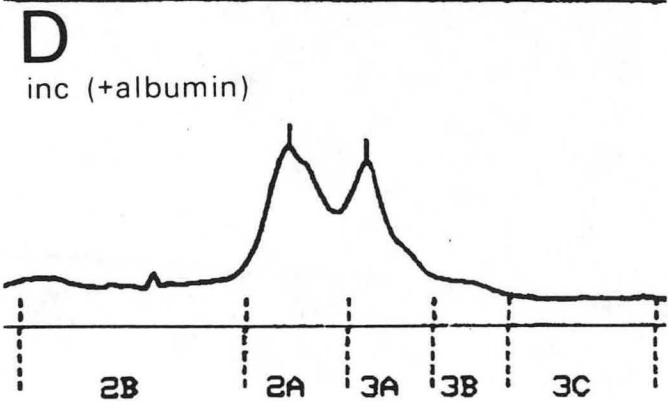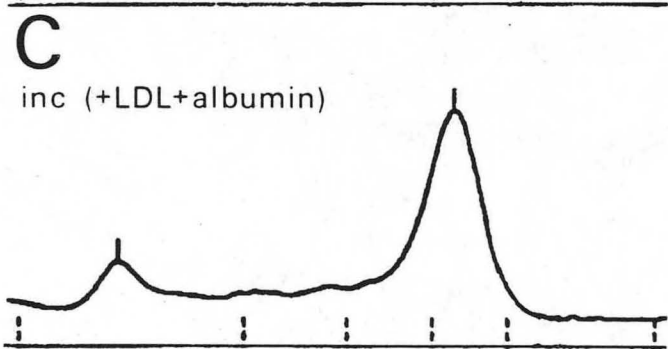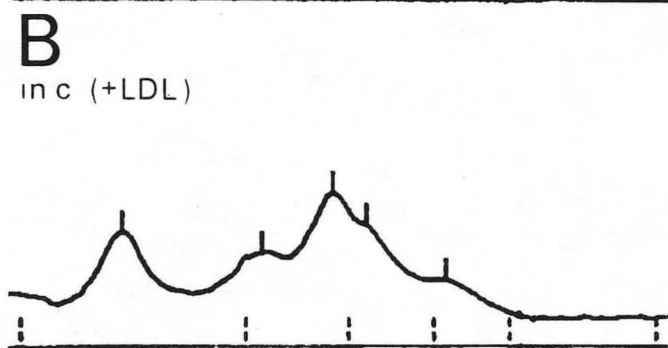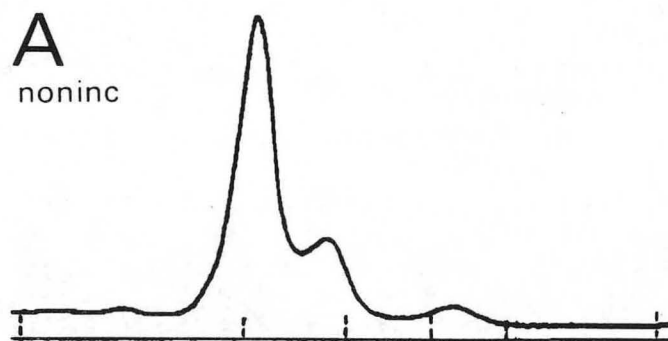
XBL 848-7873

both LDL and albumin.

4. Chemical Characterization of LDL following Incubation with Discoidal Complexes and either Albumin or the Plasma d>1.20 g/ml Fraction

In order to directly evaluate the role of BF and albumin in enhanced LDL APD increase, changes in chemical composition of LDL (subjects DJ and LS) were compared for class I products formed during incubation (37°C, 6h) of LDL (DJ, LS) and discoidal complexes (0.4 mg/ml PC) in the presence and absence of albumin or BF. After incubation, the incubation mixtures were fractionated by gel filtration under conditions previously described (91). The LDL peak (subject DJ) in the elution profile of the incubation mixtures containing LDL, discoidal complexes, and either albumin (fraction 25; not shown) or BF (fraction 25; not shown) was shifted to a lower elution volume compared to that obtained in the absence of albumin and BF (fraction 26). These results were consistent with the larger APD values of LDL observed by GGE for the mixtures containing albumin (major LDL component: nonincubated, 268A and 262A; incubated (+DC), 270A and 265A; incubated (+DC+albumin), 281A; incubated (+DC+BF with LCAT inhibitor), 280A). The larger APD values (by 9-10A) were associated with 12-13% higher PL/protein weight ratios than the ratios in incubation mixtures containing only LDL and discoidal complexes (0.98). A decrease in LDL UC/protein weight ratio (nonincubated LDL, 0.31) in the presence of BF (by about 40%) was seen, comparable to that in its absence

(by about 35%), but more than that in the presence of albumin (by about 26%).

The LDL peak (subject LS) of the elution profile of the incubation mixture containing albumin (Fig 31C) was slightly shifted to lower elution volume compared to that (Fig 31B) in the absence of albumin. The increase in PL/protein weight ratio (40%) in the incubation mixture containing LDL, DC and albumin was more than that in the absence of albumin (30%). The decrease in UC/protein in the mixture containing albumin (25%) was less than that in the absence of albumin (35%). These data indicated that, irrespective of the initial particle size of LDL enhanced LDL transformation occurred in the presence of albumin, which was related to enhanced PL uptake by LDL and a smaller decrease in UC content of LDL. In addition, the larger the initial LDL size, the less the extent of enhancement by albumin of both LDL APD increase and uptake of PL.

The changes in LDL PL content were associated with reciprocal changes in the PL content of the discoidal complexes. Thus, the PL/protein weight ratio of the d 1.063–1.20 g/ml fraction obtained from the incubation mixtures (LDL plus DC) decreased by 31% in the absence and by 63% in the presence of albumin. This ratio in the initial disc preparation was 2.53. Incubation of albumin with DC in the absence of LDL resulted in a 17% decrease in PL content of DC, indicating that both PL removal from the discoidal complexes and the shift in their pattern to one indicating

formation of smaller species are more extensive in the pres-
ence of both LDL and albumin (e.g. 63% decrease in
PL/protein) compared to the sum (48%) of the effects of
either LDL (31%) or albumin (17%) alone.

These observations were consistent with enhanced PL
transfer from discoidal complexes to LDL in the presence of
albumin. Albumin and not PLTP was thus found to be one of
the factors in BF that behaved as a facilitation factor; the
possibility of other facilitation factors in BF awaits addi-
tional studies.

5. Susceptibility of Apo B to Trypsin Attack Following
Interaction of LDL with Discoidal Complexes and Albumin

In Results, section D5, we showed an altered rate of
trypsin digestion of apo B within class I products formed
during incubation of small, major LDL components (TI, see
Fig 34) with discoidal complexes. We also found that when
changes in PL content and APD value were minimal, as in the
case of large, major LDL components (e.g. subject DJ), no
effect on the rate of trypsin attack on apo B was observed.
In the preceding sections, we observed PL uptake and APD
increase for a large, major LDL component (subject DJ, Table
13), when incubated with DC and albumin. Thus,we expected
that class I products from this incubation mixture (i.e.,
with added albumin) might also show an altered proteolytic
pattern compared to either nonincubated LDL or LDL incubated
with DC alone. Indeed, the SDS-PAGE pattern of apo B from
DJ's LDL in incubation mixtures containing discoidal

complexes, and LDL, and albumin showed less degradation (see Fig 34, lane 7) than LDL from mixtures containing LDL and DC only (Fig 34, lane 5). It is interesting that SDS-PAGE pattern of trypsin-treated LDL isolated from an incubation mixture containing DJ's LDL plus DC and albumin (Fig 34, lane 7) was similar to the pattern of trypsin-treated LDL isolated from an incubation mixture containing TI's LDL plus DC without albumin (Fig 34, lane 11). These data were consistent with the notion of altered accessibility of apo B to trypsin following PL uptake and APD increase.

6. Reversibility of Changes in Electrophoretic Properties of LDL Exposed to DC: Roles of HDL and Albumin

Using radiolabelled PL several studies have shown that most of the PL of LDL is both accessible to hydrolysis by phospholipase (92) and can readily exchange with HDL-PL. Although the location and exchangeability of the additional PL taken up by LDL from DC is not known, it is likely that this is also within an exchangeable pool on the LDL surface. Based on this assumption, it was of interest to establish whether removal of the added PL from the LDL surface was possible and whether it would reverse the APD increase previously induced by PL uptake. Of plasma factors that are known to have a high capacity for PL uptake, HDL was chosen as acceptor for excess PL from LDL. Following incubation ($37^{\circ}C$, 6h) of DR's LDL (initial particle diameters, 240A and 229A; Fig 28 and Fig 11, lane 1) with DC, HDL (HDL-PL/LDL-PL mole ratio approximately 10:1) was added, and incubation was

resumed for another 6h. GGE was performed directly on the incubation mixture (Fig 41). In the absence of HDL, both class I and class II products were observed (Fig 41, lane 2). Following the second incubation with HDL, a decrease in the APD values of class I components (from 248A and 239A to 245A and 232A, Fig 41, lane 3) was observed and the bands corresponding to class II products appeared less intense. Addition of albumin (35 mg/ml) plus HDL to the incubation mixture, further decreased the APD values of class I products (240A and 230A; Fig 41, lane 5) to the original value.

The above results indicate that a decrease in the APD values of class I species is effected by HDL, and that reversal of APD values to those observed for nonincubated LDL is possible by a combination of HDL and albumin. When HDL, without (Fig 41, lane 6) or with (Fig 41, lane 7) albumin, were present in the initial incubation mixture containing LDL and DC, no change in LDL pattern was observed, most likely because HDL competed with LDL for the PL provided by the DC.

Addition of albumin following incubation of a mixture of LDL and discoidal complexes, and resumption of incubation for another 6h, resulted in an increase, instead of a decrease (as seen in the presence of HDL), in the APD values of LDL components (Fig 41, lane 4). Also, transformation of the intial bimodal pattern to a single peak pattern was observed. This was consistent with our previous observation (e.g., see Table 13), in which albumin (initially present in

Fig 41. Reversal of changes in particle size distribution (2-16% gel) of discoidal complex-exposed LDL induced by HDL (with or without albumin). Lane 1, nonincubated LDL (subject DR); lane 2, LDL incubated (6h) with discoidal complexes; lane 3, LDL was first incubated (6h) with discoidal complexes, followed by addition of HDL and a second incubation (6h); lane 4, LDL incubated (6h) with discoidal complexes and albumin; lane 5, same as lane 3 except that both HDL and albumin were added prior to the second incubation; lane 6, LDL incubated (6h) with discoidal complexes and HDL; lane 7, same as lane 6 except that albumin was also added. For apparent particle diameters of each component, see text.
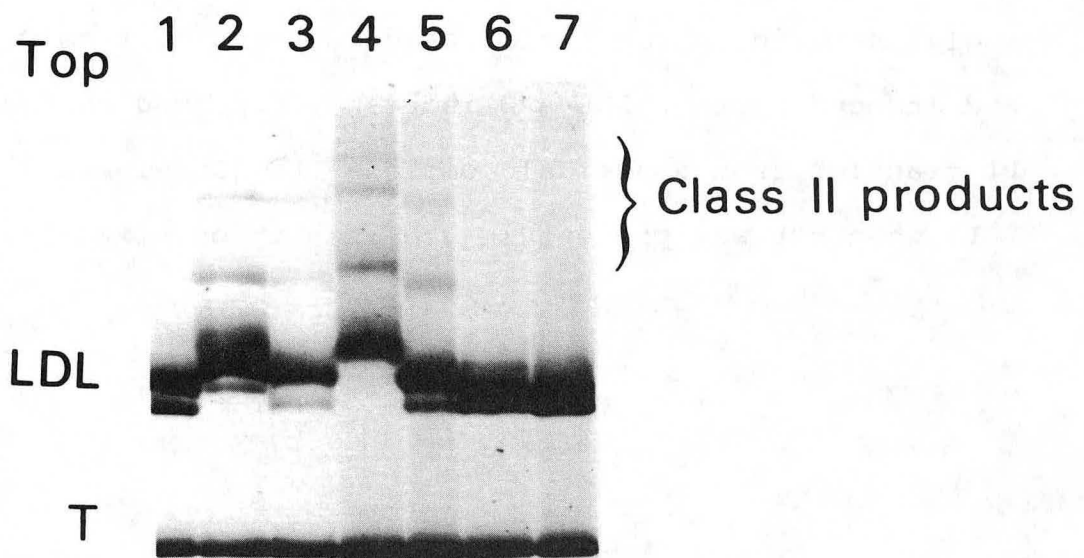
XBB 848-6386A

the incubation mixture of LDL and DC) facilitated transformation of LDL pattern to one with a single component with larger APD values.

Thus, the APD increase in LDL, induced during interaction of DC with LDL, could be reversed by HDL. Interestingly, albumin, which facilitated PL transfer from DC to LDL and induced further LDL APD increase, appeared to facilitate PL transfer from discoidal complexes to HDL instead of to LDL, when HDL was present in the incubation mixture.

7. Summary of Studies Using Discoidal Complexes and LDL
in the Presence of Plasma Components

Incubation studies with discoidal complexes proved
valuable in elucidating the nature of LDL interaction with
sources of PL and its modulation by plasma factors. Of the
PCV-induced effects (Effects I, II, III, aggregate forma-
tion), we focused primarily on Effect II because that was
the only effect observed with DC, and that was the effect in
which BF played a major and interesting role. Thus, we
showed LDL APD increase by DC is comparable to that produced
by PCV. We showed this effect to be a result primarily of
PL uptake by LDL and minimal physical changes (e.g.,
hydrated density, peak S^o_f rate, or morphology). We showed
that APD change due to PL uptake was associated with changes
in apo ⌐ structure on the surface of intact LDL.

In both the PCV and the DC incubation systems, BF
enhanced LDL APD increase, primarily due to enhanced PL
uptake by LDL. Albumin alone could simulate the effect of
BF in both cases. Finally, in the presence of a PL acceptor
(HDL), albumin enabled reversal of LDL APD change back to
the original particle size.

Our studies established that PL, found as a surface
component in lipoproteins, can be taken up by LDL from
external sources (e.g. PCV or DC) with an increase in APD
value (class I products) and formation of class II products.
Other workers have shown (93) that LDL can take up other
surface-reactive agents (e.g. detergents like sodium

deoxycholate). At appropriate concentrations that do not disrupt LDL structure, uptake of sodium deoxycholate by LDL also induces an increase in apparent particle size. Another surface-reactive agent is lysophosphatidylcholine (LPC). LPC is a surface component of lipoproteins which is metabolically released, similar to PC, during lipolysis of the TG-rich lipoproteins (94) and LCAT activity (95). Although it is thought that the LPC released during lipolysis is removed by albumin (96), other studies (97) have indicated that LDL also has a high affinity for LPC. We were interested in evaluating possible changes in LDL APD value upon interaction with another surface-active agent, namely LPC.

F. Interaction of LDL with Lysolecithin: Effect on the Apparent Particle Size Distribution of LDL

To investigate the GGE properties of LDL following interaction with LPC, LDL (subject EB; 0.6 mg/ml protein) was incubated (37°C, 6h) with egg yolk lysolecithin (0.5-3.9 mM* in Tris buffer) and the total incubation mixture was directly applied to the gel. The nonincubated LDL pattern showed a small, major peak (245A; Fig 42, lane 1). With increasing added LPC levels, a progressive increase in LDL APD value (0.5 mM LPC, 253A Fig 42, lane 2; 1.5 mM LPC, 270A, Fig 42, lane 3) was observed. In addition, minor components (298-339A) within the size range of class II products were produced. At a LPC-PL/LDL-PL molar ratio (1.85) within the range of PCV-PL/LDL-PL molar ratio (0.7-3) used in PCV incubation studies, a comparable APD increase was noticed with either of the agents (about 15-17A). This observation suggests that a common mechanism may be involved in producing alterations in LDL GGE distribution, i.e. uptake of a surface-reactive agent. At higher LPL levels (3.9 mM), LDL was completely transformed to species within class II product range (303A; Fig 42, lane 4). In contrast, at similar PCV molar concentrations in the incubation mixtures containing LDL, PCV, and BF, marked aggregation of LDL with PCV occurred.

---

*The concentration of LPC was in the range of three to eight times the concentration of LPC normally found in plasma (240 µM (98)).

Fig 42. Effect of incubation of LDL with lysolecithin (LPC) on the particle size distribution of LDL. Lane 1, nonincubated LDL. Lanes 2 and 5, 0.5 mM LPC; lanes 3 and 6, 1.5 mM LPC; lanes 4 and 7, 3.9 mM LPC. Lanes 2-4 contained only LDL and LPC; lanes 5-7 contained LDL, LPC, and plasma d>1.20 g/ml fraction.

Top

1 2 3 4 5 6 7

LDL

T
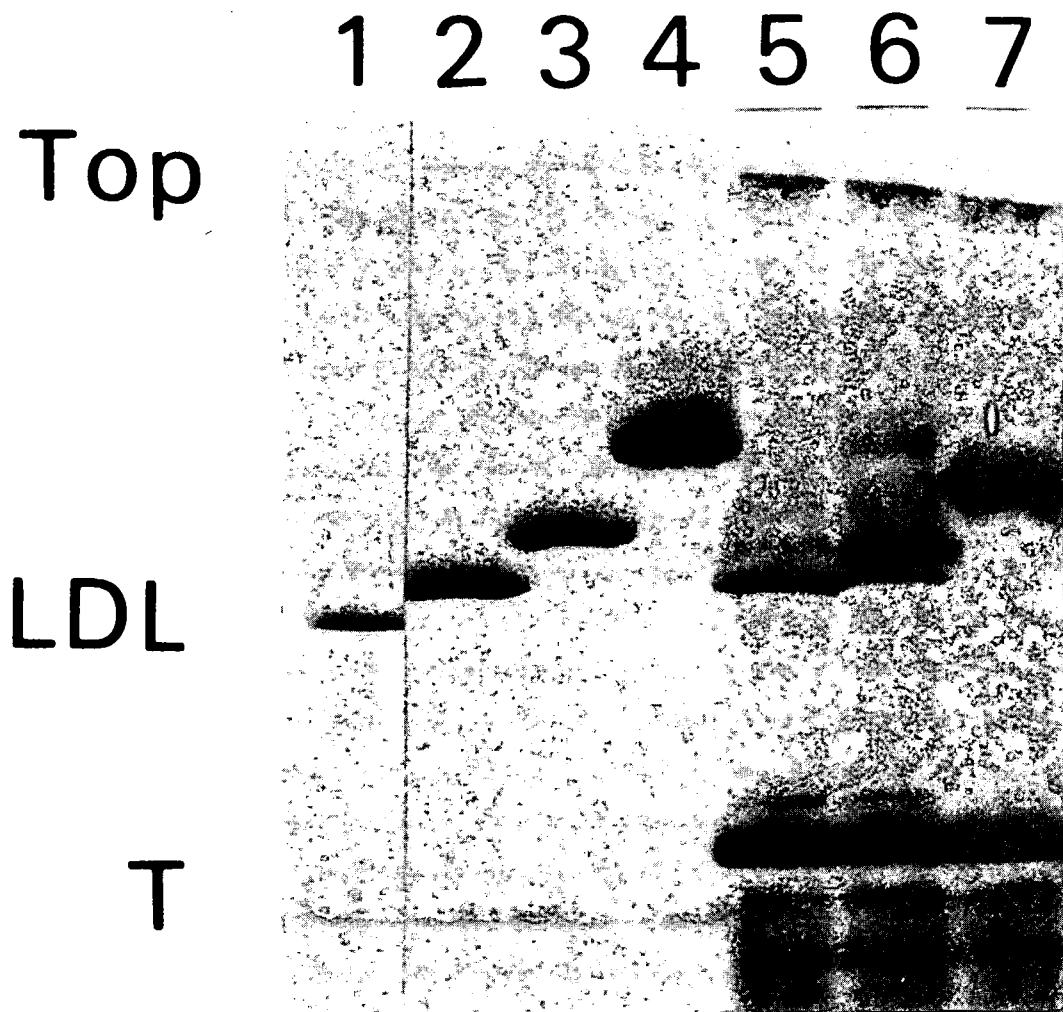
XBB 849-6751

We expected that the addition of ⁻F or albumin, which would likely complete with LDL for LPC uptake, might attenuate both LPC uptake and APD increase. In fact, addition of BF as a source of albumin to incubation mixtures of LDL and LPC (0.5-3.9 mM) did indeed attenuate the increase in APD value of LDL (Fig 42, lanes 5-7)). At 1.5 mM LPL, a bimodal LDL pattern (peak APD values, 258A and 264A; Fig 42, lane 6) was seen, similar to that observed during incubation of whole plasma with PCV (i.e. during Effect III). More studies are needed to show if such observations can be repeated and if the comparable sequence of bimodal to single-peak pattern transformation characteristic of Effect III would be observed using LPC and BF (instead of PCV HDL, and BF). The LPC esterifying activity of LCAT (designated LAT activity or lysolecithin acyltransferase activity), which is activated solely by LDL (99), may play a role in producing E III during incubation of LDL, LPC, and BF. It is possible that the two components within the bimodal LDL pattern represent differential interaction of LDL with LPC during LAT activity.

In summary, the similarity of action of LPC to that of DC or PCV is striking and studies on LPC interaction appear promising in providing insight into the transformation processes involved.

V. Discussion

Lipolysis of the triglyceride-rich lipoproteins within the plasma milieu results in the production of polydisperse species of particles within LDL density range. The contribution of plasma factors (e.g. HDL, lipid transfer proteins, lecithin:cholesterol acyltransferase (LCAT), albumin) in the origins of LDL polydispersity is not well-established. Studies on the origins of LDL subpopulations have generally been directed to examination of the "core pathway", mainly interconversion from larger, less dense to smaller, more dense species via lipolysis and remodelling of core composition (59). Recent studies indicate that other factors in plasma may modulate LDL structure. One such factor is phospholipid (PL) which is transiently released during lipolysis of TG-rich lipoproteins is in the form of vesicles and/or discoidal complexes of phospholipid and apoproteins. Although HDL has been shown to interact with PL and to be a major acceptor for such PL (66,67), the interaction of PL with LDL and its effect on LDL polydispersity have been little studied. In the case of HDL, _in vivo_ (65) and _in vitro_ (66,67) uptake of PL results in HDL transformations to larger, less dense species. Plasma phospholipid transfer protein facilitates PL uptake by HDL and transformation to larger, less dense species _in vitro_. Apo AI, released from HDL during such interaction, becomes associated with the PL and forms discoidal complexes. These complexes can be rapidly converted to core-containing spherical HDL species

via LCAT activity (20). In addition to PL, other surface-reactive components such as lysolecithin and unesterified fatty acids are released into plasma during lipolysis. Plasma albumin binds to and modulates the plasma level of such surface-reative agents. In this thesis, we investigate the influence of lipolysis-related surface-reactive molecules and relevant plasma components (phospholipid, lysolecithin, HDL, lecithin:cholesterol acyltransferase, lipid transfer proteins, albumin) on LDL polydispersity.

A. Interaction of LDL with Phospholipid Vesicles

Incubation of LDL from normolipidemic and a mildly hypertriglyceridemic subject with vesicles alone (for 6h) produced no change in LDL apparent particle diameter (APD). LDL from a severely hypertriglyceridemic subject (plasma triglyceride level greater than 1000 mg/dl) showed a slight increase in APD under the same conditions. Large (>400 nm) aggregates of LDL and PCV were formed when LDL from all subjects were incubated with vesicles. This was not due to oxidative degradation of LDL protein or lipids, as indicated by similarity of gradient gel electrophoretic results when incubation was carried out either in the presence or absence of a sulfhydryl reducing agent (glutathione). GGE results were also similar in the presence or absence of an inhibitor of plasma proteases (phenymethylsulfonyl fluoride). The structural and/or conformational integrity of apo B appeared important for aggregate formation, since proteolytic

cleavage of apo B by trypsin prior to interaction with vesicles prevented aggregation of LDL and vesicles (see Appendix B and ref 67). Aggregation with vesicles was specific for apo B-containing lipoproteins (VLDL, IDL, LDL, Lp(a)). Studies on the mechanism of LDL-vesicle aggregation have been reported previously by us (87).

B. Interaction of LDL with Vesicles and Plasma Components

Short term (6h) incubation of LDL (from normolipidemic and mildly hypertriglyceridemic subjects) with vesicles alone did not result in any change in LDL APD. Addition of the plasma d>1.20 g/ml fraction induced an increase in APD value of LDL. This was designated Effect II. Facilitation of APD increase by plasma d>1.20 g/ml fraction was observed for both the large (262-268A), and small (229-243A), major LDL components, although the extent of APD increase was greater in the small. The greater interactive capability with vesicles of the small LDL species (particularly those from hypertriglyceridemic individuals), compared with the large LDL species, may reflect differences in (1) core composition (i.e., triglyceride enrichment of the small LDL) and/or (2) apoprotein properties. By use of specific antibodies, differences in apoprotein epitope expression in LDL with low cholesterol ester/protein (hence smaller particle size) have been observed.[†]

[†]Krauss, R.M. and Marcel, I., personal communication.

Although aggregation of LDL with vesicles still occurred in the presence of plasma d>1.20 g/ml fraction, it was attenuated (about 40% less decrease in area under LDL pattern at each PL level) relative to that in the absence of plasma d>1.20 g/ml fraction. The ability of plasma d>1.20 g/ml fraction to take up PL has been reported (100).

Incubation of LDL, vesicles, and plasma d>1.20 g/ml fraction in the presence of an LCAT inhibitor did not alter the course of APD increase. This was not surprising in view of the fact that LCAT has both a low binding affinity and a low enzyme activity towards LDL (101,102) or vesicles.

Of the different components present in plasma d>1.20 g/ml fraction, albumin alone produced an effect similar to that of plasma d>1.20 g/ml fraction on LDL APD values (when LDL, vesicles, and albumin were incubated for 6h). This relates to the presence in albumin of hydrophobic domains that can accomodate lipid components such as PC and facilitate their transfer/exchange to acceptors such as LDL.

In contrast to the effect of albumin, phospholipid transfer protein did not produce an APD increase when added to incubation mixtures of LDL and vesicles. This was surprising in view of the fact that plasma phospholipid transfer protein facilitates both PC uptake by HDL (from vesicles) and HDL particle size interconversion (100). It is possible that phospholipid transfer protein is more reactive towards HDL than LDL. Previous studies have shown that plasma phospholipid transfer protein can promote PL uptake

by LDL from vesicles of dimeristylphosphatidylcholine (103).
It is possible, however, that some of the apparent PL uptake
may represent aggregates of LDL with vesicles rather than
actual incorporation of PL by LDL.

C. Interaction of LDL with Vesicles in the Presence of Plasma d>1.20 g/ml Fraction and HDL

The presence of HDL in incubation mixtures containing
LDL, vesicles, and plasma d>1.20 g/ml fraction considerably
attenuated APD increase (i.e., Effect II) and aggregate for-
mation. Attenuation of APD change was proportional to HDL
concentration such that at 0, 0.5, and 1.0 mg/ml HDL protein
concentration, the APD increase (in the PC range of 0.4-1.2
mg/ml) was 17-34A (mean, 21A), 7-30A (mean, 18A), and 3-21A
(mean, 12A), respectively. Since such attenuation was asso-
ciated with an increase in HDL particle size the data indi-
cated a competition between HDL and LDL for PC.

During Effect II (in the presence or absence of HDL),
larger (290-412A) but minor components (designated class II
products) also appeared, in addition to components (desig-
nated class I products) which remained within the usual LDL
particle size range (218-278A). Class II products appeared
to be association complexes of LDL particles. Apo B of LDL
was important in their formation, since trypsinized LDL did
not form class II products, and conversely, trypsinization
of class II products released LDL species. Class II pro-
ducts were produced not only in the presence of PL, but upon

exposure of LDL·to surface-reactive agents like lysolec-ithin, and to promoters of apo B conformational change like guanidine hydrochloride (see Appendix C). Recently, components within class II size and density range have been identified in media of hepatic tumor (Hep-G2) cell cultures, and their formation has been associated with intermolecular disulfide binding of apo B (personal communication, R. Thrift).

In addition to Effect II, incubation of LDL, HDL, and the plasma d>1.20 g/ml fraction with vesicles above a certain concentration can lead to major changes in the LDL pattern (designated Effect III). During Effect III, a shoulder appears on the larger APD side of the major LDL component; then the LDL profile converts to a bimodal, and subsequently a single-peak pattern. The mechanism of Effect III is unknown. We showed that the presence of HDL (but not the plasma d>1.20 g/ml fraction) was required to produce the bimodal pattern and speculated that Effect III may be a result of LDL interaction with products of HDL interaction with PC. HDL can interact with vesicles to produce discoidal complexes of apo AI and PC (66,67). It is possible that the two components within the bimodal pattern represent products of interaction of (1) LDL with vesicles and plasma d>1.20 g/ml fraction, and (2) LDL with discoidal complexes and plasma d>1.20 g/ml fraction.

An important feature of Effect III was the apparent participation of apo B in the production of the bimodal

pattern. When trypsinized LDL were incubated with HDL, d>1.20 g/ml fraction, and vesicles, a bimodal pattern was not produced. Instead, the APD value of trypsinized LDL increased up to that of the smaller component of the bimodal pattern produced by native LDL (see Fig 46, Appendix B). Conversely, trypsinization of native LDL undergoing Effect III resulted in the elimination of the larger component, within the bimodal pattern (data not shown). In view of these findings, we speculate that the smaller component of the bimodal pattern may be a precursor to the larger one. Since the APD differential between the smaller and the larger components within the bimdal pattern is about 7-10A, the latter cannot be an association complex of LDL with either vesicles or apo AI-PC discoidal complexes,[*] but may be an LDL particle with altered (i.e., swollen) apoprotein configuration. Preliminary studies showed decreased exposure of apo B to proteolytic attack during Effect III (not shown). Other studies on apo B propeties, as well as LDL composition, during Effect III may be useful in elucidating the nature of bimodal pattern formation, and bimodal to single-peak pattern transformation.

---

[*] A 1:1 complex of LDL (245A) and vesicles (250A) is expected to have an APD value of about 310A; a 1:1 complex of LDL (245A) and discoidal complexes (90A) is expected to have an APD value within the range of 276A (if the complex migrates as a fusion product) to 335A (if the complex migrates as a binary complex). These APD values are larger than that reached during Effect III.

Finally, our reconstitution experiments established that vesicle-induced changes in LDL GGE pattern were similar to those observed during incubation of whole plasma with vesicles. Although the changes were consistent with PL uptake as well as with alterations in apo B conformation, we could not characterize the properties of LDL undergoing Effects II and III, because of difficulties in product separation from vesicles and LDL-vesicle aggregates in reconstitution mixtures of whole plasma.

D. Interaction of LDL with Discoidal Complexes

While little or no change in APD value occurred during incubation of LDL with vesicles, an increase in LDL APD vlaue was observed during exposure of LDL to discoidal complexes (for 6h). This increase was similar to that observed during Effect II in interaction mixtures of LDL, vesicles, and d>1.20 g/ml fraction. In both cases (1) an APD increase occurred in both the small, and the large major LDL components, but the extent of increae was greater with the former; (2) the increases in APD value were not associated with major changes in LDL hydrated density and S_f^o rate; and (3) minor components larger than LDL (class II components) were formed. No Effect III and no aggregates containing LDL and discoidal complexes were observed, in contrast to the results obtained using vesicles.

Unique to the interaction between LDL and apo AI-PC discoidal complexes was the transformation of an initial

multicomponent LDL patterns to a single-peak pattern (at 24h) with LDL attaining a limiting APD value. The limiting APD value was smaller for the initially smaller species, possibly due to limitations in core expandibility. Some class II products were observed in interaction mixtures of LDL and discoidal complexes.

Chemical analysis of class I products isolated from incubation mixtures comprised of LDL and discoidal complexes, showed PL uptake and loss of unesterified cholesterol by LDL. The extent of APD increase (30A, 12A, 10A, 0-2A, using LDL from different individuals) was proportional to the extent of PL uptake by LDL (increase in PL/protein weight ratio, 40%, 30%, 13%, 7%, respectively). The extent of depletion in unesterified cholesterol (33-39%) from LDL did not change with increasing APD value. No other compositional changes occurred, strongly suggesting that PL uptake was the main determinant of LDL APD increase.

Our studies showed that an increase in APD was closely associated with an increase in LDL PL content. An earlier report (87) describing LDL interaction with vesicles alone noted no change in APD value during an aparent increase in PL content of 31%. It is likely that the apparent PL increase in LDL may have been due to contamination of LDL fractions with complexes of LDL and vesicles and not actual incorporation of PL into LDL. In another study (104) which have reported uptake of PL (bound covalently to nucleosides) by LDL, the properties of LDL were not examined. By small

angle neutron scattering, a 5A increase in LDL size was noted in association with PL uptake from sonicated complexes of apo AI and PC (105). In a study investigating interaction of surface-reactive agents with LDL (93), uptake of about 250 molecules of sodium deoxycholate by LDL was associated with about 27A increase in LDL apparent size, using scanning molecular sieve chromatography. In our incubation studies using apo AI-PC discoidal complexes, maximal PL uptake by a small LDL species corresponded to an increase of about 230 PL molecules per LDL particle and was associated with an APD increase of about 30A.

The mechanism of APD change induced by uptake of surface-reactive agents is unknown. Based on calculations of the increase in LDL surface area (assuming a spherical particle) produced by uptake of 230 PL molecules (molecular area, $68A^2$), an increase of about 12A in diameter would be expected, i.e., about 20A less than actually observed by GGE or electron microscopy. Since no major shape changes were observed by electron microscopy, we conclude that the structural changes in LDL, associated with PL uptake and an increase in APD value, were more complex than those predictable by the simple model of Shen et al (2). The Shen model does not take into account possible changes in LDL apoprotein configuration, or the disposition of PL head groups that may influence the effective LDL size. The additional PL taken up by LDL may promote protrusions of apo B and perhaps PL above the LDL surface that are not detectable by

electron microscopy, but which can affect LDL APD. In fact, a change in LDL surface organization was implied from our observation of a decreased susceptibility of apo B to proteolytic attack, using either apo AI-PC discoidal complexes, or d>1.20 g/ml fraction plus high levels of vesicles. Decreased susceptibility may have resulted from shielding of lysine and arginine residues of apo B by PL, and/or a conformational change in apo B. Although circular dichroic spectroscopy (data not shown) did not reveal any significant change in apo B conformation following maximal (40% increase in PL/protein weight ratio) PL uptake, this technique may not be sufficiently sensitive to subtle changes in apo B conformation as enzymatic recognition of specific amino acids. Another sensitive technique for assessing alterations in LDL protein conformation following PL uptake by LDL might be one utilizing the binding properties of monoclonal anti-apo B antibodies that recognize different apo B domains. Such studies would be helpful in elucidating the mechanism of PL-induced increase in LDL APD.

Alterations in LDL APD value were associated with PL uptake by LDL and loss of unesterified cholesterol from LDL. This lead to a drop in unesterified cholesterol/PL molar ratio of about 50%. Such a chemical alteration would result in changes in LDL surface fluidity and could probably alter protein-protein and/or protein-PL interaction at the LDL surface and lead to altered apo B conformation. A change in surface chemistry may also alter interactions between the

core lipids and surface components. Such alterations might produce core expansion (during PL-induced APD increase) without addition of any core components.

E. Interaction of LDL with Discoidal Complexes and Plasma Components

During incubation of LDL with only discoidal complexes, PL uptake by LDL and subsequent APD increase was noted. In the vesicle incubation system, the presence of plasma d>1.20 g/ml fraction was necessary to produce APD increase. Apo AI in the discoidal complexes presumably behaves as a facilitation factor. Although some residual apo AI is usually found in plasma d>1.20 g/ml fraction preparations, it apparently does not promote APD increase when LDL, vesicles, and plasma d>1.20 g/ml fraction are incubated.

The factors in plasma d>1.20 g/ml fraction responsible for vesicle-induced changes in LDL APD also promoted additional LDL APD increase when PL was provided by discoidal complexes. In both cases albumin could promote LDL APD increase, whereas phospholipid transfer protein could not. Albumin facilitated a greater extent of LDL APD increase (during incubation of LDL, discoidal complexes, and albumin) an enhanced PL uptake and a lower loss of unesterified cholesterol by LDL, compared to changes in these parameters occuring during incubation of LDL and discoidal complexes alone. Once again, our data point to the importance of surface lipid components (mainly PL) in determining LDL APD

value.

Changes in LDL properties were associated with transformation of discoidal complexes from discoidal to spherical species (with an LCAT inhibitor in plasma d>1.20 g/ml fraction) or to core-containing HDL_{2a}-like species (without an LCAT inhibitor). During such transformations, LDL were the donor of unesterified cholesterol to discoidal complexes and the acceptors of PC from discoidal complexes.

F. Interaction of LDL with Discoidal Complexes in the Presence of Plasma d>1.20 g/ml Fraction and HDL

Addition of HDL to incubation mixtures of LDL and discoidal complexes produced a reversal of the LDL APD increase. This reversal was complete (i.e., LDL APD values completely reversed back to those of the original LDL) when albumin was added with the HDL. These studies provided insight into the disposition of PC between LDL and HDL, and the role of factors in plsma d>1.20 g/ml fraction, such as albumin. Albumin apparently facilitates transfer of the PL of discoidal complexes to HDL, instead of to LDL. Although some studies (92) have shown that more than 95% of the LDL PL head groups were hydrolysable by phospholipase A_2, electron paramagnetic resonance (106) and ^{31}P-nuclear magnetic resonance (107) studies have indicated that 1/5th of LDL PL content is immobilized in LDL (presumably tightly bound to apoprotein), suggesting the existence of a close interaction between apo B and surface PL. Our demonstrations of the

reversibility of APD increase by HDL suggests that PL taken up by LDL is available for exchange or removal. It is most intriguing to examine whether, like APD, apo B susceptibility to trypsin attack is also reversible following incubation of PL-enriched LDL with HDL.

G. Interaction of LDL with Lysolecithin

Incubation of LDL with increasing levels of egg yolk lysolecithin (0.5-3.9 mM), much greater than its critical micelle concentration $0.02-o.2x10^{-4}$ M (108)) produced an increase in APD value of about 8-53A. This range of lysolecithin was about 3-8 times higher than levels usually present in total plasma ($2.4x10^{-4}$ M (98)) and about 1-10 times greater than levels produced following lipolysis of triglyceride-rich lipoproteins.[*] The APD increase (about 25A' at a lysolecithin-PL/LDL-PL molar ratio of 1.85 was comparable to that (about 17A) at a discoidal complexes-PL/LDL-PL molar ratio of 1.33, suggesting a common mechanism, between the two systems, for APD increase (namely, lipid uptake). We did not characterize the composition of LDL following interaction with lysolecithin. Published studies (104) have shown that LDL have a high affinity for lysolecithin. Although as little as a few µmoles

---

[**]Assuming a level of plasma very low density lipoproteins of about 300 mg/dl in response to a fat-free diet and 35% hydrolysis of the very low density lipoprotein PL by lipoprotein lipase during lipolysis, about 0.18 mg/ml lysolecithin is expected to be produced, using a very low density lipoprotein PL content of 18%.

lysolecithin (relative to about 10^4 cell membrane PL) are disruptive to the bilayer structure of biological membranes (109,110), another study (104) has indicated that LDL can take up as much as 798 molecules lysolecithin per particle and still appear intact within the density range of 1.019-1.063 g/ml. The separation of the intact lysolecithin-enriched LDL and the properties of such LDL were not examined in those studies. Assuming that LDL remains intact upon uptake of 798 molecules of lysolecithin, an increase of about 25A would be expected (molecular area of $50A^2$ (108)). This increase falls within the range of APD values that we observed in our studies with lysolecithin. Further work is needed to evaluate the extent of lysolecithin uptake by LDL and the consequent changes in LDL size and/or shape. Since lysolecithin has an inverted cone structure (111), it may affect packing at the surface of LDL such that it may actually extrude apo B domains above the LDL surface; lysolecithin uptake may give rise to a "swollen" LDL particle. Changes in apo B and LDL structure during uptake of sodium deoxycholate, an even smaller (molecular dimensions, 3.1x6.4A) surface-reactive agent, have been proposed (93).

H. Interaction of LDL with Lysolecithin and Plasma d>1.20 g/ml Fraction

More than 80% of lysolecithin produced during extensive in vitro lipolysis (96) in plasma is found in plasma d>1.20 g/ml fraction, mainly associated with albumin. In our

studies, competition between plasma d 1.20 g/ml fraction and LDL for lysolecithin was suggested by an attenuation of LDL APD increase when plasma d>1.20 g/ml fraction was present in the incubation mixture of LDL and lysolecithin. Such attenuation was clearly apparent at high lysolecithin-PL/LDL-PL molar ratios (1.9 and 4.9) but not at a lower molar ratio (0.6), suggesting that LDL was the primary acceptor for lysolecithin at a level of lysolecithin which was comparable to that calculated for post-meal conditions (see previous Footnote). On a molar basis, LDL have an 8-fold higher affinity for lysolecithin than albumin (97). Hence, LDL could potentially be an important acceptor for lysolecithin during slow lipolysis.

I. Biological Implications

1. Evidence for PL-Enriched, Large LDL In Vivo

Whether PL enrichment of LDL associated with APD increase occurs in vivo remans to be elucidated. The major process which produces a flux of PL in plasma occurs during lipolysis of the triglyceride-rich lipoproteins. The amount of PL flux during lipolysis has not been quantitated and the properties of LDL during both in vivo and in vitro lipolysis have not been characterized. Intravenous injection of radiolabelled chylomicrons into rats resulted in a marked increase in PL mass, first in the LDL (about 3-fold), then in the HDL density range (112). It is not certain how much of this PL was actually incorporated into the lipoprotein

particles themselves, since large (300-650A) flattened vesicular structures with a double bilayer thickness (about 100A) appeared in both LDL and HDL density ranges. Vesicular structures represented only 4% of the particles within the LDL density range, suggesting that a substantial increase in PL content of the LDL might have occurred. No other properties of these LDL were evaluated.

In one set of fat-feeding experiments (one bolus of 100 g corn oil) with healthy subjects, major changes in HDL properties were found, but changes in LDL distribution were not assessed (65). In another fat feeding experiment (one bolus of 100 gm safflower oil)* no major changes in the GGE pattern of LDL were noted. In view of the changes in apo B properties following PL uptake by LDL, alterations in receptor binding properties may occur which may lead to rapid in vivo removal of PL-enriched LDL species. Tracer studies, using radiolabelled LDL and a high level fat load, need to be carried out to elucidate the possible transient appearance of PL-enriched LDL in vivo.

Since HDL in plasma is a major acceptor of PL, the LDL/HDL molar ratio may serve as an indicator of the extent of PL uptake by LDL. Our GGE data show that a 50% drop in LDL/HDL molar ratio is required for a 50-70% increase in the extent of LDL APD increase. Thus, changes in LDL APD value following fat loading would be expected only in individuals

*Krauss, R.M., personal communication.

with very low HDL levels In addition, since excess surface components of lipolysis are LCAT substrates, the likelihood of encountering large, PL-rich LDL would be greater in individuals with low LCAT activity.

Extremely low HDL levels (and subnormal LCAT activity) are present in patients with apo AI-apo C III- deficiency (19). Some HDL (containing apo A II) can be detected by GGE and electron microscopy and about 12% of the particles within the HDL density range are discoidal (113). Fat loading (100g safflower oil) did not produce a change (4h-8h following fat load) in LDL APD value (using GGE) in these individuals, but an unexpected increase in S_f^o rate was observed. The LDL in these patients were large (260A) and, as shown by our studies,the extent of APD change of a large LDL is usually small upon interaction with vesicles or apo AI-PC discoidal complexes. Although fat load experiments did not show a change in LDL particle size, an extra component, 300A in diameter, consistently appeared with a similar density and apoprotein moiety as LDL. It is tempting to speculate that this component is a class II product formed during LDL exposure to lipolysis-generated PL.

An intriguing finding in apo AI-CIII-deficiency is that the LDL are much larger than expected from the normal interrelationship found between LDL S_f^o rate and HDL levels (42).[*] The appearance of a relatively large LDL in these

---

*In other words, a person with as low HDL level as that found in the apo AI-C III-deficient patients would nor-

patients suggests that LDL particle size in the steady state may in part be determined by PL loading. Thus, PL interaction with LDL may transiently give rise to PL-enriched LDL in plasma which in turn could have a higher capacity for LCAT-related core CE enrichment. Support for this hypothesis is provided by a report describing the transfer of cholesterol esters from HDL to PL-enriched LDL during in vivo lipolysis of intravenously infused rat chylomicrons (112). Work is needed to determine the capacity of PL-enriched LDL to undergo further remodeling of their core structure. These studies may elucidate the physico-chemical bases of characteristic LDL patterns found in individuals in similar metabolic states (see Introduction section).

In familial LCAT deficiency, discoidal HDL structures accumulate (20). The LDL are heterogeneous and enriched in PL and UC, but the particle size ditribution is not well characterized. In a recent case of familial partial LCAT deficiency in Japan (114), a 60-80% reduction in LCAT activity was associated with the presence of discoidal HDL particles and a heterogeneous (200-350A) primarily PL-enriched LDL species. The effect of fat loading on the LDL in these individuals remains to be examined.

Tangier disease is a case of very low HDL level (115). The LDL particles in these individuals have not been characterized. It should be pointed out that fat feeding in

mally have a very small (<240A) LDL species.

Tangier disease leads to the appearance (in electron micro-graphs of HDL) of large (680A), flattened and translucent vesicular structures (20). These components could interact with LDL and lead to the formation of larger species.

Lipolytic activity due to intravenous heparin injection produces large (400-1200A) vesicular structures in both the LDL and the HDL density ranges (89) associated with a shift in HDL to faster floating species. The physical propeties of LDL during such studies have not been reported and might show changes associated with PL uptake.

2. Role of Phospholipid and LCAT on LDL Polydispersity

Considerable particle size versus density polydisper-sity is normally observed for LDL in plasma of human sub-jects. Our studies on incubation of whole plasma with a range of vesicle concentrations (0.2-1.8 mg/ml PC), indi-cated little change in LDL density (0.002-0.004 g/ml) for a major increase in APD (5-40A). PL enrichment could be a basis for such size versus density heterogeneity. During incubation of plasma alone, small, minor species (240-250A) are found with density comparable to the larger, major com-ponent. This alteration requires LCAT activity and may con-tribute to polydispersity observed in human plasma. LCAT-induced formation of small, minor LDL species observed dur-ing whole plasma incubation may contribute to the origins of the LDL distribution found in patients with familial hyper-cholesterolemia (116). These patients have variable plasma lipid phenotypes and are highly prone to atherosclerosis.

They also have cholesterol ester-poor LDL of 252±2 A parti-
cle size with a hydrated density of 1.036 g/ml (117). In
vitro incubation of whole plasma from normolipidemic sub-
jects (our present work) can produce small, minor species
with similar size and density as that found in patients with
familial hypercholesterolemia. Since ultracentrifugal tech-
niques could not separate these minor components from the
major, larger species, we did not define their chemical com-
position. With the use of other fractionation techniques,
such as gel filtration, it should be possible to character-
ize their properties and gain further insight into the
mechanism of their formation.

The role of LCAT activity in producing changes in LDL
properties (mainly decrease in APD value) was revealed not
only during plasma incubation but during interaction of the
reconstituted mixture of LDL, discoidal complexes, and
plasma d>1.20 g/ml fraction (without an LCAT inhibitor).
Recent findings (132) show direct LDL-LCAT interaction that
can result in direct incorporation of cholesterol ester into
LDL, bypassing transfer of cholesterol ester from HDL to LDL
via lipid transfer proteins. Although this is a minor path-
way accounting for only 5% increase in CE content of LDL,
the possible contribution of direct LCAT-LDL interaction to
changes in LDL distribution during plasma incubation needs
to be assessed.

3. In Vivo Interconversions Among LDL Subpopulations:
"Surface Pathway" versus "Core pathway"

In <u>vivo</u> interconversion of radiolabelled less dense LDL to more dense species has been reported (63). Our <u>in vitro</u> observation of interconversion of LDL to smaller, more dense species during whole plasma incubation could provide a possible explanation for the above-mentioned <u>in vivo</u> observations. The <u>in vivo</u> more dense species exhibit a longer half times in plasma (64). The observation indicating that the <u>in vitro</u>-produced LDL species show a lower binding affinity to apo B-receptors in fibroblasts (63), provides further support for the hypothesis that LCAT activity in plasma may contribute to LDL interconversion to smaller, more dense species.

In <u>vivo</u> interconversion of LDL to less dense species, on the other hand, may be initiated by PL enrichment of the LDL, followed by core enrichment of the PL-enriched LDL species. In addition to the above-mentioned "surface pathways", "core pathways" may be operational <u>in vivo</u>. One such process was suggested during long term (24h) incubation of whole plasma with high triglyceride levels. During such incubation, LDL interconversion to larger species was noted, presumably due to triglyceride enrichment of the LDL core via lipid transfer proteins.

In summary, the lipoprotein subpopulations appearing in the LDL density range can undergo interconversion to smaller, or larger, species. Our findings provide insight into the role of PL, HDL, triglycerides, and plasma factors, such as albumin and LCAT, in modulating LDL propeties. Our

studies were primarily directed at "surface pathways" and complement the "core pathway" described by us and other investigators (59).

VI. Appendix

A. Effect of Whole Plasma Incubation on Particle Size Distribution of Lp(a)

The strong similarities that exist between the properties of LDL and Lp(a) (118-122) prompted us to investigate the effects of plasma incubation on these two lipoprotein classes. Apo B is the major apoprotein component in both lipoproteins, although the presence of an antigenically distinct protein (designated protein (a)) in Lp(a) differentiates Lp(a) from LDL (119). Both LDL and Lp(a) have the same lipid composition (119) and core phase transition properties (120). We previously reported (87) similarities between Lp(a) and LDL in their interaction with PC vesicles. Others (121) have shown similarities between Lp(a) and LDL in binding to apo B receptors on fibroblasts. Lp(a) is larger (>290A) than LDL, yet is more dense (found mainly in the d 1.055-1.19 g/ml plasma fraction). Another way of distinguishing Lp(a) is by its higher content of carbohydrates in the protein moiety (119). This leads to pre-beta mobility of Lp(a) on agarose gel electrophoresis. Since VLDL also has pre-beta mobility, the presence of lipoproteins with pre-beta mobility but with density greater than that of VLDL (d 1.006) is indicative of presence of Lp(a). This explains the designation "sinking pre-beta" which has also been assigned to Lp(a) (122).

Plasma from subject GH (diameter of major LDL component, 258A, minor component, 247A; Fig 43A) was used for incubation studies. Both the presence of a component beyond LDL size range (290A) within the d 1.055-1.19 g/ml plasma fraction (Fig 43B) and the detection of arcs of partial identity between LDL and the d 1.055-1.19 g/ml plasma fraction during radial immunodiffusion (Fig 44), were indicative of the presence of Lp(a) in GH's plasma. Incubation (37°C, 6h) of GH's plasma produced a decrease in particle size of Lp(a) species (nonincubated: 290A, Fig 45, lane 3; incubated (6h): 286A, Fig 45, lane 4). This was associated with a decrease in particle size of LDL (nonincubated LDL: 258A, 247A; Fig 43, lane 1; incubated (6h) LDL: 251A, 239A; Fig 43, lane 2) and formation of a smaller minor species (235A). Our observation suggests another possibly "functional" similarity between LDL and Lp(a). In Results, section B, we showed that similar changes in LDL pattern following whole plasma incubation were dependent on the presence of LCAT activity in plasma. The effect of LCAT activity on Lp(a) has not been studied; our plasma incubation studies suggest possible utilization of Lp(a) surface components by plasma LCAT, leading to a decrease in Lp(a) particle size.

Fig 43. Particle size distributions (2-16% gel) of LDL (plasma d 1.019-1.055 g/ml fraction; subject GH) and Lp(a) (plasma d 1.055-1.19 g/ml fraction).

A

LDL

258

247

T

B

Lp(a)

290

T
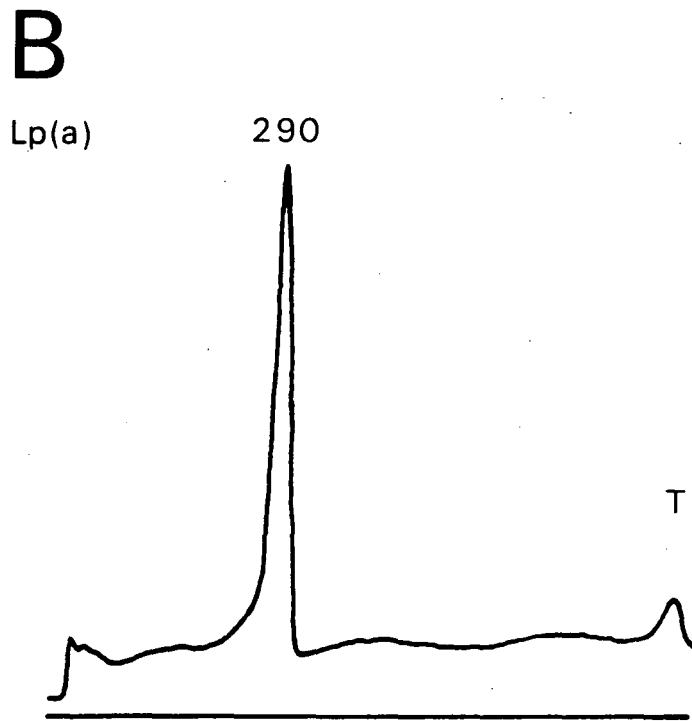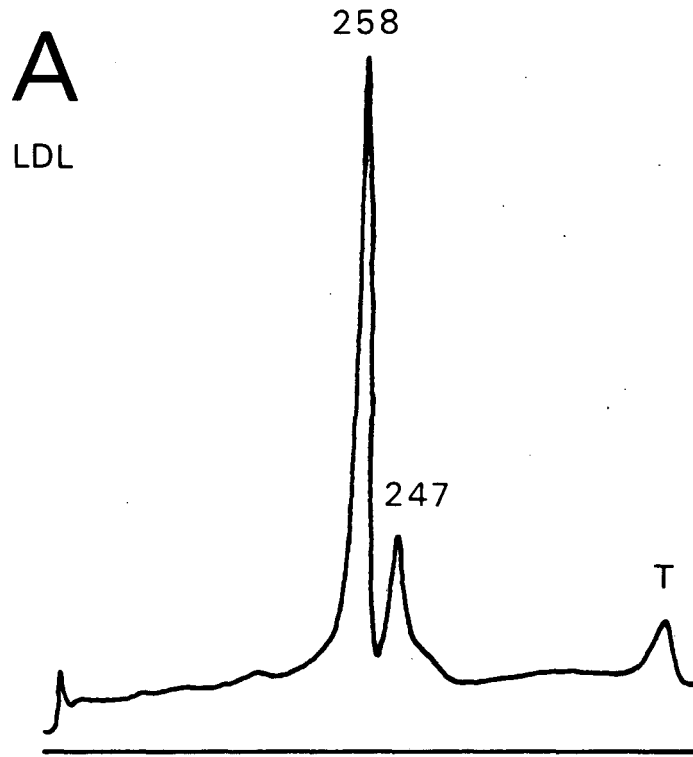
XBL 848-7878

Fig 44. Assay of plasma fractions for Lp(a) by radial immu-
nodiffusion against anti-Lp(a) antiserum. Wells 1 and 4, 10
μl Lp(a)-rich fraction (plasma d 1.055-1.19 g/ml fraction),
wells 2 and 6, 10 μl LDL (d 1.019-1.055 g/ml fraction; 6
Co), wells 3 and 5, not part of this experiment, middle
well, anti-Lp(a) antiserum obtained from intramuscular
injection of rabbits with an Lp(a)-rich fraction (obtained
by gel filtration of plasma d 1.055-1.19 g/ml fraction).
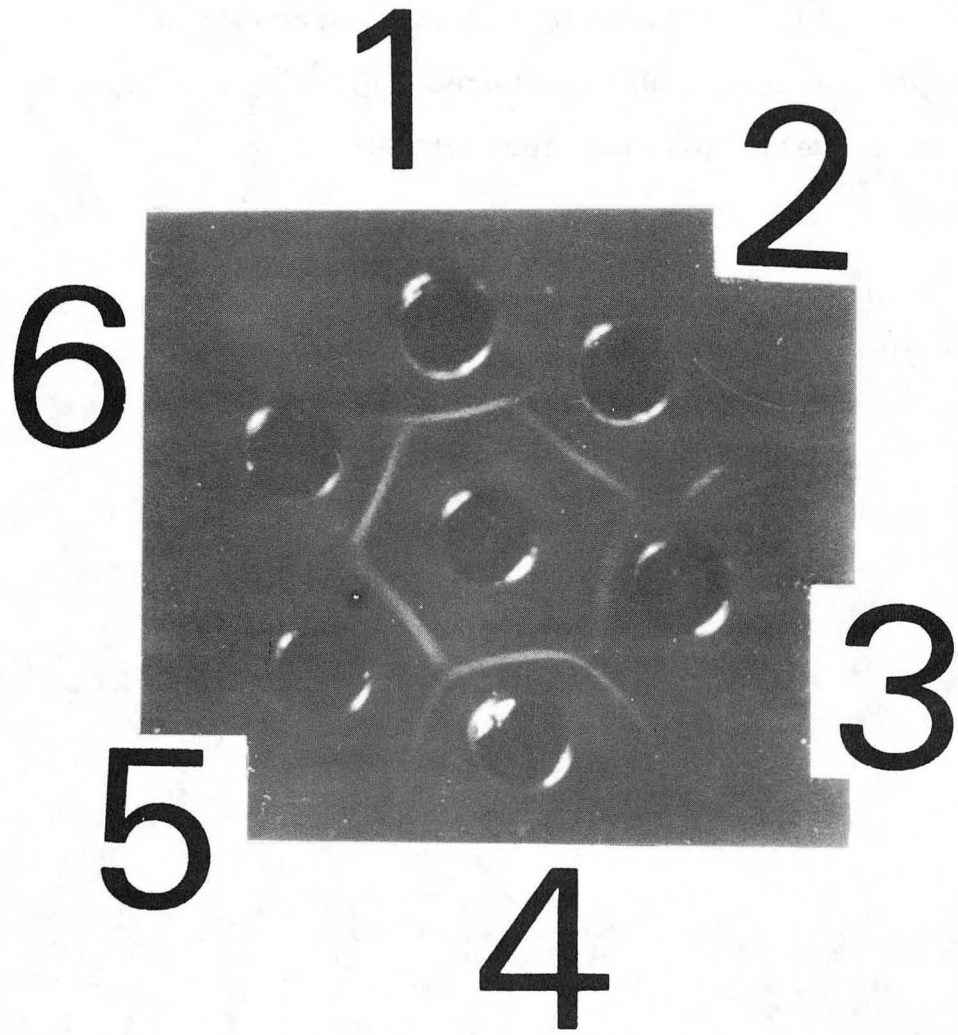
Fig 45. Particle size distribution (2-16% gel) of LDL (plasma d 1.019-1.055 g/ml fraction) and Lp(a) (plasma d 1.055-1.19 g/ml fraction) from nonincubated (lanes 1 and 3, respectively) and incubated (37°C, 6h; lanes 2 and 4, respectively) plasma (subject GH).
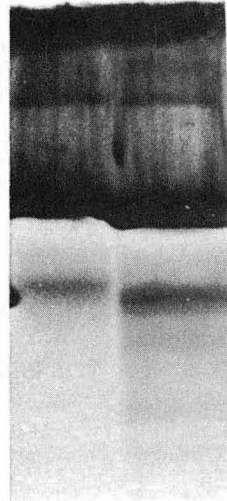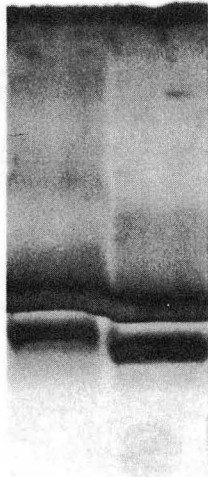
XBB 849-6750

B. Interaction of Trypsin-Treated LDL with Phosphatidylcholine Vesicles

In Results, section D5, we showed that with the major increase in LDL APD (upon PL uptake) there occurs some alteration in the accessibility of apo B to trypsin digestion. Such alteration suggests the possibility of change in apo B organization which might contribute to APD change. To gain further insight into the role of apo B in influencing LDL APD, the properties of LDL, modified in its apo B by trypsin, and the interaction of such modified LDL (designated as T-LDL) with PCV were studied.

It has been shown (59,123) that trypsin-treatment of LDL removes at most 20-25% of LDL-protein without change in lipid composition. We found that T-LDL had an APD value which was about 5-10A smaller than untreated LDL (e.g., subject BG: noninc LDL, 262A, T-LDL, 252A; Fig 46). Both the T-LDL and native LDL (N-LDL) showed similar rates of GGE electrophoretic mobility (between 24h and 36h electrophoresis time; see Fig 5, Results, section A1). Thus, GGE measurements should provide meaningful APD values for T-LDL. By EM (not shown), T-LDL appeared as widely-dispersed particles that never associated closely, in contrast to the tight-packing or even clumping and chaining often observed in N-LDL. Such spreading of T-LDL under the conditions of negative staining may be due to their increased negative charge (following loss of most arginine and lysine residues), as indicated both by our agarose gel electrophoresis

Fig 46. Effect of trypsin pretreatment of LDL (T-LDL) on interaction with PC vesicles. Native LDL (N-LDL, subject BG, approximately 0.6 mg/ml protein) and T-LDL (see Methods, section J for conditions of preparation) were incubated (6h) with PC vesicles (range, 2.5-4 mg/ml PC), HDL (approximately 1 mg/ml protein) and BF (1 Co). Inset: gradient gel electrophoresis of incubation mixtures using either N-LDL (odd-numbered lanes) or T-LDL (even-numbered lanes). Lanes 1-2, 2.5 mg/ml PC; lanes 3-4, 3.0 mg/ml PC; lanes 5-6, 3.5 mg/ml PC; lanes 7-8, 4.0 mg/ml PC.

XBB 849-6748
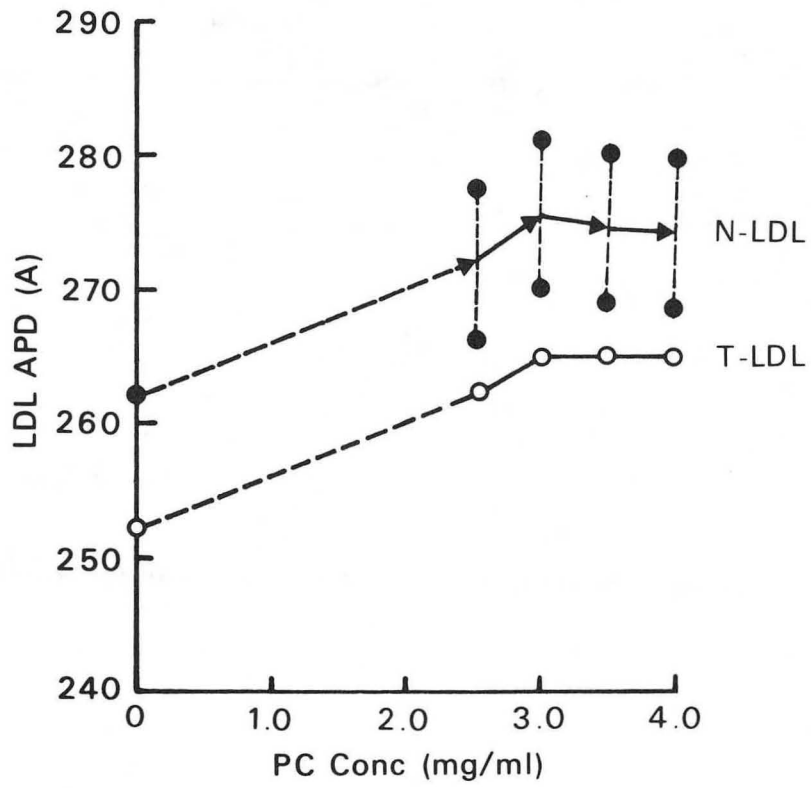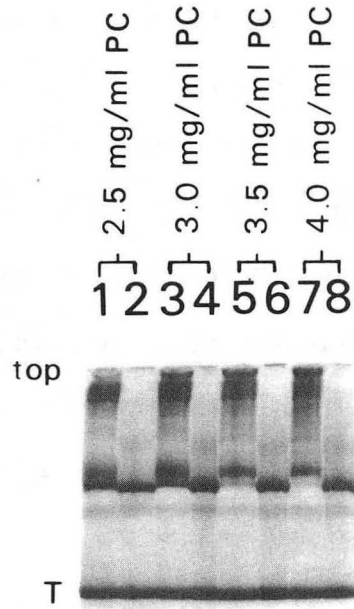
data (not shown) and by others (124).

To evaluate the interactive properties of LDL, modified in its apoprotein, with PL, APD changes following interaction of T-LDL with PCV, BF, and HDL were examined by GGE. Incubation ($37^{O}C$, 6h) of T-LDL, BF (1 Co), and HDL (approximately 1 mg/ml protein) with increasing PCV concentrations (2.5-4.0 mg/ml PC) resulted in an increase in APD values (Fig 46, empty circles). Under identical conditions, N-LDL showed a similar APD change (Fig 46, solid circles). Since T-LDL was about 10A smaller than N-LDL, the PCV-exposed T-LDL, at all PC levels, remained about 10A smaller than the PCV-exposed N-LDL, at the corresponding PC level. Thus, trypsin attack does not interfere with processes leading to Effect II despite loss of apoprotein integrity. In contrast, at PCV concentrations high enough to induce bimodal LDL pattern transformations (Effect III) in N-LDL, T-LDL did not show the expected bimodal pattern. For the same PCV level, the APD value of T-LDL was only about 4A smaller than the smaller component within the bimodal pattern of N-LDL, indicating that it is the larger component within the bimodal pattern which does not form with T-LDL. Using N-LDL, protein staining materials appeared at APD values >319A all the way to the top of the gel (Fig 46, insert, odd-numbered lanes) which consisted of both class II products and aggregated of LDL and PCV. In contrast, using T-LDL, no protein staining material at APD values >319A was observed; only a faint band appeared at about 309A (Fig 46, insert, even-

numbered lanes). Thus, intactness and/or proper conformation of apo B appear important in processes leading to aggregation of LDL with PCV, formation of class II products, and appearance of a bimodal LDL, from an originally unimodal pattern. In view of its high affinity for PL, apo B's role in these three cases may come from bridging between LDL and PL interfaces of another particle.

C. Apparent Particle Size Distribution of Guanidine Hydrochloride-Treated LDL

Two lines of evidence in this thesis suggested a role for apo B in influencing APD values of LDL on GGE: (1) modification of LDL apo B (e.g., by trypsin treatment) leads to smaller APD values and altered reactivity with PCV, and (2) modification of LDL APD upon exposure of LDL to PCV was associated with alterations in apo B organization (e.g., trypsin accessibility). We thus evaluated possible changes in LDL APD when apo B conformation was changed during exposure to relatively mild denaturing conditions (e.g., guanidine hydrochloride, GnHCl) which do not disrupt the lipoprotein molecule (125). Separate incubation ($37^{O}C$, 6h) of large (DJ and AP, not shown) and small (TI, Fig 47) major LDL components with increasing GnHCl concentrations was carried out and the total incubation mixture, still containing the GnHCl, was applied directly to the gradient gel. A progressive increase in APD values of LDL components and a decrease in the number of LDL components occurred with increasing GnHCl concentrations (Table 14, top). At 2M GnHCl, species with APD values (371A, 351A, 305A) beyond the normal particle size range of LDL also appeared in DJ's pattern. These latter components had APD values similar to class II products noted in the DC incubation system. In addition, the area under all LDL peaks decreased at GnHCl concentrations >4M, in conjunction with the appearance of flocculent material in the sample. It should be noted that

Fig 47. Effect of exposure of LDL to guanidine hydrochloride (GnHCl) on the particle size distribution (2-16% gel) of LDL. Incubation (37°C, 6h) mixtures contained LDL (0.1 mg/ml protein) in the presence of GnHCl (0-6 M) in a total volume of 1 ml. After incubation, samples were directly applied to the gradient gel (2-16% gel). Lane 1, nonincubated LDL; lane 2, LDL incubated with 1 M GnHCl; lane 3, LDL incubated with 2 M GnHCl; lane 4, LDL incubated with 4 M GnHCl; lane 5, LDL incubated with 6 M GnHCl. GnHCl induced changes in the apparent particle diameter of thyroglobulin, when added to sample aliquots just prior to electrophoresis; the thyroglobulin peak disappeared at or above 2 M GnHCl. Some protein staining material appear at the top of the gel when GnHCl concentrations were equal to or greater than 2M. Lane 6 contains particle size calibration proteins: latex beads (L), thyroglobulin (T) and apoferritin (A).
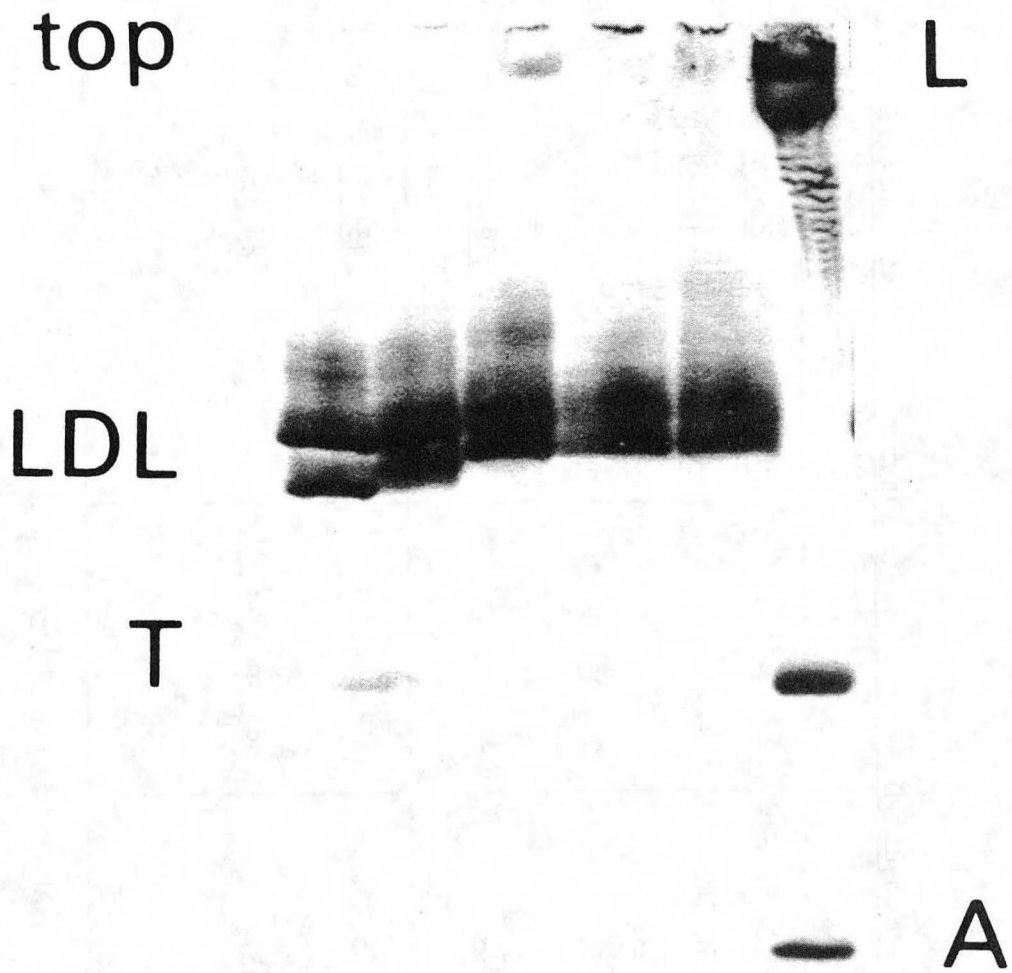
Table 14 -Apparent particle diameter (APD, A) of LDL following treatment with guanidine hydrochloride (GnHCl).

sample treatment	subject DJ class I products	class II products	subject AP class I products	subject TI class I products
noninc LDL	270*,262,255,245	----	260,253	242,226
inc (1M GnHCl; nondial**)	269,257,245	----	263,257	244,233
inc (2M GnHCl; nondial)	269,260	391,351,305	265	244,233
inc (4-6M GnHCl; nondial)	281,273	335	268	244,233
inc (1M GnHCl; dial**)	270,255,245	318,354,302	not done	245,231
inc (2M GnHCl; dial)	271,257,245	392,380,358,308	" "	248,238
inc (4-6M GnHCl; dial)	272,260,248	390,380,358,311	" "	248,239

* underlined values are APD of major LDL components.

** nondial, nondialysed LDL incubated (37°C, 6h) in GnHCl was directly applied to gradient gels (2-16%) for electrophoresis; dial, LDL incubated with GnHCl was dialysed against buffer B (see Methods, section B) and subsequently applied to gels.

the denaturing effect of GnHCl, associated with APD increase, was also observed in the internal standard protein (thyroglobulin). Denaturation occurred within the time it took to mix and apply the samples for GGE (about 10 min).

To evaluate whether GnHCl-induced changes in LDL properties could be reversed by removal of the denaturant, GGE patterns of GnHCl-treated LDL species, after extensive dialysis to remove the GnHCl, were obtained. Instead of the two major (270A, 262A) and two minor (255A, 245A) components of DJ's nonincubated LDL, one major and two minor components were observed upon GnHCl treatment (Table 14, bottom). Also, the APD value of the major component of DJ's LDL following removal of GnHCl (in range of 1M-4M), returned to initial values (272-268A). However, the increase in APD of TI's initially small LDL component was not reversed by removal of GnHCl (Table 14, bottom). These data indicate that GnHCl-induced change in LDL APD, even after removal of GnHCl, is reversible for large, major components of LDL but not for the small, major components. In addition, even after removal of GnHCl, components with APD values in the range of class II products (DJ) were still present (Table 14, bottom). Since the increase in APD of initially small LDL components, even after removal of GnHCl, correlates with the GnHCl concentration present in the incubation mixture prior to removal, exposure of LDL to conditions favorable to conformational change in its apoprotein moiety results in alterations qualitatively similar to those induced by PL

during Effect II.

D. Lipoprotein Distribution in Patients with Cystic Fibrosis

1. Introduction

Cystic fibrosis (CF) is the most common congenital disease among Caucasians transmitted via an autosomal recessive inheritance (for reviews see ref 126,127). It affects one in every 1000-2000 newborns and is usually lethal in early childhood. Today, early diagnosis and comprehensive therapy have increased the mean survival age to 20 years. Carriers of the disease are clinically nonsymptomatic and 3-5% of Causacian population is estimated to carry the CF gene. The molecular basis of CF is still unknown, but it is classified under the category of exocrinopathy. The sweat glands fail to reabsorb electrolytes leading to a salty sweat. In the lung, the secretion of a viscous mucus causes pulmonary obstruction and facilitates pulmonary infection. Salivary secretions contain increased amounts of enzymes, glycoproteins, and electrolytes. Obstruction of the pancreatic ducts leads to diminished exocrine pancreatic secretion. The liver, kidney, and genito-urinary tract are also involved.

The phenotypic expression of CF is complex. In few individuals, no abnormality other than sweat electrolyte imbalance is noticed. More than 95% of patients, however, die of progressive pulmonary dysfunction. Lipid malabsorption secondary to pancreatic lipase deficiency occurs in 60-90% of cases and generally results in negative energy

balance, decreased essential fatty acids (128,129) and fat-soluble vitamins (A, E, K) in plasma.

Lipids, essential fatty acids, and β-carotene, a pre-cursor to vitamin A, all require lipoproteins for transport from intestine to various tissues. Abnormal lipoprotein dis-tributions would be expected in cases of fat malabsorption. Earlier studies have reported low serum cholesterol in CF (130). Recently, Vaughan et al (131) reported depressed apo B, LDL, and HDL levels in plasma from children with CF, most of which had pancreatic insufficiency. In that study, a more severe gastro-intestinal problem correlated with a more depressed plasma LDL concentration, suggesting that LDL and its apoprotein may be depressed secondary to fat malabsorp-tion.

In addition to their role in fat absorption and tran-sport from the intestine to blood, lipoproteins also tran-sport fatty acids to the lungs for production of surfactants that are essential for reducing surface tension at the air-fluid interface of alveoli. Abnormal lipoprotein concentra-tion and/or composition may contribute to deterioration of lung function by affecting membrane structure, fluidity, and transport. In fact, Vaughan et al (131) reported that the more severe the lung involvement, the lower the HDL, LDL, and VLDL concentrations. Although deterioration of health status of CF patients seemed to be reflected in low levels of total plasma lipids, other lipoprotein abnormalities were also found in CF. Despite low HDL levels, HDL_{2a} showed

higher contribution to total HDL distribution, and positively correlated with the degree of gastro-intestinal involvement.

To investigate further the above preliminary observations, we characterized lipoprotein distributions in relation to lung and GI involvement in another CF population. Older individuals with relatively mild conditions were chosen, and lipoprotein levels, polydispersity in particle size, flotation properties, and apoprotein distribution were examined.

2. Methods

a. Source of CF Plasma

Eight to ten ml plasma containing Na_2EDTA from outpatient CF subjects at NIH and healthy volunteers were shipped on ice (courtesy of Dr. V.S. Hubbard, Pediatric Metabolism Division, NIH) at monthly intervals. The study followed the Human Use Protocol of NIH (NIAMDO) and was approved by the LBL and UCB Human Use Committees. At the time the studies were carried out, diagnostic information on the subjects (i.e. whether they had CF or not) was blinded.

Separation of various lipoprotein classes is described in the Methods, section A of this thesis. Particle size measurement using GGE (71), flotation properties using the analytical ultracentrifuge (70), and apoprotein distribution using SDS-PAGE (74) were carried out as previously

discussed.

b. Radial Immunodiffusion

For measurment of Lp(a) concentrations by radial immu-nodiffusion, samples were sent to Dr. Albers, University of Washington, Seattle. Plasma concentrations of β2-Glycoprotein-1 were measured by radial immunodiffusion using the Boehringer β-2-glycoprotein-1 Measurement Kit.

3. Results and Discussion

a. Patient Data

Clinical information on six CF patients with pancreatic insufficiency (CFPI+, age, 22±5) and four CF patients without pancreatic insufficiency (CFPI-; age, 18±3) are listed in Table 15a and 15b. There was one female in each group. Five healthy males were used as age-matched normal (N) controls (age, 23±7). For each patient a clinical score was constructed at NIH so as to give 75% of the weight to the pulmonary manifestations and 25% to the nutritional aspects of the disease. This test assesses a patient's past and current clinical status and provides a numerical predic-tion of life expectancy. As expected, CFPI+ who were on pancreatic enzyme replacement therapy had lower scores (CFPI+, 74±3; CFPI-, 84±3). The CFPI+ patients also had abnormal glucose tolerance tests.

b. Plasma Lipid and Lipoprotein Concentrations

Table 15a -List of subjects (CFPI+)[*] and their plasma lipid and lipoprotein concentrations (mg/dl).

| | subjects | | | | | | |
	CF3	CF4 (♀)	CF6	CF1	CF15	CF7	mean (S.D.)[##]
health score[**]	50	70	75	80	80	88	73.8 (13)
age (years)	27	22	14	25	26	19	22 (5)
plasma TG[***]	110	109	132	295	68	201	162 (66)
plasma CS[***]	95	94	107	32	97	161	98 (46)
VLDL (S_f^o 20-400)	4	83	40	109	70	240	91 (81)
LDL (S_f^o 0-12)	106	115	145	156	172	197	148 (35) #
peak S_f^o rate	5.76	6.65	5.56	6.65	5.39	6.27	6.05 (0.55) #
HDL ($F_{1.20}^o$ 0-9)	226	205	178	244	207	271	222 (33) #
%HDL$_{2a}$[+]	49.9	42.4	54.3	31.5	48.2	38.8	44.2 (11.4)
%HDL$_3$[+]	38.0	57.1	43.4	61.9	44.9	61.2	51.1 (10.2)

[*]CFPI+, cystic fibrosis patients with pancreatic insufficiency. They were free-living subjects on regular diet who were on pancreatic enzyme replacement therapy. Fecal fat levels ranged from 14-37 g/day in these subjects. All subjects except CF7 showed an abnormal glucose tolerance test. CF3 and CF4 were being treated with antibiotics.

[**]Health scores were designated at NIH and reflected the degree of gastro-intestinal and pulmonary involvement.

[***]TG, triglyceride; CS, total cholesterol.

[#]Significantly (t-test two-tailed probability<0.05) different from normal.

[+]Plasma lipoprotein levels were obtained by ultracentrifugation. %HDL$_{2a}$ and %HDL$_3$ are percentages of total HDL concentration. Levels of HDL subpopulations were determined by three component analysis of total HDL ($F_{1.20}^o$ 0-9) according to Anderson et al (132).

[##]S.D., standard deviation.

Table 15b -List of subjects (CFPI-)[*] and their plasma lipid and lipoprotein concentrations (mg/dl).

	subjects				
	CF12	CF8 (♀)	CF11	CF5	mean (S.D.)
health score	80	85	85	88	85 (3)
age (years)	16	22	18	16	18 (3)
plasma TG	74	63	116	34	72 (34)
plasma CS	134	191	175	142	161 (27)
VLDL (S_f^o 20-400)	34	85	78	0	49 (40) #
LDL (S_f^o 0-12)	271	270	229	225	249 (25)
peak S_f^o rate	6.79	6.69	6.79	7.43	6.92 (0.34)
HDL ($F_{1.20}^o$ 0-9)	169	266	197	212	211 (40) #
%HDL$_{2a}$	42.9	49.7	39.9	31.1	40.9 (7.7)
%HDL$_3$	52.1	41.2	60.0	55.6	52.2 (8.0)

[*]CFPI-, cystic fibrosis patients without pancreatic insufficiency and fat malabsorption (fecal fat<7 g/day).
For explanation of symbols and abbreviations, see legend to Table 15a.

Table 15c -List of subjects (normal controls) and their plasma
lipid and lipoprotein concentrations (mg/dl).

	subjects					
	N2	N9	N10	N13	N14	mean (S.D.)
health score	--	--	--	--	--	--
age (years)	35	20	20	19	19	23 (7)
plasma TG	196	80	126	59	72	101 (62)
plasma CS	149	140	145	185	181	152 (16)
VLDL (S_f^o 20-400)	78	115	204	66	39	100 (64)
LDL (S_f^o 0-12)	315	231	189	186	251	234 (53)
peak S_f^o rate	6.60	6.90	6.59	6.19	6.74	6.64 (0.26)
HDL ($F_{1.20}^o$ 0-9)	258	233	263	270	334	271 (38)
%HDL_{2a}	33.8	41.4	46.7	34.7	45.9	40.4 (6.1)
%HDL_3	66.2	43.5	39.3	57.4	35.0	48.3 (13.1)

For explanation of symbols and abbreviations, see
legend to Table 15a.

Tables 15a-c lists plasma lipid and lipoprotein levels in these subjects. Plasma triglyceride levels in CFPI+ (162±66) were similar to N (106±56), but significantly* lower in CFPI- (72±34). The low plasma TG levels reflected in low plasma VLDL levels in CFPI- (49±40) compared to CFPI+ (91±81) and N (100±64). Plasma cholesterol concentrations were significantly lower in CFPI+ (98±46) compared to CFPI- (161±27) and N (152±16). This was reflected in significantly lower plasma LDL concentrations in CFPI+ (CFPI+, 148±35; CFPI- , 249±25; N, 234±53), and significantly lower HDL concentrations in both CFPI+ (222±38) and CFPI- (211±40) compared to N (271±38). Thus, LDL levels differentiated between patients with and without pancreatic insufficiency, suggesting that this abnormality is probably secondary to fat malabsorption.

c. Particle Size Distribution of LDL

To check the possibility of alterations in LDL distribution in CF subjects with fat malabsorption, we next examined the flotation properties and particle size distributions of LDL in CF. The mean peak S^o_f rate of LDL at d 1.063 g/ml (Table 15a-c) was significantly lower in CFPI+ (6.05±0.55) compared to CFPI- (6.92±0.34) and controls (6.6±0.26). However, the peak S^o_f values were within the range reported in other studies (42) for healthy males and did not approach the low values (S^o_f 4) found in the

*two-tailed probability (t-test) less than 0.05.

hypertriglyceridemic individuals. In view of the direct relationship between peak S^O_f and particle diameter (88)[†] we expected LDL in CFPI+ to exhibit relatively smaller major components. The GGE profiles of the d<1.063 g/ml plasma fraction showed up to four components within the LDL size range (218-278A) and one to two components beyond LDL size range (280-310A). The overall LDL particle size and distribution (Table 16) were not different between CF and healthy subjects.

d. Concentration and Particle Size Distribution of Lp(a)

In four out of six CFPI+ studied, a component larger than the LDL size range (e.g., 290A in CF12; Fig 48A) was consistency observed in the d<1.063 g/ml fraction. A component of similar size (e.g., 288A; Fig 48B) was detected in the d 1.055-1.19 g/ml plasma fraction from these patients suggesting that the large components were Lp(a) species. In an attempt to estimate Lp(a) concentrations in CF, the $F^O_{1.20}$ rate interval for Lp(a) in the d 1.055-1.19 g/ml plasma fraction was established, using analytical ultracentrifugation. Lp(a) floated in an $F^O_{1.20}$ rate range of 17-24 (roughly corresponding to S^O_f 0-2).[*] Using the concentration of $F^O_{1.20}$ 17-24 material as an estimate of Lp(a) levels, we

[†]diameter = (5.13)xpeak S^O_f - (218) A
[*]The peak $F^O_{1.20}$ rate for this component was similar between CF (CFPI+, 23.24±3.99; CFPI-, 20.09±0.54) and controls (19.75±2.61).

Table 16 -Particle diameters (Å) of major and minor components of LDL and Lp(a).[*]

		CF subjects									
		CF3	CF4	CF6	CF1	CF15	CF7	CF12	CF8	CF11	CF5
particle diameter of LDL	major	265	268	260	275	248	256	255,242	267	255	266
	minor	239	238	272,249,239	251,238	240	271	274,233	254	276,248,238	278,251,240
particle diameter of Lp(a)	major	292	299	---	296	292	---	290	280	--	---

		normal controls				
		N2	N9	N10	N13	N14
particle diameter of LDL	major	275	270	263	251	259
	minor	234	252,240	279	242,233	248,241
particle diameter of Lp(a)	major	295	282	---	---	---

[*]Gradient gel electrophoresis (2-16%) was performed on LDL within the plasma d<1.063 g/ml fraction and Lp(a) within the d 1.055-1.19 g/ml fraction.

Fig 48. Particle size distribution (2-16% gel) of LDL (within plasma d<1.063 g/ml fraction) and Lp(a) (within plasma d 1.055-1.19 g/ml fraction) of a patient with cystic fibrosis (CF12). Note the appearance of an Lp(a) component in both (A) (mean diameter, 290A) and (B) (mean diameter, 288A). The presence of the minor component (250A) in the pattern shown in (B) indicates incomplete separation of Lp(a) from major LDL component.
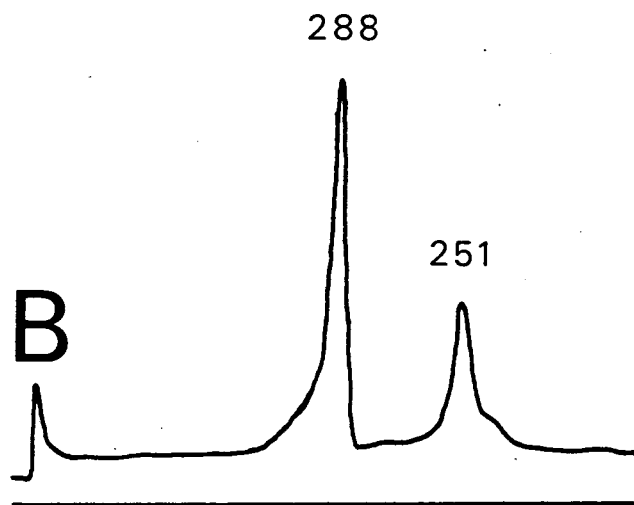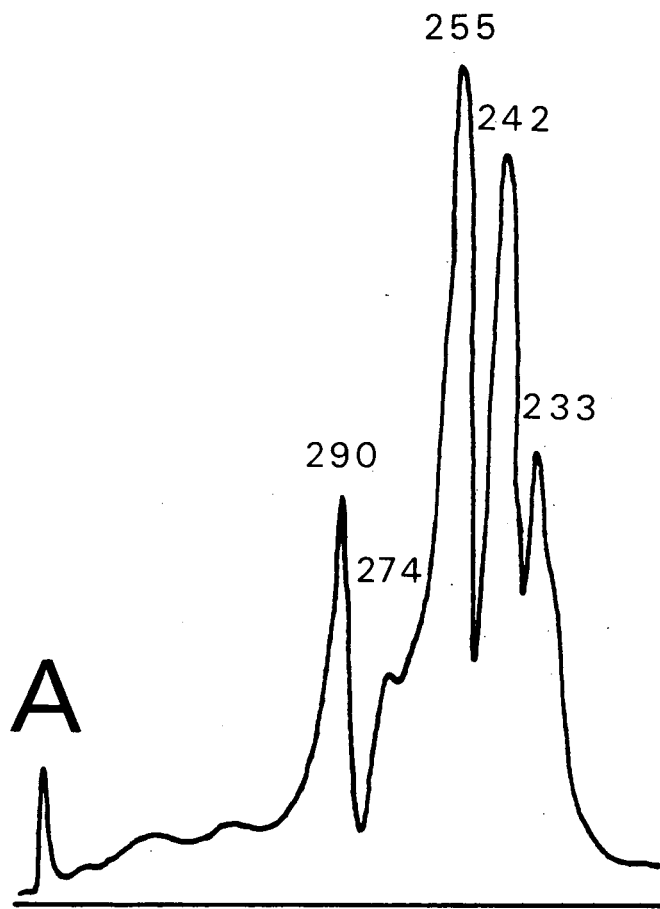
XBL 848-7888

found a higher mean concentration in CFPI+ (14.2±6.7) com-
pared to CFPI- (9.8±8.3) and healthy controls (8.3±6.6);
however, the differences were not significant due to large
variability in the values. The higher mean $F^O_{1.20}$ 17-24
levels in CFPI+ may reflect not only Lp(a) species but the
presence of minor, small (<230A' LDL species in CF. Meas-
urement of total plasma Lp(a) levels, using radial immuno-
diffusion, also did not reveal any significant differences
between CF patients (CFPI+, 7.3± 9.7; CFPI-, 9.1±6.8) and
control subjects (4.6±5.8).

e. Particle Size Distribution of HDL

We have already commented on our observation of consid-
erably lower HDL levels in CF patients with or without pan-
creatic insufficiency. Whereas low HDL levels in healthy
individuals generally reflect low levels of HDL_2 species
(Fig 49, squares), this was not the case in CF. Four out of
6 CFPI+ patterns and 3 out of 4 CFPI- patterns had a signi-
ficantly (more than one S D.) higher contribution of the
larger HDL (i.e. $(HDL_{2a})_{gge}$) species to the total HDL pat-
tern than expected from their total HDL levels (Fig 49,
solid circles). Two out of 5 control HDL patterns also
showed elevated (more than one S.D.) $\%HDL_{2a}$ (Fig 49, empty
circles). Thus, we cannot definitively establish a dif-
ferent HDL distribution pattern in CF patients and further
studies on a larger number of patients and control subjects
are needed. Nevertheless, we observed a significant posi-
tive correlation between $\%HDL_{2a}$ and health scores in CF

Fig 49. Weight percentage of HDL_{2a} in plasma of cystic fibrosis (CF) patients compared to that in normal controls as a function of total HDL concentration. Regression of $\%HDL_{2a}$ on total HD+ (solid curve) were constructed by Anderson et al (133) using 80 male (solid squares) and 80 female (empty squares) healthy subjects. CF patients and controls from our present study are identified by he following symbols: CF with pancreatic insufficiency, empty circles; CF without pancreatic insufficiency, solid circles; normal controls, solid tiangles.
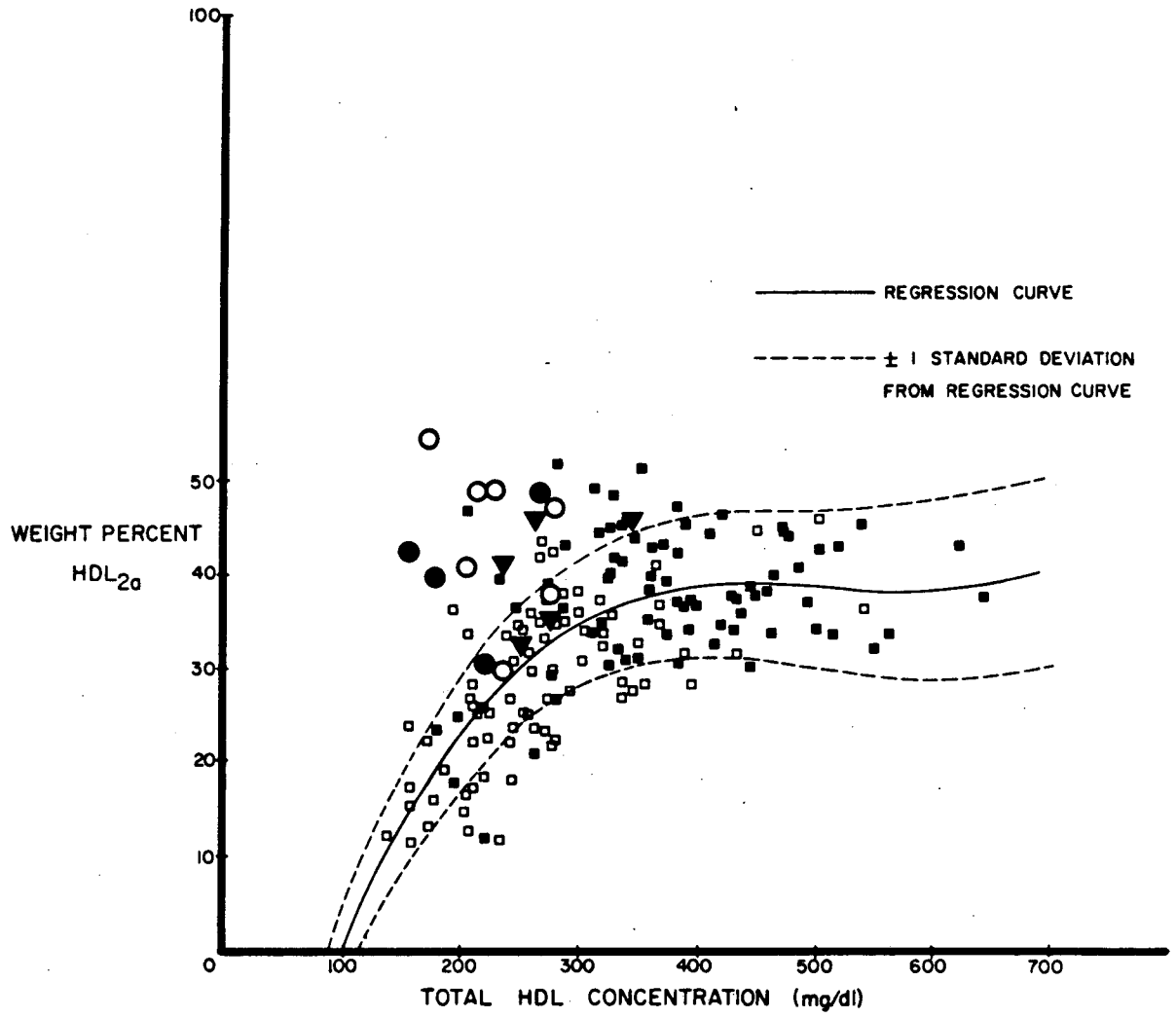
XBL 774-3268-A

patients, implying that in the face of chronic disease, alterations in HDL distribution occurs in CF. In healthy individuals, an increase in %HDL_{2a} can be induced by anaerobic exercise. We speculate that a basis for the apparent elevated %HDL_{2a} levels in CF patients in the present study may have been similar to that resulting from anaerobic work. In fact, physiological changes associated with anaerobic work, such as increased glycolysis and fatty acid turn over, and lactic acidosis, are common clinical findings in CF (134). Most recent studies suggest that some symptoms in CF such as increased salivary glycoproteins, enzymes, and electrolytes are also similar to those induced by anaerobic work (129,134). A normal energy metabolism in CF may stem from marginal energy intake, due to either fat malabsorption or drug-induced anorexia, relative to the high energy expenditure, due to lung infection and work of respiration. More studies are necessary to elucidate whether abnormal energy metabolism associated with elevated HDL_{2a} levels is a common finding in CF.

f. Interrelations Among Lipoprotein Classes from CF Patients

To gain further insight into possible metabolic interrelationships among lipoprotein subclasses in CF patients, correlations between lipoprotein levels were evaluated. In healthy subjects, a negative correlation generally exists (88) for plasma VLDL and HDL levels, particularly HDL_2 species. This was the case for our control

subjects as well (r= -0.51; slope, -0.87). However, in CFPI+, a positive (instead of negative) trend was observed between VLDL and HDL levels (r= 0.75; slope, 1.81). More data are necessary to establish the significance of this trend. The metabolic basis for the increase interrelationship between plasma VLDL and HDL in healthy individuals is currently considered to be the increase in HDL mass when there is sufficient lipolysis of VLDL coupled to transfer of VLDL surface components to HDL species. The metabolic basis for the positive, instead of the negative correlation between VLDL and HDL in CFPI+ is not apparent, but may relate to either low lipoprotein lipase activities previously reported in CF patients with pancreatic insufficiency (135), or the general deterioration of health status and low total available lipids. The latter would be consistent with the positive trends between each lipoprotein class (VLDL, LDL, HDL_3) and health score.

g. Apoprotein Distribution in Plasma from CF Patients

Abnormalities in plasma glycoprotein properties in CF have recently gained interest (136) in view of the fact that organs affected in CF all secrete glycoproteins. Increased fucose and low sialic acid content in several plasma proteins and increased plasma heparin binding capacity (136) have been reported in CF, which may have relevance to their low LpL activity (135). Since some plasma apoproteins (apo B, apo E, apo C III) are glycoproteins, we were interested to check the distribution of apoproteins and their isoforms

in CF subjects, particularly in light of their role as activators and inhibitors of lipases.

In a preliminary study of the apoprotein distribution in CF plasma, SDS-PAGE was performed on d<1.063 g/ml (3.5% polyacrylamide gels) and d 1.063-1.20 g/ml (10% gels, Fig 50) plasma fractions from a CFPI+ (CF6) and a control (N9) subject. Equal amounts of protein were applied to gels. No differences in apo B distribution in the d<1.063 g/ml fractions were observed in CF (not shown). However, of HDL apoproteins, a marked difference in the distribution of apo C was noticed. In view of the fact that apo Cs modulate lipoprotein lipase activity in plasma, the significance of our findings with respect to the reported low LPL activity in CF needs to be assessed. Of the apo C family, apo C III is a glycoprotein with several isoforms differing in sialic acid content. Since changes in the distribution of apo C (particularly apo C III isoforms) occur in healthy individuals put on a low fat, high carbohydrate diet (137), studies on the distribution of isoforms of apoproteins in CF may be promising in enhancing our understanding of the mechanisms affecting lipid transport system in CF subjects particularly those with pancreatic insufficiency.

h. Concentration of β2-Glycoprotein-1 in plasma from CF Patients

β2-glycoprotein-1 is a minor apoprotein, an activator of lipoprotein lipase (138), and has been found associated mainly with the triglyceride-rich lipoproteins and HDL

Fig 50. Apoprotein distribution of HDL (plasma d 1.063–1.20 g/ml fraction) in a healthy (N9, solid line) and a cystic fibrotic patient (CF6, dashed line). SDS-polyacrylamide gel electrophoresis (10% gel) was performed on samples (50 µg protein) as described in Methods, section G3. Apoproteins were identified according to their molecular weight: apo B, 550 kilodaltons (Kd); human serum albumin, 67 Kd; apo E covalently bound to apo AII monomer via a disulfide bond (apo E+ AII), 46 Kd; apo AIV, 46 Kd; apo E, 36 Kd; apo AI, 28.3 Kd; apo D, 22 Kd; apo AII dimer, 17.5 Kd; apo C family, 7–8.5 Kd.
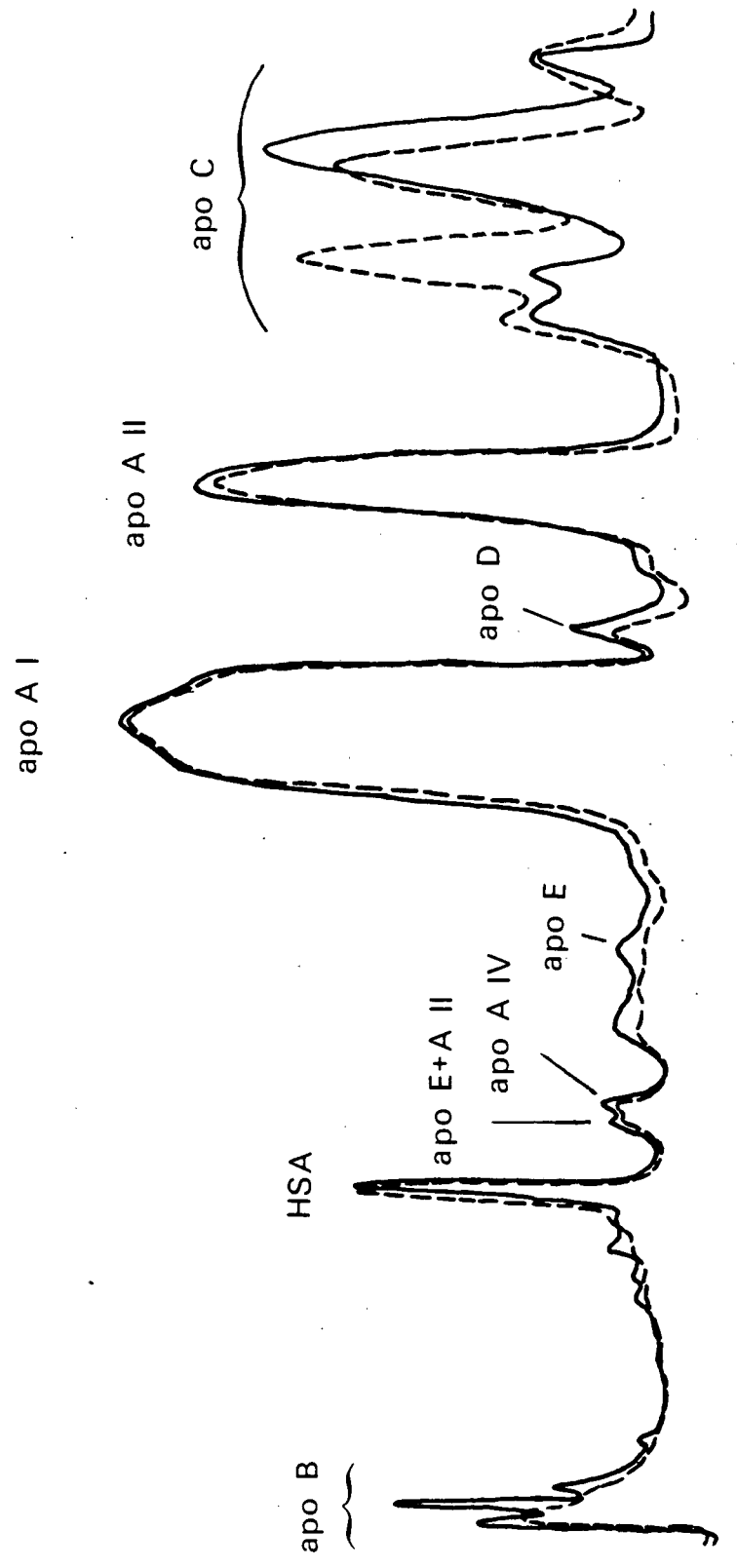
XBL 848-7883

(139). We checked the concentration of total β2-glycoprotein-1 in CF plasma and found little difference in those patients with pancreatic insufficiency (21.01$\pm$2.61 mg/ml) or without pancreatic insufficiency (19.34$\pm$2.23 mg/ml) compared to normal controls (22.54$\pm$2.27 mg/ml).

4. Conclusion

Our data on adult CF patients confirm previous findings on younger CF (131), and show the existence of markedly lower lipid levels in CF patients with pancreatic insufficiency secondary to fat malabsorption. Further work is needed to elucidate the significance of possible alterations in the carbohydrate composition of apoproteins in CF. Possible alterations in HDL distribution in CF (with or without PI) was implied which may be related to altered energy metabolism in these subjects. Information on the lipoprotein distribution in CF patients may be of value in assessment of the effectiveness of therapeutic measures in CF.

VII. References

1. Soutar, A.K., and Myant, N.B. (1979). In Offord, R.E. (ed.) "International Review of Biochemistry" Vol. 25, p.55-119. University Park Press, Baltimore.

2. Shen, B.W., Scanu, A.M., and Kezdy, F.J. (1977) Proc Natl Acad Sci 74:837-841.

3. Laggner, P., and Muller, K.W. (1978) Quar Rev Biophys II 3:371-425.

4. Scanu, A.M. (1972) Biochim Biophys Acta 265:471-508.

5. Blau, L.B., Bittman, R., Lagocki, P., Byrne, R., and Scanu, A.M. (1982) Biochim Biophys Acta 712:437-443.

6. De Lalla, O.F., and Gofman, J.W. (1954). In D. Glick (ed.) "Methods of Biochemical Analysis" Vol II, p.459. Interscience Publishers, New York.

7. Alaupovic, P., Lee, D.M., and McConathy, W.J. (1972) Biochim Biophys Acta 260:689-707.

8. Jackson, R.L., Morrisett, J.D., and Gotto, A.M., Jr. (1979) Physiol Rev 56:259-316.

9. Eisenberg, S. (1980) Ann N.Y. Acad Sci 348:30-47.

10. Tall, A.R., Green, P.H.R., Glickman, R.M., and Riley, J.W. (1979) J Clin Invest 64:977-989.

11. Eisenberg, S., and Olivecrona, T. (1979) J Lipid Res 20:614-623.

12. Chajek, T., and Eisenberg, S. (1978) _J Clin Invest_ 61:1654-1665.

13. Green, P.H.R., Tall, A.R., and Glickman, R.M. (1978) _J Clin Invest_ 61:528-534.

14. Krul, E., and Dulphin, D.J. (1982) _FEBS Letters_ 139:259-264.

15. Norum, K.R., Glomset, Glomset, J.A., Nichols, A.V., Forte, T.M., Albers, J.J., King, W.C., Mitchell, C.D., Applegate, K.R., Gong, E.L., Cabana, V., and Gjone, E. (1975) _Scan J Clin Lab Invest_ 35. Suppl. 142:31-55.

16. Patsch, J.R., Gotto, A.M., Jr., Olivecrona, T., and Eisenberg, S. (1978) _Proc Natl Acad Sci_ 75:4519-4523.

17. Goldstein, J.L., Brown, M.S. (1977) _Ann Rev Biochem_ 46:897-930.

18. Brown, M.S., and Goldstein, J.L. (1971) _Proc Natl Acad Sci_ 71:788-792.

19. Rees, A., Shoulders, C.G., Stocks, J., Galton, D.J., and Barralle (1983) _Lancet_ i:444-446.

20. Norum, K.R., Glomset, J.M., Gjone, E. (1972). In Stanberry, J.R., Wyngaarden, J.H., and Fredrickson, P.S. (eds.) "The Metabolic Basis of Inherited Disease" (3rd ed) McGraw-Hill, New York.

21. Deckelbaum, R.J., Shipley, G., and Small, D.M. (1977) _J Biol Chem_ 252:744-754.

22. Kroon, P.A. (1981) J Biol Chem 256:5332-5339.

23. Tall, A.R., Small, D.M., and Atkinson, D. (1978) J Clin Invest 62:1354-1363.

24. Lee, D.M. (1976). In Day, C.E., and Levy, R.S. (eds.) "Low Density Lipoproteins" Plenum Press, New York.

25. Kane, J.P. (1983) Ann Rev Physiol 45:637-650.

26. Steele, J.C.H., and Reynolds, J.A. (1979) J Biol Chem 254:1639-1643.

27. Socorro, L., Lopez, F., Lopez, A., and Camejo, G. (1982) J Lipid Res 23:1283-1291.

28. Shuh, I. Fairclough, G.F., Jr., Haschemeyer, R.M. (1978) Proc Natl Acad Sci 75:3173-77.

29. Lee, D.M., Valente, A.J., Kuo, W.H., Maeda, H. (1981) Biochim Biophys Acta 666:133-146.

30. Cardin, A.D., Witt, K.R., Barnhart, C.L., Jackson, R.L. (1982) Biochem 21:4503-11.

31. Margolis, S., Langdon, R.G. (1966) J Biol Chem 241:469-476.

32. Hahn, K-S, Tikkanen, M.J., Dargar, R. Cole, T.G., Davie, J.M., and Schonfeld, G. (1983) J Lipid Res 24:877-885.

33. LeBoeuf, R.C., Miller, C., Schively, J.E., Schumaker, V.N., Balla, M.A., and Lusis, A.J. (1984) FEBS Letters 170:105-108.

34. Cardin, A.D., Witt, K.R., Chao, J., Margolius, H.J., Donaldson, V.H., and Jackson, R.L. (1984) J Biol Chem 259:8522-28.

35. Schumaker, V.N., Robinson, M.T., Curtiss, L.K., Butter, R. and Sparkes, R.S. (1984) J Biol Chem 259:6423-30.

36. Mao, S.J.T., Patton, J.G., Badimon, J.J., Kottke, B.A., Alley, M.C., and Cardin, A.D. (1983) Clin Chem 29:1890-97.

37. Bautovich, G.J., Dash, M.J., Hensley, W.J., and Turtle, J.R. (1973) Clin Chem 1:415-418.

38. Krauss, R.M., and Burke, D.J. (1982) J Lipid Res 23:97-104.

39. Fisher, .R. (1983) Metabolism 32:283-291.

40. Kahlon, T.S., Adamson, G.L., and Shen, M.M.S. (1982) Lipids 17:323-330.

41. Shen, M.M.S., Krauss, R.M., Lindgren, F.T., and Forte, T.M. (1981) J Lipid Res 22:236-244.

42. Krauss, R.M., Lindgren, F.T., Ray, R.M. (1980) Clinica Chimica Acta 104:275-290.

43. Lindgren, F.T., Jensen, L.C., Wills, R.D., and Freeman, N.K. (1969) Lipids 4:337-344.

44. Adams, G.H., Schumaker, V.N. (1969) Ann N.Y. Acad Sci 164:130-146.

45. Fisher, W.R., Zech, L.A., Bardalaye, P., Warmke, G., and Berman, M. (1980) J Lipid Res 21:760-774.

46. Krauss, R.M., Williams, D.T., Lindgren, F.T., and Wood, P.D. (1984) submitted for publication.

47. Deckelbaum, R.J., Garnot, E., Oschery, Y. Rose, L. and Eisenberg, S. (1984) Arterio 4:255-231.

48. Sniderman, A.D., Shapiro, S., Marpole, D., Skinner, B., Teng, B., Kwiterowitch, P.O., Jr. (1980) Proc Natl Acad Sci 77:604-608.

49. Tikkanen, M.J., Dargar, R. Pfleger, B., Gonen, B., Davie, J.M., and Schonfeld, G. (1982) J Lipid Res 23:1032-38.

50. Chapman, M.J., Goldstein, S., Miller, G.L. (1978) Eur J Biochem 87:475-488.

51. Eisenberg, S., Bilheimer, D.W., Levy, R.I., Lindgren, F.T. (1973) Biochim Biophys Acta 326:361-377.

52. Eaton, R.P., Allen, R.C., and Schade, D.S. (1982) J Lipid Res 23:738-746.

53. Janus, E.D., Nicoll, A.M., Turner, P.M., and Lewis, B. (1980) Eur J Clin Invest 10:161-172.

54. Ginsberg, H.N., Le, N-A, Melish, J., Steinberg, D., and Brown, W.V. (1981) Metabolism 30:343-348.

55. Eaton, R.P., Allen, R.C., and Schade, D.S. (1983) J Lipid Res 24:1291-1303.

56. Fidge, N.H., and Poulis, P. (1978) J Lipid Res 19:342.

57. Raymond, T.L., and Reynolds, S.A. (1983) J Lipid Res 24:113-119.

58. Bell-Quint, J., and Forte, T.M. (1981) Biochim Biophys Acta 663:83-98.

59. Eisenberg, S. (1983) Klin Wochenschr 61:119-132.

60. Deckelbaum, R.J., Eisenberg, S. Fairnau, M., Barenholz, Y., and Olivecrona, T. (1979) J Biol Chem 254:6079-87.

61. Krauss, R.M., Musliner, T.A., and Giotas, C. (1983) Arterio 3:510a.

62. Barter, P.J., Hopkins, G.J., and Calvert, G.D. (1982) Biochem J 208:1-7.

63. Zechner, R., Dieplinger, H., Roscher, A. Krempler, F., Kostner, G.M. (1982) Biochim Biophys Acta 712:433-435.

64. Burke, D.J., Kesaneimi, A, Beltz, W., Grundy, S.M., and Krauss, R.M. (1982) Arterio 2:417a.

65. Tall, A.R., Blum, C.B., Forester, G.P., and Nelson, C.A. (1982) J Biol Chem 257:198-207.

66. Tall, A.R., Green, P.H.R. (1981) J Biol Chem 256:2035-2044.

67. Hunter, J.A. (1983) PhD thesis.

68. Langer, T., Strober, W., and Levy, R.I. (1972) J Clin Chem 51:1528.

69. Nichols, A.V., Gong, E.L., Blanche, P.J., and Forte, T.M. (1983) <u>Biochim Biophys Acta</u> 750:353-364.

70. Barter, P.J. (1983) <u>Biochim Biophys Acta</u> 751:261-270.

71. Blanche,P.J., Gong, E.L., Forte, T.M., and Nichols, A.V. (1981) <u>Biochim Biophys Acta</u> 665:408-419.

72. Hatch, F.T., Lindgren, F.T., Adamson, G.L., Jensen, L.C., Wong, A.W., and Levy, R.I. (1977) <u>J Lab Clin Med</u> 81:946-960.

73. Shore, V.G., and Shore, B. (1967) <u>Biochem</u> 6:1962.

74. Swaney, J.B., and Kuehl, K.S. (1976) <u>Biochim Biophys Acta</u> 446:561-565.

75. Williams, I.H., Kuchman, M., and Witter, R.F. (1966) <u>Lipids</u> 1:89-97.

76. Bartlett, G.F. (1959) <u>J Biol Chem</u> 234:466-468.

77. Lowry, O.H., Rosebrough, N.J., Farr, A.L., and Randall, R.J. (1951) <u>J Biol Chem</u> 193:265-275.

78. Hindricks, F.R., Walthers, B.G., and Groen, A. (1977) <u>Clin Chim Acta</u> 74:207-215.

79. Chen, C., and Albers, J.J. (1982) <u>J Lipid Res</u> 23:680-691.

80. Glomset, J.A., Janssen, E.T., Kennedy, R., and Dobbins, J. (1966) <u>J Lipid Res</u> 7:638-648.

81. Hopkins, G.L., and Barter, P.J. (1982) <u>Metabolism</u> 31:78-81.

82. Nichols, A.V., Gong, E.L., and Blanche, P.J. (1981) Biophys Biochem Res Commun 100:391-399.

83. Schmitz, G., Assman, G., Melnik, B. (1981) Clin Chim Acta 119:225-236.

84. Gambert, P., Lallemant, C., Athias, A., and Padieu, P. (1982) Biochim Biophys Acta 713:1-9.

85. Ihm, J., Ellsworth, J.L., Chataing, B., and Harmony, J.A.K. (1982) J Biol Chem 257:4818-27.

86. Tall, A.R., Abreu, E., Schuman, J. (1983) J Biol Chem 258:2174-80.

87. Hunter, J.A., Shahrokh, Z., Forte, T.M., and Nichols, A.V. (1982) Biophys Biochem Res Commun 105:828-834.

88. Burke, D.J., Krauss, R.M., and Forte, T.M. (1984) manuscript in preparation.

89. Forte, T.M., Krauss, R.M., Lindgren, F.T., and Nichols, A.V. (1979) Proc Natl Acad Sci 76:5934-38.

90. Brown, J.R., and Shockley, P. (1982). In Jost, P.C., and Griffith, O.H. (eds.) "Lipid-protein Interaction" Vol 1, p. 25-68. Wiley-Interscience Publication, New York.

91. Nichols, A.V., Gong. E.L., Blanche, P.J., Forte, T.M., and Shore, V.G. (1984) Biochim Biophys Acta 793:325-337.

92. Aggerback, L.P., Kezdy, F.J., aND Scanu, A.M. (1976) J Biol Chem 251:3823.

93. Oeswein, J.Q., and Chun, P.W. (1983) J Biol Chem 258:3645-54.

94. Scow, R.O., and Egelrud, T. (1976) Biochim Biophys Acta 431:538-549.

95. Aron, L., Jones, S., and Fielding, C.J. (1978) J Biol Chem 253:7220-26.

96. Switzer, S., and Eder, H.A. (1965) J Lipid Res 6:506.

97. Portman, O.W., and Illingworth, D.R. (1973) Biochim Biophys Acta 326:34-42.

98. Takeda, A., Pafree, R.G.E., Foradyke, D.R. (1982) Biochim Biophys Acta 710:87-98.

99. Subbaiah, P.V., Albers, J.J., Chen, C.H., and Bagdade, J.D. (1980) J Biol Chem 255:9275-80.

100. Tall, A.R., Forester, L.R., and Bongiovanni, G.L. (1983) J Lipid Res 24:277-288.

101. Barter, P.J. (1983) Biochim Biophys Acta 751:261-270.

102. Yamazaki, S., Mitsunaga, T., Furukawa, Y., and Nishida, T. (1983) J Biol Chem 258:5847-53.

103. Jackson, R.L., Cardin, A.P., Barnhart, R.L., Johnson, J.D. (1980) Biochim Biophys Acta 619:408-413.

104. Macloss, M., Edwards, J.J., Lagocki, P., and Rahman, Y-E. (1983) Biophys Biochem Res Commun 116:368-374.

105. Laggner, P., Kostner, G.M., Rakusch, U., and Worcester, D. (1981) _J Biol Chem_ 256:11832-9.

106. Keith, A.D., Melhorn, R.J., Birnbauer, M.E. (1973) _Chem Phys Lipids_ 10:223.

107. Yeagle, P.L., Langdon, R.G., Martin, R.B. (1977) _Biochem_ 16:4345.

108. Saunders, L. (1966) _Biochim Biophys Acta_ 123:70-74.

109. Lucy, J.A. (1970) _Nature_ 227:816.

110. Weltzien, H.U. (1979) _Biochim Biophys Acta_ 559:259-287.

111. Haydon, D.A., and Taylor, J. (1963) _J Theor Biol_ 4:281-299.

112. Tall. A.R., Green. P.H.R., Glickman, R.M., and Riley, J.W. (1979) _J Clin Invest_ 64:977-989.

113. Forte, T.M., Nichols, A.V., Krauss, R.M., and Norum, R.A., in press.

114. Kodama, T., Akanuma, Y., Okazaki, M., Abunatani, H. Itakura, H., Takahashi, K., Sakuma, M., Takaku, F., Hara, I. (1983) _Biochim Biophys Acta_ 752:407-415.

115. Fredrickson, D.S., Altrochi, S.P.H., Avioli, L.V., Goodman, D.S., and Goodman, H.C. (1961) _Ann Int Med_ 55:1016-31.

116. Goldstein, J.L., Schrote, H.G., Hazzard, W.R., Bierman, E.L., and Motulsky, A.G. (1973) _J Clin Invest_ 52:1544-68.

117. Krauss, R.M., Albers, J.J., and Brunzell, J.D. (1983) Clin Res 31:503A.

118. Kostner, G.M. (1976). In Day, C.E., and Levy, R.S. (eds.) "Low Density Lipoproteins" Chap 9. Plenum Press, New York.

119. Ehnholm, C., Garoff, H., Renkonen, O., and Simons, J. (1972) Biochem 11:3229-32.

120. Nothg-Laslo, V., and Jurgens, G. (1981) Biophys Biochem Res Commun 101:158-164.

121. Havekes, L., Vermeer, B.J., Brugman, T., and Emeis, J. (1981) FEBS Letters 132:169-173.

122. Kallberg, L.M., Gustafson, A., and Dahlen, G. (1976) Scand J Clin Lab Invest 36:51-65.

123. Triplett, R.B., and Fisher, W. (1978) J Lipid Res 19:478-488.

124. Chana, G.S., Chapman, M.J., Sheppard, R.J., Mills, G.L., Goldstein, S., and Grant, E.H. (1980) J Supramol Structure 13:47-52.

125. Ikai, A. (1975) J Biochem 77:321-331.

126a. di Sant'Agnese, P.A., Talamo, R.C. (1967) N Engl J Med 277:1287-95.

126b. Ibid, p.1344-52.

126c. Ibid, p.1399-1408.

127. Wood, R.E., Boat, T.F., Doershurk, C.F. (1976) Am Rev Respir Dis 113:833-878.

128. Rosenberg, M.L., Kim, H.K., Kritchevsky, D. (1970) Nature (London) 251:719.

129. Hubbard, V.S. (1983) Eur J Pediatr 141:68-70.

130. Weiss, H.F., Bennet, M.J., Braun, I., Yamanaka, W., Coon, E. (1966) Am J Clin Nutr 18:155.

131. Vaughan, W.J., Lindgren, F.T., Whalen, J.B., Abraham, S. (1978) Science 199:783-785.

132. Anderson, D.W., Nichols, A.V., Forte, T.M., and Lindgren, F.T. (1977) Biochim Biophys Acta 493:55-68.

133. Anderson, D.W. (1977) PhD thesis.

134. Kollberg, H., Bardon, A., Ceder, O. (1983) Acta Paediatr Scand Suppl 309.

135. Slack, J., Nair, S., Traisman, H., Becker, G., Hahler, S., Yi-Yang, D. (1962) J Lab Clin Med 59:302.

136. Pearson, R.D., and Lubin, A.H., (1979) Pediat Res 13:834-840.

137. Kashyap, M.L., Barnhart, R.L., Srivstava, L.S., Perisutti, G., Vink, P., Allen, C., Hogg, E., Brady, D., Glueck, C.J., and Jackson, R.L. (1982) J Lipid Res 23:877.

138. Nakaya, Y., Schaefer, E.J., and Breuer, H.B., Jr. (1980) Biophys Biochem Res Commun 95:1168-72.

139. Polz, E., and Kostner, G.M. (1979) <u>Biophys Biochem Res Commun</u> 90:1305-12.

140. Thrift, R.N., Forte, T.M., and Shore, V.G. (1984) <u>Fed Proc</u> 43:621A.